iScience

CellPress
OPEN ACCESS

Review

Biogas Reforming to Syngas: A Review

Xianhui Zhao,[1,2,*] Babu Joseph,[1,*] John Kuhn,[1] and Soydan Ozcan[3,4]

Interest in novel uses of biogas has increased recently due to concerns about climate change and greater emphasis on renewable energy sources. Although biogas is frequently used in low-value applications such as heating and fuel in engines or even just flared, reforming is an emerging strategy for converting biogas to syngas, which could then be used to obtain high-value-added liquid fuels and chemicals. Interest also exists due to the role of dry, bi-, and tri-reforming in the capture and utilization of CO_2. New research efforts have explored efficient and effective reforming catalysts, as specifically applied to biogas. In this paper, we review recent developments in dry, bi-, and tri-reforming, where the CO_2 in biogas is used as an oxidant/partial oxidant. The synthesis, characterization, lifetime, deactivation, and regeneration of candidate reforming catalysts are discussed in detail. The thermodynamic limitation and techno-economics of biogas conversion are also discussed.

INTRODUCTION

Research on renewable energies has been carried out due to concerns related to global warming and depletion of petroleum-based resources. Renewable power sources have entered the energy markets due to their promising sustainable development, reduced environmental pollution, and enhanced domestic energy supply (NREL, 2013). Biogas, which has been considered as a sustainable and renewable gaseous fuel (EPA, 2014), is suitable for direct conversion into syngas (i.e., a mixture of H_2 and CO) via a reforming. The removal of CO_2 is not required, which avoids substantial cost related to gas purification.

Biogas dry reforming could make a significant contribution to future hydrogen production, as H_2 allows for highly efficient generation of electricity in vehicles and fuel cell plants (Charisiou et al., 2019). However, biogas dry reforming involves a highly endothermic reaction because CH_4 and CO_2 have high bond-dissociation energies (435 and 526 kJ/mol, respectively). Thermodynamically, an increase in the reaction temperature favors biogas dry reforming. In addition, a number of simultaneous side reactions (e.g., reverse water–gas shift [rWGS] reaction) can influence the catalytic performance and reactant conversions (Charisiou et al., 2019). Another issue for biogas dry reforming is coke formation through the methane decomposition and/or Boudouard reaction. The coke deposited on the outer and/or inner catalyst surfaces can cause catalyst deactivation and plugging of the reforming reactor (Jabbour et al., 2019). Linde (News, 2016) had built a pilot reformer to test dry reforming technology, and there could be others at similar stage. However, there are not any commercial plants using CO_2 as a feed in the reformer to the best of our knowledge.

Compared with biogas dry reforming, the steam reforming reaction (without the CO_2 separation step) is less energy intensive. The steam reforming of CH_4 has been an established technology. The addition of steam to the biogas dry reforming process can lead to significant mitigation of coke deposition on the catalyst. Combined CO_2 and steam reforming of methane is referred as bi-reforming or "steam biogas reforming" (Equations 1 and 2) (Roy et al., 2018). However, the O_2 (if a high content) has to be separated from the biogas to allow the bi-reforming process to take place.

Tri-reforming is a combination of three methane reforming processes: carbon dioxide reforming (Equation 1), steam reforming (Equation 2), and partial oxidation reforming (Equation 3).

$$CH_4 + CO_2 \leftrightarrow 2CO + 2H_2 \quad \Delta H^\circ = 247 kJ/mol \quad \text{(Equation 1)}$$

$$CH_4 + H_2O \leftrightarrow CO + 3H_2 \quad \Delta H^\circ = 206 kJ/mol \quad \text{(Equation 2)}$$

$$CH_4 + 1/2O_2 \leftrightarrow CO + 2H_2 \quad \Delta H^\circ = -36 kJ/mol \quad \text{(Equation 3)}$$

In addition, there are other reactions taking place during the tri-reforming process (Walker et al., 2012).

$$CO + H_2O \leftrightarrow CO_2 + H_2 \quad \Delta H^\circ = -41 kJ/mol \quad \text{(Equation 4)}$$

$$C + H_2O \leftrightarrow CO + H_2 \quad \Delta H^\circ = 131 kJ/mol \quad \text{(Equation 5)}$$

[1]Department of Chemical & Biomedical Engineering, University of South Florida, Tampa, FL 33620, USA

[2]Chemical Sciences Division, Oak Ridge National Laboratory, 1 Bethel Valley Road, Oak Ridge, TN 37831, USA

[3]Manufacturing Demonstration Facility, Energy and Transportation Science Division, Oak Ridge National Laboratory, Knoxville, TN 37932, USA

[4]Department of Mechanical, Aerospace, and Biomedical Engineering, University of Tennessee, Knoxville, TN 37996, USA

*Correspondence: zhaox@ornl.gov (X.Z.), bjoseph@usf.edu (B.J.)

https://doi.org/10.1016/j.isci.2020.101082

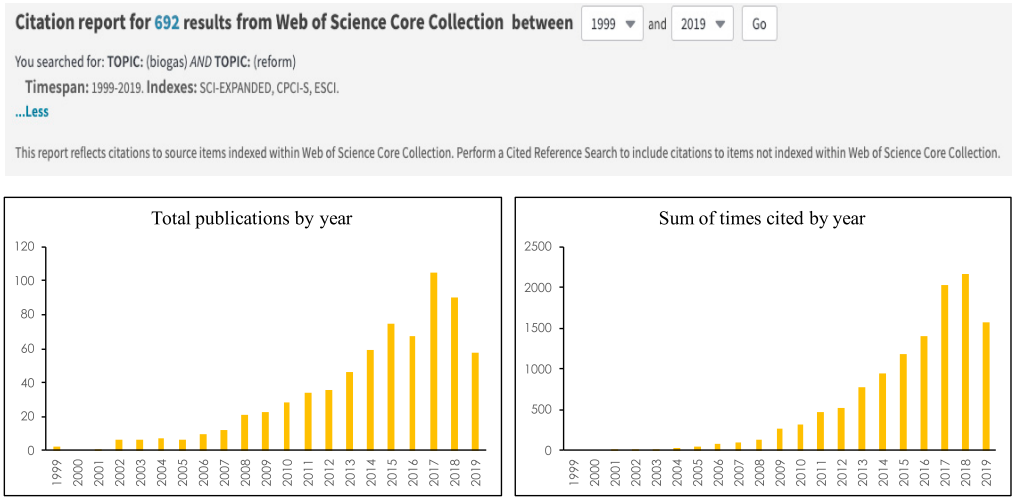

Figure 1. Search Results on Web of Science for "Biogas" and "Reform"

The graphs show exponential increases in research publications and citations for these two terms. Web of Science search and citation report conducted on 08/05/2019.

$$C + O_2 \leftrightarrow CO_2 \quad \Delta H^{\circ} = -\ 394 kJ/mol \qquad \text{(Equation 6)}$$

The tri-reforming technology has numerous advantages: the environmental advantage of carbon dioxide reforming, the high economical advantage of steam reforming due to the utilization of CO_2, no need to remove O_2, coke inhibition due to the presence of H_2O and O_2, high energy efficiency of exothermal partial oxidation reaction, and relatively lower energy consumption compared with dry and bi-reforming (Kozonoe et al., 2019; Lino et al., 2019; Paladino Lino et al., 2019; Yoo et al., 2015). However, there is a risk of oxidation of catalysts due to the oxygen present in the feed (Majewski and Wood, 2014). Despite the fact that tri-reforming is energy efficient, avoiding the oxidation of catalysts during the tri-reforming process is a challenge.

The syngas produced from methane reforming could be used to make methanol, ethanol, hydrogen, gasoline, diesel, jet fuel, dimethyl ether, and other chemicals (Gangadharan et al., 2012; He et al., 2019; Vita et al., 2014). For example, hydrogen is an important energy carrier due to its highly specific energy density, abundance, and eco-friendliness (Yoo et al., 2015). The past 20 years have seen an exponential increase in technical articles and citations on syngas production from biogas reforming, including dry reforming, bi-reforming, and tri-reforming (Figure 1).

Catalysts for reforming must be thermally stable and coke resistant due to the endothermic nature of key reactions (Anchieta et al., 2019; Singha et al., 2016b). Conventional supported nickel catalysts tend to deactivate due to coke formation and metal sintering (Yoo et al., 2015). Noble metal catalysts generally have higher coke resistance than conventional nickel catalysts during the methane reforming process (Jiang et al., 2007). Nickel is less expensive than noble metals. Well-developed mesoporous nickel-based catalysts exhibited excellent activity due to high mass transfer rate of reactants (Yoo et al., 2015). The popular catalysts for biogas tri-reforming use are nickel supported by a wide range of materials including CeO_2, ZrO_2, and Al_2O_3 (Kozonoe et al., 2019).

This review focuses on the reforming of biogas to syngas; the comparison between tri-reforming and other biogas reforming reactions (i.e., dry and bi-reforming); and recent research of biogas reforming at low temperatures. The properties of reforming catalysts, catalyst lifetime, catalyst dimension, and catalyst regeneration are discussed. The composition of biogas, thermodynamic limitations or consideration of biogas reforming, application of syngas produced from biogas, techno-economics of biogas conversion, challenges, and future directions will be discussed as well.

BIOGAS PRODUCTION, COMPOSITION, AND IMPURITIES

Biogas can be produced in many ways, and the incidence of its generation is growing fast. The feedstocks for biogas generation include farm-based wood residues, crops, livestock, and manure (Lin et al., 2018; Sarker

Ref.	Biogas Source	CH_4 (%)	CO_2 (%)	N_2 (%)	O_2 (%)	H_2S (%)	Other
(Chen et al., 2017)	Agricultural gases, landfill gas (LFG)	45–75	25–55	0–25	0.01–5	Trace	Trace composites (e.g., NH_3)
(Vita et al., 2014)	[a]Biogas from a variety of organic raw materials	50–75	25–45	2	Trace	<1	H_2O: 2%–7% at 20–40°C H_2: <1% Trace composites (e.g., NH_3, siloxane, and halides)
(Yentekakis et al., 2015)	Biogas from digestion or anaerobic fermentation of most waste materials	50–70	25–50	–	–	–	–
(Zhang et al., 2015)	Biogas from urban organic waste	40–70	30–60	–	–	–	–
(Broun and Sattler, 2016)	Biogas from solid waste in landfill	45–60	40–55	–	–	–	–
(del Valle-Zermeño et al., 2015)	Biogas from organic fraction of municipal solid waste	55–70	30–45	–	–	–	Some trace other gases
(Díez-Ramírez et al., 2016; Fei et al., 2016)	LFG	25–60	7–60	–	0.6–3	–	H_2O: 3%–20% Trace amounts of other gases
(Vita et al., 2015)	Biogas from biomasses	55–70	27–44	–	–	<3	H_2: <1% Traces of siloxanes, NH_3, and halogenates

Table 1. Composition of Biogas Derived from Different Sources

[a]Biogas composition is related to the starting source.

et al., 2018). The most common source is anaerobic digestion of biomass, either in commercial digesters, landfills, or wastewater treatment plants. Biogas compositions (CH_4: ~25%–75%, CO_2: ~7%–60%) are affected by the type of waste source utilized (Vita et al., 2015). World biogas production increased by 357% to 59 billion m^3 from 2000 to 2014 (Scarlat et al., 2018). Approximately 78 biogas plants were built in Japan by 2012 (Sarker et al., 2018). The potential volume of biogas production from farm animal manure and slaughterhouses in Malaysia was approximately 49.5 million m^3/year. The potential volume of biogas production from slaughterhouse waste and livestock manure in Iran was 8,600 million m^3/year (Zareei, 2018). The increase of biogas production is encouraged by the sustainable, economic, climate, and environmental benefits. However, the distributed nature of waste/biomass that generates biogas, which leads to small-scale reforming reactors, is a major challenge of biogas application. The supply chain logistics for biogas production faces challenges in feedstock hub location, road network design to transport feedstock to hub, and site selection of biogas reactors (Sarker et al., 2019). The location and allocation of a biogas plant is an issue because transportation cost is affected by distance (Sarker et al., 2018). Optimum biogas plant location selection, efficient management, and appropriate planning are crucial to reduce supply chain cost.

Table 1 shows the typical composition and impurities of biogas from different sources. Biogas contains CH_4, CO_2, N_2, O_2, H_2O, and trace amounts of other gases (e.g., H_2S, NH_3, and H_2). Biogas composition differs based on the feedstocks used, but CH_4 and CO_2 are the main components. The ratio of CH_4 to CO_2 is mainly in the range of 1.0–2.3. The CH_4 to H_2O ratios and CH_4 to O_2 ratios in biogas are typically higher than 3 and higher than 20, respectively. The large variance of the CH_4, CO_2, H_2O, and O_2 content in biogas from different sources is a major challenge for biogas reforming. The reaction conditions in the anaerobic digestion can be controlled to obtain appropriate ratios of components in biogas. The biogas composition can be influenced by the feed composition (Bierer et al., 2019), temperature, and organic loading rate (Bi et al., 2019). In addition, a large number of experiments (Gao et al., 2020; Hossain et al., 2019; Saebea et al., 2019) examining the reforming of biogas with different component ratios at different reaction conditions can be carried out. Artificial intelligence methods can be used on the obtained data to predict what reaction condition (e.g., temperature, pressure, and gas hourly space velocity [(GHSV]) is needed for the efficient

reforming of biogas with a specific composition to obtain high reactant conversions and the desired H_2/CO ratio (Alsaffar et al., 2020). The fast development of artificial intelligence in recent years provides an opportunity to assist the optimization of biogas utilization and application.

Biogas without purification contains small amounts of impurities such as siloxanes, NH_3, and H_2S (Elsayed et al., 2017). Volatile methyl siloxanes consist of silicon, oxygen, and methyl groups. Manufacturers have started to set limits on allowable siloxanes in the feed, considering the harmful effect of siloxane decomposition to biogas processing reactors (Elsayed et al., 2017). However, these impurities can limit the biogas application and generate harmful environmental emissions (Abdullah et al., 2018). To utilize the biogas efficiently, undesired components need to be removed (Sun et al., 2015). The H_2S can be adsorbed using porous materials such as activated carbon and ZnO-impregnated zeolite (Abdullah et al., 2018). Other materials such as Sulfatreat and silica gel can be used to remove H_2S and NH_3. Elsayed et al. (Elsayed et al., 2017) studied the effect of silicon poisoning on biogas dry reforming performance, finding that the addition of silicon decreased CH_4 and CO_2 conversions by up to >80% with increased deposited silica amounts. Siloxanes can irreversibly decompose to silica, which can become deposited on the equipment. It is suggested that the biogas should be scrubbed of impurities, including siloxanes and sulfur species, to avoid the frequent replacement of catalysts (Elsayed et al., 2017). Some biogases also include nitrogen, which is an inert gas during the biogas reforming. It is not easy to separate or remove nitrogen from the biogas. The presence of nitrogen in biogas can increase the energy consumption to reach the desired reaction temperature for biogas. Therefore, effective removal of nitrogen can be explored and developed in the future.

THERMODYNAMIC LIMITATIONS OR CONSIDERATIONS

Thermodynamic calculation can be conducted to evaluate biogas reforming performing Gibbs-free energy minimization and is common in different software packages such as Aspen Plus and HSC Chemistry. The temperature, pressure, and feed composition are the primary factors investigated.

Dry Reforming of Biogas to Syngas

The side reactions occurring during biogas reforming are an issue for the efficient utilization of biogas because they can decrease the reactant conversions. However, selection of the appropriate reaction conditions can lessen the side reactions and promote the conversions of reactants. Han et al. (Han et al., 2020) found that the CO_2 conversion and H_2/CO ratio both increased with the increase of the CH_4 to CO_2 ratio (0.5, 1.0, and 2.0) at 700–950°C. Cao et al. (Cao et al., 2018) studied the effect of the CH_4 to CO_2 molar ratio (3/6, 4/6, 6/6, 9/6, 12/6) and pressure (0.5, 1, 10, and 50 bar) on the biogas dry reforming performance at 800°C. The CH_4 conversion increased but the CO_2 conversion decreased with the decrease in CH_4 to CO_2 molar ratio. The CH_4 conversion and CO_2 conversion both increased with the decrease in pressure. Cui et al. (Cui et al., 2007) found that the dry reforming was accompanied by some side reactions such as CO disproportionation reaction, CO_2/H_2 methanation reaction, CO/H_2 methanation reaction, CO/H_2 reduction reaction, and rWGS reaction, as shown in Equations 7, 8, 9, and 10. When the reaction temperature was higher than 450°C, the CO/H_2 methanation reaction was thermodynamically forbidden. When the reaction temperature was higher than 550°C, the CO disproportionation and CO/H_2 reduction reaction were thermodynamically forbidden. When the reaction temperature was higher than 550°C, the thermodynamic equilibrium conversion of CO_2 for the CO_2/H_2 methanation was lower than 3%. Figure 2A shows the variation of CH_4 conversion with the reaction temperature at the equilibrium state. The CH_4 conversion increased greatly from 58% to 98%, with temperature increasing from 550°C to 750°C (Cui et al., 2007). These results suggest that a high temperature (e.g., 750°C) lessens side reactions.

$$2CO \rightarrow C + CO_2, \quad CO \text{ disproportionation} \qquad \text{(Equation 7)}$$

$$CO + 3H_2 \rightarrow CH_4 + H_2O, \quad CO/H_2 \text{ methanation} \qquad \text{(Equation 8)}$$

$$CO_2 + 4H_2 \rightarrow CH_4 + 2H_2O, \quad CO_2/H_2 \text{ methanation} \qquad \text{(Equation 9)}$$

$$CO + H_2 \rightarrow C + H_2O, \quad CO/H_2 \text{ reduction} \qquad \text{(Equation 10)}$$

A relatively low reaction temperature without the presence of H_2O and/or O_2 in feed gas generally tends to cause coke formation. The higher conversions at higher temperatures were due to the dry reforming being an endothermic reaction. Coke formation during biogas reforming is a major challenge for the efficient utilization of biogas. Nandini et al. (Nandini et al., 2005) reported that temperatures higher than 870°C are needed to prevent coke formation when CH_4/CO_2 feed ratio is 1 and pressure is 1 bar. Chen et al. (Chen et al., 2017) found with a temperature change from 500°C to 800°C, the generated solid carbon was negligible. The conversions of CH_4 and CO_2 increased with the temperature increase, but the rate of conversion increase was slower at higher

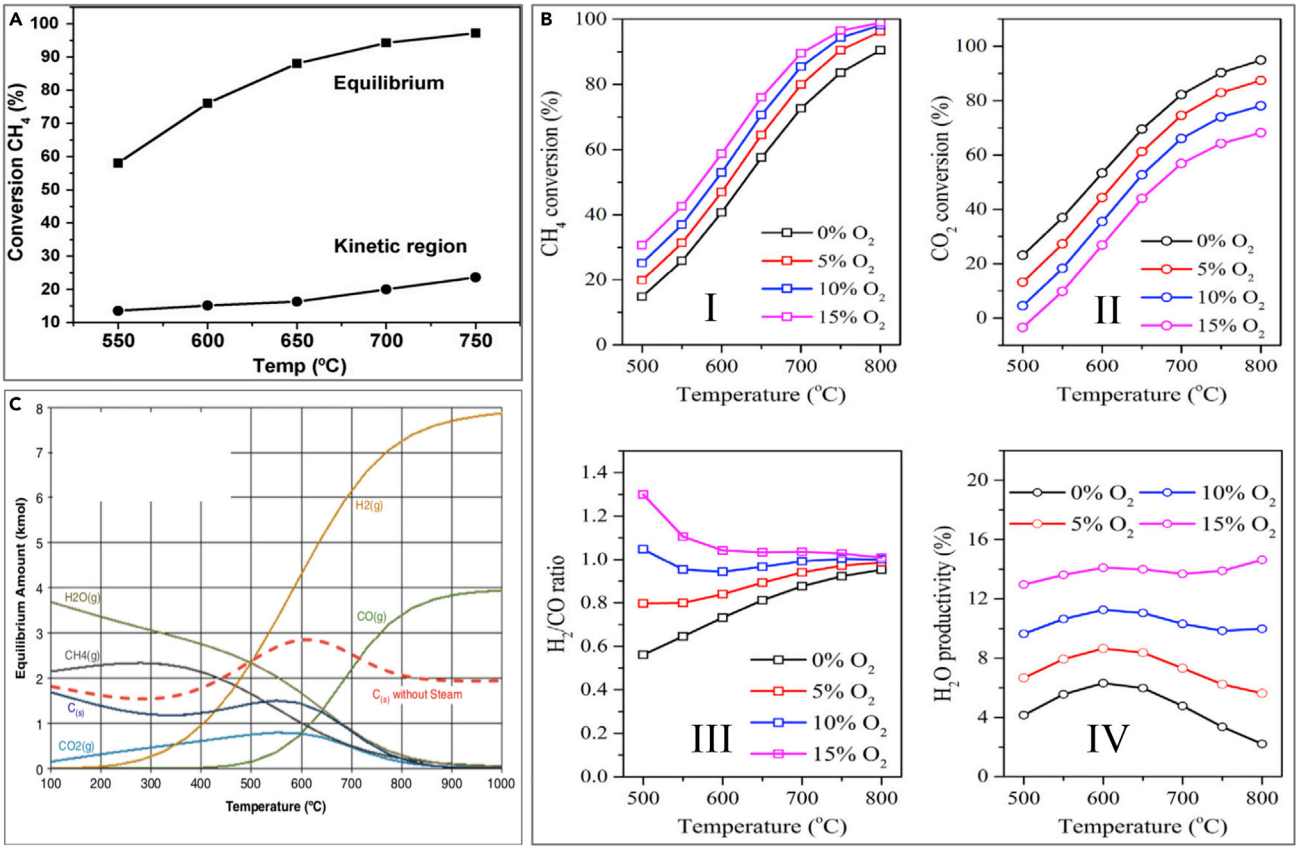

Figure 2. The Equilibrium State of Biogas Reforming

(A) Variation of CH_4 conversion with the reaction temperature (the feed molar ratio of CH_4:CO_2 = 1:1). Reproduced with permission from (Cui et al., 2007). Copyright © 2006 Elsevier B.V.

(B) Conversion efficiencies and selectivity: (I) CH_4 conversion, (II) CO_2 conversion, (III) H_2 to CO ratio, (IV) H_2O productivity. Reproduced with permission from (Chen et al., 2017). Copyright © 2016 Elsevier Ltd.

(C) Equilibrium composition for biogas bi-reforming at different temperatures and 1 bar. The initial amounts of reactants in kmol are CH_4 = 3, CO_2 = 1, and H_2O = 2. Allowed products are H_2, CO, and $C_{(s)}$. The dotted curve shows $C_{(s)}$ formation under the same conditions, but in the absence of steam. Reproduced with permission from (Kumar et al., 2015). Copyright © 2015 Elsevier Ltd.

temperatures (Figure 2B) (Chen et al., 2017). Ayodele and Cheng (Ayodele and Cheng, 2015) found that the yield of H_2 and CO increased with increased temperature from 200°C to 1,000°C. However, the syngas formation was not thermodynamically favored at 200–400°C (Ayodele and Cheng, 2015).

For dry reforming of biogas, some side reactions such as rWGS, CO/H_2 methanation reaction, and CO_2/H_2 methanation reaction take place. A high temperature (e.g., 870°C) is needed to prevent the coke formation on catalysts. With suitable increased temperature range, the conversions of CH_4 and CO_2 increase, and the yield of H_2 and CO increase due to the endothermic reaction of the dry reforming. The CO_2 is a relatively weak oxidant during biogas reforming, and its conversion increases with the increase of the CH_4 to CO_2 ratio (0.5–2.0). The CH_4 and CO_2 conversions both increase with the decrease in pressure (0.5–50 bar) because high pressure can suppress the reactions. For rWGS, the equilibrium toward products can be shifted by their separation.

Bi-reforming of Biogas to Syngas

The reaction conditions have a large effect on the biogas bi-reforming process. Jang et al. (Jang et al., 2016) investigated the effects of the (CO_2 + H_2O) to CH_4 ratio (0.9–2.9) and temperature (500–1000°C) on the thermodynamic equilibrium. For all (CO_2 + H_2O) to CH_4 ratios, the CH_4 conversion increased with the increase in temperature due to the endothermic nature of the steam reforming of methane. Almost all CH_4 was consumed above 850°C, except the lowest (CO_2 + H_2O) to CH_4 ratio (0.9). This indicates that oxidizing agents were limiting reactants so that insufficient amounts of oxidizing agents caused a lower

CH_4 conversion. The CO_2 conversion exhibited an increasing trend above 550°C, suggesting carbon dioxide reforming of methane was dominant at a high temperature. The coke yield decreased with the increase in temperature. The coke yield here is determined based on the mass of feed unless specified. In addition, the coke yield decreased largely with the increase in the (CO_2 + H_2O) to CH_4 ratio (Jang et al., 2016).

Elsayed et al. (Elsayed et al., 2018) found that the methane reforming was not possible thermodynamically below 350°C. The H_2 to CO ratio decreased as the reaction temperature increased from 450 to 600°C. The CO_2 conversion increased with an increase in the reaction temperature as the WGS reaction was favored at lower temperatures (<500°C) (Elsayed et al., 2018). Kumar et al. (Kumar et al., 2015) found that temperatures above approximately 850°C were required to reach basically complete equilibrium to H_2 and CO (Figure 2C). There was a significant thermodynamic driving force for carbon formation at temperatures below ~800°C. In addition, the presence of H_2O decreased carbon formation (Kumar et al., 2015).

Challenges related to coke prevention in biogas reforming include the use of low reaction temperatures due to energy saving and catalyst deactivation prevention, varying content of H_2O due to various biogas sources, and catalysts not being advanced. A high reaction temperature (≥500°C) and high (CO_2 + H_2O) to CH_4 ratio are needed for the biogas reforming to prevent coke formation. The addition of H_2O into biogas reduces coke formation due to their capability of initiating reactions that result in coke destruction.

Tri-reforming of Biogas to Syngas

To obtain desired reactant conversions and H_2 to CO ratio, additional components (H_2O and O_2) can be added into the biogas. Maintaining a high reforming performance with a low processing cost is a challenge. Diez-Ramirez et al. (Díez-Ramírez et al., 2016) studied the thermodynamic analysis of the biogas tri-reforming process at different temperatures (850–1000°C) and feed compositions. The optimal molar feed composition was identified as CH_4/CO_2/H_2O/O_2 = 4:1:4:2, where the high thermal efficiency (>70%), high methane conversion (>90%), and desirable H_2 to CO molar ratio (2:1) were achieved. The reaction temperature of 950°C led to higher methane conversion (~98%), a desirable H_2 to CO molar ratio, and superior exergy efficiency value. The exergy destruction mainly occurred in the reactor, mostly due to the high irreversibility of the chemical reactions. Future research should focus on decreasing the exergy destruction within the reactor and heat exchanger (Díez-Ramírez et al., 2016). A high reaction temperature (≥850°C) is helpful for the biogas reforming to improve the conversions of CH_4 and CO_2. However, a high reaction temperature needs a high energy consumption. To reduce the energy consumption, the biogas reforming at low temperatures (<600°C) has been investigated and developed (see Low Temperature Biogas Reforming).

Zhang et al. (Zhang et al., 2014) investigated the effects of process variables such as pressure (1–20 bar), inlet composition (CH_4, CO_2, H_2O, and O_2), and temperature (200–1000°C) on the product distribution of tri-reforming. As the temperature increased from 200 to 850°C, the H_2 molar fraction increased from 0 to ~0.6 (Figure 3). At temperatures <600°C, the CO_2 molar fraction was high, indicating the overall reaction favored the WGS reaction instead of dry reforming. The H_2 composition decreased, and the CH_4 composition increased with increased pressure from 1 to 20 bar. Relatively low pressure allowed the researchers to obtain products rich in H_2 and CO. A high temperature and low pressure favor the high CO_2 conversion and H_2 production rate during tri-reforming. With an increased O_2 to CH_4 ratio, the CH_4 conversion increased greatly, especially at temperatures below 850°C (Zhang et al., 2014). Methane is a limiting reactant during the tri-reforming process. With the increase of H_2O content, the CO_2 conversion decreases because H_2O is more chemically reactive to CH_4 than CO_2. Increased H_2O and O_2 in the feed can result in decreased CO_2 conversion and H_2 yield. A relatively low pressure is helpful to improve the conversion of CO_2. However, the syngas produced from biogas reforming needs to be synthesized to liquid hydrocarbon fuels through Fischer-Tropsch synthesis (FTS) at a high pressure (e.g., 20 bar). When combining the biogas reforming and FTS systems, a relatively high pressure in the biogas reforming section will be helpful for the compressor to easily reach the high pressure needed in the FTS section for industrial-scale application. The gas exiting the reformer needs to be cooled to knock out the water.

In our previous study (Zhao et al., 2018a), the thermodynamic equilibrium analysis of tri-reforming was investigated at conditions of pressure (3 bar), temperatures (830°C and 860°C), and H_2O to CH_4 molar ratios (0.34, 0.69, 1.40, and 2.10). The equilibrium O_2 conversions were nearly 100% at all conditions. The equilibrium CH_4 conversion increased from 95% to 99%, whereas the equilibrium CO_2 conversion decreased from 71% to 8% with the increase of the H_2O to CH_4 molar ratio. In addition, the produced H_2 to CO molar ratio increased as the H_2O/CH_4 molar ratio increased (Zhao et al., 2018a).

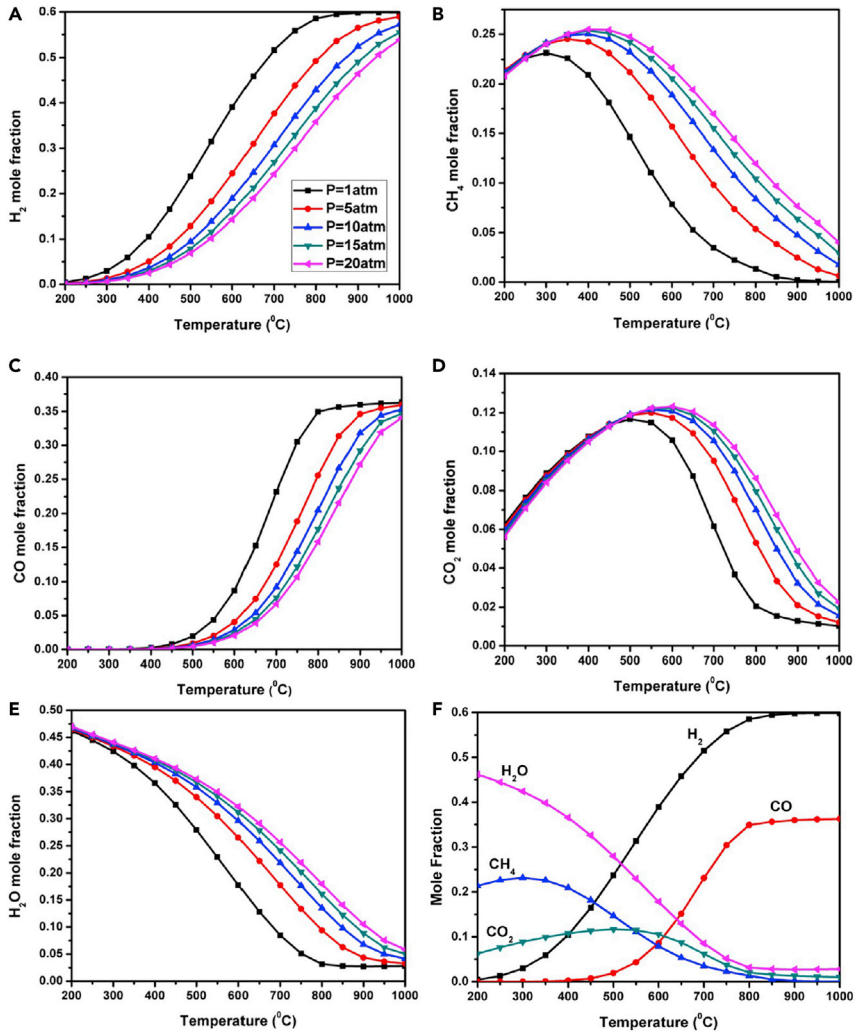

Figure 3. The Equilibrium State of Biogas Tri-reforming

Effect of the pressure on (A) H_2, (B) CH_4, (C) CO, (D) CO_2, and (E) H_2O mole fractions and (F) effect of the temperature on product mole fractions. Reproduced with permission from (Zhang et al., 2014). Copyright © 2014 American Chemical Society.

The appropriate amount of O_2 in biogas is helpful to improve the CH_4 conversion because the presence of O_2 can compensate for some energy consumption and prevent coke formation. In addition, the O_2 is nearly all consumed. With the increase of the H_2O to CH_4 molar ratio in a range, the equilibrium CH_4 conversion increases. However, the presence of O_2 and H_2O can decrease the CO_2 conversion because they are more chemically reactive with CH_4 than CO_2. The produced H_2 to CO molar ratio increased as the H_2O to CH_4 molar ratio increased due to the potential 3:1 H_2 to CO ratio resulting from the steam reforming reaction. It is flexible for biogas reforming to add necessary components into biogas based on the biogas composition to obtain desired reactant conversions and H_2 to CO ratio. However, the addition of other components can increase the biogas reforming cost.

REFORMING TECHNOLOGIES OF CONVERTING BIOGAS TO SYNGAS

Dry Reforming of Biogas to Syngas

The dry reforming of biogas is a highly endothermic process typically taking place at temperatures of 700–900°C (Table 2). Generally, the pressure of 1 bar and a CH_4 to CO_2 ratio of 1.0–2.0 in a quartz reactor were utilized for the dry reforming of biogas. The typical CH_4 to CO_2 ratio (1.0–2.0) falls in the range of that in biogas according to biogas composition study described above. The catalysts used in biogas dry

Catalyst	Reaction Conditions	CH_4 Conv. (%)	CO_2 Conv. (%)	H_2/CO	Coke Rate ($g_{coke}/(g_{cat}*h)$)	Ref.
$Ni/SrZrO_3$	700–900°C, CH_4/CO_2/He = 1/0.5/18.5, 1 bar, quartz reactor	43–55	86–99	~1.0	0.018–0.042	(Evans et al., 2014)
Ni/Al_2O_3	750°C, CH_4/CO_2 = 1/1, 18,000 mL(STP)*$g^{-1}h^{-1}$, Inconel tubular reactor	65–97	–	–	[7.5×10^{-4}, 8.1×10^{-4}]	(Lee et al., 2003a)
$5Ni\text{-}10W/Al_2O_3$	750°C, CH_4/CO_2/Ar = 1/1/1, 36,000 mL*$g^{-1}h^{-1}$, 1 bar, quartz tubular fixed-bed reactor	60	~75	~0.8	–	(Arbag et al., 2015)
$Ni@SiO_2$	750°C, $CH_4/CO_2/N_2$ = 1/1/2, 48,000 mL(STP)*$g^{-1}h^{-1}$, 1 bar, fixed-bed reactor	~71	~58	~0.7	4.9×10^{-4}	(Zhang and Li, 2015)
Ir/Al_2O_3	750°C, CH_4/CO_2 = 1/1.8, 9,000 h^{-1}, 1 bar, fixed-bed quartz reactor	~90	~68	~1.0	–	(Yentekakis et al., 2015)
$Ir/Zr_{0.92}Y_{0.08}O_{2-\delta}$	750°C, CH_4/CO_2 = 1/1.8, 11,000 h^{-1}, 1 bar, fixed-bed quartz reactor	~87	~65	~1.0	–	(Yentekakis et al., 2015)
$Ir/Ce_{0.9}Gd_{0.1}O_{2-\delta}$	750°C, CH_4/CO_2 = 1/1.8, 18,000 h^{-1}, 1 bar, fixed-bed quartz reactor	~90	~63	~0.9	–	(Yentekakis et al., 2015)
Ni-Mg PSNTS (phyllosilicate nanotubes)	750°C, CH_4/CO_2/He = 1/1/1, 60,000 mL*$g^{-1}h^{-1}$, 1 bar, quartz tube reactor	~85	~89	~0.7	0.022	(Bian et al., 2016)
Ni-Mg PSNTS@silica	750°C, CH_4/CO_2/He = 1/1/1, 60,000 mL*$g^{-1}h^{-1}$, 1 bar, quartz tube reactor	85	89	0.8	Negligible	(Bian et al., 2016)
Ni-Y/KIT-6	750°C, CH_4/CO_2/Ar = 1/1/8, 20,000 h^{-1}, 1 bar, fixed-bed quartz reactor	~65	~72	~0.8	–	(Świrk et al., 2019)
Ru/SiO_2	700°C, CH_4/CO_2/Ar = 1/1/8, 10,000 mL*$g^{-1}h^{-1}$, 1 bar, fixed-bed quartz reactor	~93	~93	~1.0	3.8×10^{-4}	(Das et al., 2019)
$Sr_{0.92}Y_{0.08}Ti_{1-x}Ru_xO_{3-d}$	800°C, $CH_4/CO_2/N_2$ = 1/1/2, 12,000 h^{-1},1 bar, fixed-bed quartz reactor	~82	~90	~0.9	–	(Kim et al., 2019a)
$La(Co_{0.1}Ni_{0.9})_{0.5}Fe_{0.5}O_3$	750°C, CH_4/CO_2 = 1/1, 12,000 mL*$g^{-1}h^{-1}$, 1 bar, fixed-bed quartz reactor	70	80	~0.9	Negligible	(Wang et al., 2019)
Rh/Al_2O_3	750°C, CH_4/CO_2 = 1/1, 120,000 mL*$g^{-1}h^{-1}$, 1 bar, fixed-bed quartz reactor	~80	~88	~1.0	8.8×10^{-4}	(Yentekakis et al., 2019)

Table 2. Recent Studies on Dry Reforming of Biogas to Syngas (the Unit g_{cat} Refers to Grams of Catalyst)

reforming were mainly Ni-based and Ir-based catalysts, which showed high activity. Ir is a noble metal, and its use in large amounts could increase costs. However, noble metals in small amounts can decorate the cheaper metals (e.g., Ni) on the catalysts. Nickel is one of the most popular metals used in dry reforming. Al_2O_3 and SiO_2 were the common supports utilized for dry reforming of biogas. The CH_4 and CO_2 conversions obtained were generally higher than 42% and 57%, respectively. The produced H_2 to CO ratio was 0.7–1.0, which is close to the equilibrium calculation. The coke rate varied depending on the reaction conditions (including time-on-stream, temperature, pressure, and GHSV) and catalyst performance.

The carbon deposition on the catalyst, low reactant conversion, and high reaction temperature are the main challenges for the dry reforming of biogas.

The high endothermic characteristics of the biogas dry reforming reaction cause a high reaction temperature required, which can cause the deactivation of catalysts. The catalyst deactivation is a drawback of biogas dry reforming applied in the industry. To prevent the catalyst deactivation and maintain the catalyst stability, researchers have investigated and developed different catalysts. Evans et al. (Evans et al., 2014) studied the dry reforming of biogas over Ni/$SrZrO_3$ catalysts, which exhibited a high selectivity toward the reforming reaction (i.e., syngas formation). The CH_4 conversion was limited due to CO_2 as a limiting reactant (Evans et al., 2014). Zhang and Li (Zhang and Li, 2015) found that the core-shell Ni@SiO_2 catalysts exhibited a high stability and activity. Both micropores and mesopores were created in the amorphous SiO_2 shell, which suppressed carbon filament growth. The Ni cores (nanoparticles) were accessible to gas molecules through the pores of the SiO_2 shell (Zhang and Li, 2015). The catalyst species, catalyst structure, and interaction between metal and support play a significant role in the resistance of carbon deposition on the catalyst. Other factors such as metal particle size, metal particle distribution, metal content, metal oxide interface, promoter, and support can affect the performance of catalysts.

Bian et al. (Bian et al., 2016) studied the dry reforming of biogas over multicore-shell Ni-Mg PSNTS@silica catalysts, which exhibited a stable and high conversion during a run of 72 h. Without the silica coating, the Ni-Mg PSNTS exhibited a high carbon deposition due to the decomposition of nanotubular structure at a high temperature (e.g., 750°C). After coating, the thermal stability of Ni-Mg PSNTS@silica was significantly improved, as silica was expected to form a strong interaction with the outer and inner surfaces of the PSNTS. The high activity and carbon resistance of the Ni-Mg PSNTS@silica catalyst was ascribed to the confinement effect and interaction between metal and nanotubular support given by the unique multicore-shell structure. The Ni-Mg PSNTS@silica catalyst is believed to be used for other high temperature and carbon-coking reactions (Bian et al., 2016). Cruz-Flores et al. (de la Cruz-Flores et al., 2020) found that the Ni-SiO_2 catalysts exhibited a low carbon deposition at a short time-on-stream (e.g., ~4 h), but a severe sintering of Ni particles at a long time-on-stream (e.g., 50 h). Understanding the reaction mechanism on the catalyst will be helpful to design the catalysts, perform the biogas reforming reactions, and analyze the reaction results. Das et al. (Das et al., 2019) studied the dry reforming of biogas over the Ru-modified catalyst (Ru-Mg-Ce/SiO_2). The proposed reaction mechanism (Figure 4A) included adsorption of CO_2 preferentially occurred over MgO surface, forming a layer of surface-adsorbed CO_2. The adsorbed CO_2 transformed over the Ce_2O_3. A fraction of the CO_2 activated over the catalyst surface to oxidize activated metallic Ru. The oxidized Ru metal was reduced to metallic Ru by the generated H_2. The selective dissociation of CH_4 occurred over the Ru metal surface, which yielded a layer of carbon over the Ru metal surface. The deposited carbon was oxidized by the catalyst surface oxygen to generate CO (Das et al., 2019). Khoja et al. (Khoja et al., 2018) proposed a reaction mechanism of dry reforming of biogas over Ni/Al_2O_3-MgO catalysts (Figure 4B). The reaction mechanism included activation of CH_4 on Ni and gasification of deposited carbon on MgO. The adsorption of elementals and intermediates containing H, O, C, and oxy-carbonates occurred on the surface and active sites of the catalyst support. The dissociation of CH_4 and CO_2 was initiated by plasma (Khoja et al., 2018).

Bobadilla et al. (Bobadilla et al., 2017) proposed a reaction mechanism of biogas dry reforming over Rh/$MgAl_2O_4$ catalysts (Figure 4C). The dissociative adsorption of CO_2 initially occurred, and the active oxygen species formed on the Rh metallic sites. The oxygen species promoted the CH_4 activation to produce H_2. The produced H_2 initiated a bi-functional mechanism, where CO_2 was activated on the basic sites of the support surface. CO_2 can be transformed into CO through the H-assisted dissociation on the metal support interface and the direct dissociation on Rh metallic sites (Bobadilla et al., 2017). The reaction mechanism of biogas reforming has been proposed to some extent. It is proposed that the dissociation of CH_4 typically occurs on the active metal surface, and CO_2 prefers to be activated on the support surface. Carbon is typically deposited on the active metal surface, and the deposited carbon is oxidized by the catalyst surface oxygen. However, it will be important for researchers to study more on the reaction mechanism over various catalysts, which can promote biogas application.

Hossain et al. (Hossain et al., 2019) found that GHSV (10,000–60,000 h^{-1}) had an influence on the CH_4 and CO_2 conversions, where the highest CH_4 and CO_2 conversions were obtained at 35,000 h^{-1}. At a higher temperature during biogas dry reforming, the pyrolysis of methane can become a primary carbon-forming reaction because the Boudouard reaction ($2CO \rightarrow CO_2 + C$) becomes more thermodynamically

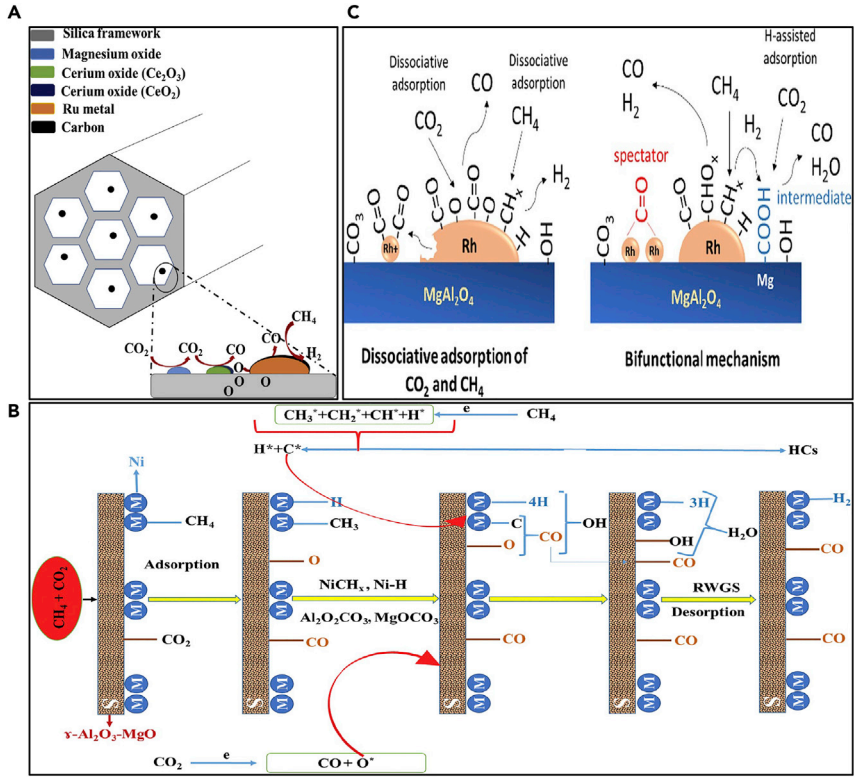

Figure 4. Proposed Mechanism of Biogas Dry Reforming over Different Catalysts

(A) Ru-Mg-Ce/SiO_2 catalysts. Reproduced with permission from (Das et al., 2019). Copyright © 2018 Elsevier Ltd.

(B) Ni/Al_2O_3-MgO catalysts in a cold plasma dielectric barrier discharge reactor. Reproduced with permission from (Khoja et al., 2018). Copyright © 2018 Elsevier B.V.

(C) Rh/$MgAl_2O_4$ catalysts. Reproduced with permission from (Bobadilla et al., 2017). Copyright © 2017 Wiley-VCH Verlag GmbH & Co. KGaA, Weinheim.

unfavorable (Evans et al., 2014). With the increase of the reaction temperature from 700 to 900°C, the CH_4 conversion increased from 43% to 55% and the CO_2 conversion increased from 86% to 99%, respectively (Evans et al., 2014). In summary, dry reforming of biogas has been frequently studied by academia. A relatively lower GHSV indicates a higher residence time of reactants on the catalyst surface, probably leading to higher reactant conversions. The CH_4 conversion increases with increased reaction temperature. The noble metal–based catalysts (e.g., Ru/SiO_2 and Ir/Al_2O_3) seem to exhibit a higher dry reforming performance than Ni-based catalysts (e.g., Ni-W/Al_2O_3 and Ni@SiO_2) due to the high stability of noble metals. Significant advances on the catalyst development have been made to reduce the carbon deposition. Incorporation of appropriate metals (e.g., La, Fe, Sn, and Zr) (Chen et al., 2020; Li et al., 2020; Zhang et al., 2020a, 2020b) to Ni-based catalysts has proven to improve the coke-resistance property. Some catalysts (e.g., Ni-Mg PSNTS) showed a high coke rate up to 0.022 $g_{coke}/(g_{cat}*h)$. However, the Ni-Mg PSNTS@silica catalysts showed negligible coke rate due to the oxygen vacancy of MgO and the function of the silica support. The addition of H_2O and O_2 into the biogas can help prevent the coke formation, discussed in below bi-reforming and tri-reforming sections. The produced H_2/CO ratio in biogas dry reforming is not suitable to produce many hydrocarbon products. Developments on the reaction condition optimization and catalysis mechanism have been made in recent years, which promote the biogas dry reforming performance. The choice of appropriate metal and support for catalyst synthesis (e.g., Ni-Zr on the CeO_2 support), reaction temperature (≥800°C), pressure (e.g., 1 bar), and composition of reactants, is significant in the stable catalytic performance and low deactivation for the dry reforming of biogas.

Bi-reforming of Biogas to Syngas

The bi-reforming of biogas typically takes place at temperatures of 800–850°C and pressure of 1–7 bar (Table 3). The CH_4 to CO_2 ratio and CH_4 to H_2O ratio are typically in the range of 1–3 and 0.5–2.5, respectively.

Catalyst	Reaction Conditions	CH_4 Conv. (%)	CO_2 Conv. (%)	H_2/CO	Coke Rate ($g_{coke}/(g_{cat}*h)$)	Ref.
NiO/MgO	830°C, $CH_4/CO_2/H_2O$ = 3/1.2/2.4, 60,000 mL*$g^{-1}h^{-1}$, 7 bar, tubular flow reactor	71	~73	2.0	–	(Olah et al., 2013)
LaSrNi/Al/SiC	850°C, $CH_4/CO_2/H_2O$ = 1/0.34/1.2, 18,000 mL*$g^{-1}h^{-1}$, 1 bar, fixed-bed Incoloy reactor	95	34	2.1	Negligible	(Kim et al., 2015)
Ni/Al_2O_3	850°C, $CH_4/CO_2/H_2O$ = 1/1/2, fixed-bed reactor	~99	~47	~1.5	–	(Park et al., 2015)
Mo_2C-Ni/ZrO_2	850°C, $CH_4/CO_2/H_2O/N_2$ = 1/0.4/0.8/1.6, 60,000 mL*$g^{-1}h^{-1}$, 1 bar, quartz tube fixed-bed reactor	~98	~79	~1.9	~6×10^{-3}	(Li et al., 2015b)
NiO/MgO	830°C, $CH_4/CO_2/H_2O$ = 3/1/2, 600,000 mL*$g^{-1}h^{-1}$, 7 bar, tubular flow reactor	~70	~72	2.0	~7.3×10^{-5}	(Olah et al., 2015)
NiO/MgO	830°C, $CH_4/CO_2/H_2O/N_2$ = 3/1/2/2.25, 60,000 mL*$g^{-1}h^{-1}$, 1 bar, tubular flow reactor	86	94	~1.9	~7.3×10^{-5}	(Olah et al., 2015)
$La_{0.9}Ce_{0.1}NiO_3$	800°C, $CH_4/CO_2/H_2O$ = 1/1/1, 3,000 h^{-1}, 1 bar, fixed-bed down flow reactor	100	~61	–	Negligible	(Yang et al., 2015)
Ni/ZrO_2	850°C, $CH_4/CO_2/H_2O/N_2$ = 1/0.8/0.4/0.2, 48,000 mL*$g^{-1}h^{-1}$, 1 bar, quartz tube fixed-bed reactor	~90	~88	1.1	5×10^{-5}	(Li et al., 2015a)
LA-Ni/ZrO_2 (ligand-assisted)	850°C, $CH_4/CO_2/H_2O/N_2$ = 1/0.8/0.4/0.2, 48,000 mL*$g^{-1}h^{-1}$, 1 bar, quartz tube fixed-bed reactor	~94	~92	1.1	1.7×10^{-4}	(Li et al., 2015a)
Ni/SBA-15	800°C, 36,000 mL*$g^{-1}h^{-1}$, 1 bar, quartz tube fixed-bed reactor	~62	~59	2.1	–	(Singh et al., 2018)
Ni/La-Si	800°C, $CH_4/CO_2/H_2O$ = 1/0.4/0.8, 1.584×10^5 mL*$g^{-1}h^{-1}$, 1 bar, fixed-bed quartz reactor	~90	~75	~2.0	4.7×10^{-4}	(Chen et al., 2019)
B-Ni/SBA-15	800°C, $CH_4/CO_2/H_2O$ = 1/0.33/0.67, 36,000 mL*$g^{-1}h^{-1}$, 1 bar, packed-bed quartz reactor	~67	~60	~2.7	–	(Siang et al., 2019)
$Ni/MgAl_2O_4$	700°C, $CH_4/CO_2/H_2O$ = 1/0.52/3.71, fixed-bed reactor	~98	~60	~2.6	–	(Rahmat et al., 2019)
Mo_2C-Ni/ZrO_2	700°C, $CH_4/CO_2/H_2O$ = 1/0.4/0.8, 1 bar, quartz tube fixed-bed reactor, 36,000 mL/(g*h)	~74	~54	–	Negligible	(Ren and Zhao, 2019)
Ni/Mg-Al mixed oxide	775°C, $CH_4/CO_2/H_2O$ = 1/0.4/0.73, 1 bar, fixed-bed reactor, 86,000 h^{-1}	73	64	2.0	–	(Li and van Veen, 2018)

Table 3. Recent Studies on Bi-reforming of Biogas to Syngas

Ni-based catalysts, with different supports such as Al_2O_3, SiC, and ZrO_2, are mainly utilized. The produced H_2 to CO ratio is generally 1.1–2.7, which is higher than that obtained from biogas dry reforming. However, the main challenges for bi-reforming of biogas include low reactant conversions and catalyst deactivation. The CH_4 and CO_2 conversions are generally higher than 61% and 33%, respectively. The coke rates of catalysts varied from being negligible to ~0.006 $g_{coke}/(g_{cat}*h)$.

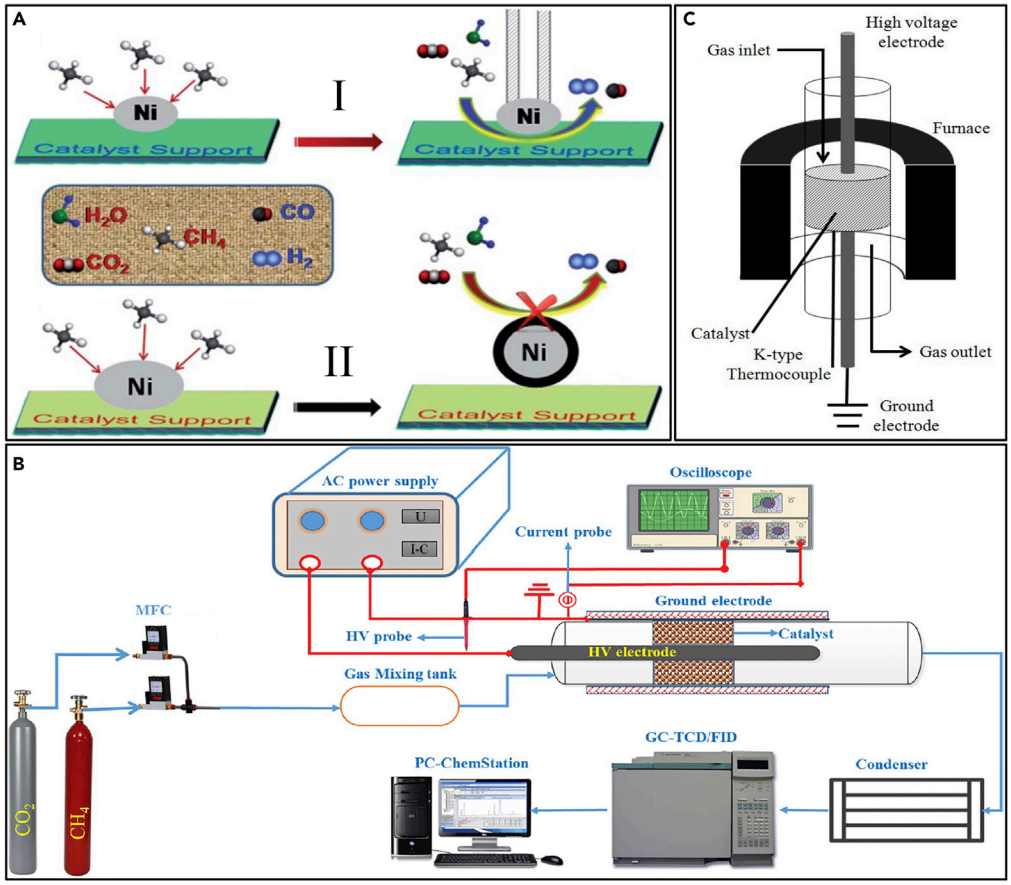

Figure 5. The Images

(A) A proposed mechanism of biogas bi-reforming over (I) Mo_2C-Ni/ZrO_2 and (II) Ni/ZrO_2 catalysts. Reproduced with permission from (Li et al., 2015b). Copyright © 2015 Royal Society of Chemistry.

(B) A schematic diagram of the biogas dry reforming in a cold plasma dielectric barrier discharge reactor. Reproduced with permission from (Khoja et al., 2018). Copyright © 2018 Elsevier B.V.

(C) The image of the electrode reactor for biogas tri-reforming. Reproduced with permission from (Yabe et al., 2018). Copyright © 2018 American Chemical Society.

Researchers have developed different catalysts to obtain desired reactant conversions and H_2 to CO ratios. Kim et al. (Kim et al., 2015) reported that the conversions of CH_4 and CO_2 both increased by 14% and 129%, respectively, with the increase of Al_2O_3 content from 0 to 10 wt% in the LaSrNi/Al/SiC catalysts, and then decreased by 13% and 42%, respectively, with the further increase of Al_2O_3 content to 20 wt%. The higher catalytic activity of LaSrNi/Al(10)/SiC (with 10 wt% of Al_2O_3 content) catalysts might be mainly ascribed to the suppressed aggregation of nickel crystallites, which caused a stronger interaction of Al_2O_3 modified SiC with La_2NiO_4 crystallites. The LaSrNi/Al(10)/SiC catalysts exhibited a larger surface area and higher dispersion of Al_2O_3 particles on SiC, compared with other Al_2O_3 concentrations. The nickel-containing crystallites seemed to be well dispersed on the SiC surface, forming intimately and strongly interacted La_2NiO_4-Al_2O_3 particles (Kim et al., 2015). Ren and Zhao (Ren and Zhao, 2019) found the catalytic activity and stability of Mo_2C-Ni/ZrO_2 catalysts were improved via a new synthesis method (glucose-assisted incipient wetness impregnation), compared with conventional incipient wetness impregnation method. Glucose was used as a metal dispersion promoting agent to improve the Ni dispersion in the catalyst.

Li et al. (Li et al., 2015b) studied the bi-reforming of biogas over Mo_2C modified Ni/ZrO_2 catalysts (0.2–3.0 wt% of Mo_2C loading), which exhibited a superior catalytic activity and stability, compared with the unmodified one. This is attributed to the catalysis of Mo_2C, improved Ni dispersion with Mo_2C addition, and the different coke morphology caused by the change in Ni-ZrO_2 interactions. A proposed reaction mechanism of biogas bi-reforming over Mo_2C-Ni/ZrO_2 and Ni/ZrO_2 catalysts is shown in Figure 5A. The Ni active sites

were accessible to the reactants for the whisker-like coke deposited on the Mo_2C-Ni/ZrO_2 catalysts. However, the Ni active sites were not accessible to the reactants for the shell-like coke deposited on the Ni/ZrO_2 catalysts. An appropriate Mo_2C loading (e.g., 0.5 wt%) was required to improve the catalytic activity and stability (Li et al., 2015b). The catalyst support (e.g., Al_2O_3) and promoter (e.g., Mo_2C) affect the metal dispersion on the catalyst. If the catalyst support and promoter content is too high, aggregation of metal particles can occur, which can decrease the catalytic performance. Optimization of the catalyst support and promoter, with a stronger interaction between metal and support, a higher dispersion of metal particles on the support, and a larger surface area, is needed for the efficient utilization of biogas.

Optimization of the reaction conditions to obtain desired reactant conversions and H_2 to CO ratio is a main challenge for the biogas reforming. Olah et al. (Olah et al., 2015) found the conversions of both CH_4 and CO_2 increased when the temperature increased from 830 to 910°C. However, the H_2 to CO ratio decreased slightly with increased temperature. The conversion of CH_4 decreased and H_2 to CO ratio increased slightly with the pressure increase from 7 to 42 bar (Olah et al., 2015). Park et al. (Park et al., 2015) also found the conversions of CH_4 and CO_2 increased with the temperature increase from 750 to 900°C, whereas the H_2 to CO ratio decreased with increased temperature. The H_2 was consumed by carbon formation on the catalyst as the temperature increased, leading to the decreased H_2 to CO ratio (Park et al., 2015).

Li et al. (Li et al., 2015a) studied the bi-reforming of biogas over LA-Ni/ZrO_2 catalysts, which exhibited a superior catalytic activity (e.g., conversions of CH_4 and CO_2), compared with classical Ni/ZrO_2 catalysts. This can be attributed to the intensified Ni-support interaction, higher Ni dispersion, enlarged oxygen vacancy, enhanced reducibility of NiO led by oxygen vacancy, and increased t-ZrO_2 content of LA-Ni/ZrO_2 catalysts. The conversions of CH_4 and CO_2 decreased with the increase of GHSV from 24,000 to 72,000 $mL*g^{-1}h^{-1}$, which might be ascribed to the decrease in the residence time on the catalyst surface and limited active sites for the increasing reactant amounts (Li et al., 2015a). Rahmat et al. (Rahmat et al., 2019) found that CH_4 and CO_2 conversions were achieved only at a suitable GHSV value (not too high or too low).

In the range of 830–900°C, a higher reaction temperature is generally favored to obtain a higher CH_4 conversion and CO_2 conversion during the biogas bi-reforming process. The high reaction temperature indicates a high processing cost due to the energy consumption. In addition, a high reaction temperature can lead to a low H_2 to CO ratio. High pressure can result in low CH_4 and CO_2 conversions. The optimization of the pressure can depend on the final application of the produced syngas due to specific requirements of the H_2 to CO ratio. A low GHSV can aid in equilibrium to be reached for obtaining high CH_4 and CO_2 conversions. However, for large-scale biogas reforming, a high GHSV may improve the feed speed. Looking for a balance between the high reactant conversions and suitable H_2 to CO ratio can be a strategy for biogas reforming.

The H_2O was added into the reactor system mainly through a syringe pump. The H_2O conversion was not reported in most biogas bi-reforming research, perhaps because the unconsumed H_2O is not easy to accurately measure. The low CO_2 conversion is a main challenge in biogas bi-reforming due to the competition between CO_2 and H_2O to react with CH_4. In addition, CO_2 is thermodynamically stable even at high temperatures. The catalyst development and reaction condition optimization have been made in recent years to look for a balance between the high CO_2 conversion and suitable H_2 to CO ratio. The produced H_2 to CO ratio is in the range of 1–3 because of the reaction of methane with CO_2 and H_2O. The catalysts exhibited different coke rates because of their characteristics and reaction conditions. Recent developments on the catalyst support have prevented the coke formation on the catalysts. The supports included MgO, ZrO_2, and ceria due to their high oxygen storage capability. The high oxygen storage property of ZrO_2 can reduce the carbon deposition on catalysts. Some catalysts, such as LaSrNi/Al/SiC and $La_{0.9}Ce_{0.1}NiO_3$, showed a negligible coke rate, probably due to the stronger metal-support interaction and higher metal particle dispersion. Utilizing noble metals (e.g., Rh) could increase the dispersion of Ni on the catalysts, thus improving catalytic performance.

Tri-reforming of Biogas to Syngas

Song and Pan (Song and Pan, 2004) first introduced tri-reforming of methane. Different catalysts with various supports and different biogas compositions have been investigated and developed to improve the catalytic performance for the biogas tri-reforming (Tables 4 and S1). Compared with dry reforming of biogas, both bi-reforming and tri-reforming can produce syngas (with a H_2 to CO molar ratio of 2:1)

Catalyst	Reaction Conditions	CH_4 Conv. (%)	CO_2 Conv. (%)	H_2/CO	Coke Rate ($g_{coke}/(g_{cat}*h)$)	Ref.
Ni/CeO_2	800°C, $CH_4/CO_2/O_2/H_2O$ = 1/0.67/0.1/0.3, 30,000 h^{-1}, 1 bar, continuous flow reactor	97.4–99.6	87.8–90.5	1.3–1.4	–	(Vita et al., 2014)
Ni/ZrO_2	800°C, $CH_4/CO_2/O_2/H_2O$ = 5/1/1/2.1, 80,000 mL/(g*h), 1 bar, fixed-bed reactor	84.4–98.5	89.3–98.5	1.6–2.2	–	(Singha et al., 2016b)
Nickel-alumina aerogel	700°C, 269,000 mL/(g*h), 1 bar, fixed-bed reactor	83.3	–	2.0–2.1	3.5×10^{-3}	(Yoo et al., 2015)
$Ni\text{-}Mg/CeO_2\text{-}ZrO_2$	800°C, 20,000 mL/(g*h), 1 bar, $CH_4/CO_2/O_2/H_2O$ = 5/1/1/2.1, fixed-bed reactor	80.9–97.2	4.4–94.8	~2.1	–	(Singha et al., 2016a)
Ni/MgO/CeZrO	850°C, 32,000 mL/(h*g_{cat}), 1 bar, $CH_4/CO_2/O_2/H_2O$ = 1/0.21/0.1/0.81, fixed-bed reactor	~94	~55	~2.1	–	(Song and Pan, 2004)
NiMoC-Ce	850°C, $CH_4/CO_2/O_2/H_2O$ = 1/0.39/0.16/0.30, fixed-bed reactor	~93	~100	–	–	(Zou et al., 2016)
$Ni/Ce\text{-}Zr\text{-}Al_2O_3$	800°C, 1 bar, 161 $g_{gas}*(g_{cat}*h)^{-1}$, $CH_4/CO_2/O_2$/liquid H_2O = 1/0.67/0.25/0.0008, fixed-bed reactor	~99	~42	~1.9	–	(Izquierdo et al., 2018)
$Ni/CeO_2\text{-}ZrO_2$	800°C, 1 bar, 17,220 $mL*(g*h)^{-1}$, $CH_4/CO_2/O_2/H_2O$ = 1/0.23/0.07/0.46, fixed-bed reactor	–	–	2.1	Negligible	(Kumar et al., 2019)
Ni/TiO_2 (calcined at 850°C)	800°C, $CH_4/CO_2/O_2/H_2O$ = 1/0.23/0.07/0.46, 1 bar, tubular reactor, 17,220 mL/(g*h)	–	–	2.0	Negligible	(Kumar et al., 2020)
$NiO\text{-}Mg/Ce\text{-}ZrO_2/Al_2O_3$	827°C, $CH_4/CO_2/O_2/H_2O$ = 1/1.33/0.47/2.47, 20 bar, multi-tubular reactor	~98	~12	~2.0	–	(Alipour-Dehkordi and Khademi, 2019)
$NiCe@SiO_2$	750°C, $CH_4/CO_2/O_2/H_2O$ = 1/0.5/0.1/0.5, 1 bar, fixed-bed reactor, 60,000 mL/(g*h)	79	75	1.7	–	(Kim et al., 2019b)

Table 4. Recent Studies on Tri-reforming of Biogas to Syngas
See also Table S1.

that can be converted into high-value products (e.g., liquid fuel) without using a WGS reactor (Zhao et al., 2018b). During the process of biogas tri-reforming, additional H_2O and O_2 are provided to obtain a H_2 to CO ratio (e.g., 1.7–2.2) suitable for FTS and to improve the CH_4 conversion. The steam reforming and partial oxidation reforming of methane can potentially provide a H_2 to CO ratio of 3:1 and 2:1, respectively. Compared with bi-reforming of biogas, the addition of O_2 in tri-reforming can help reduce the carbon deposition on the catalyst and lower the endothermic nature. Partial oxidation of methane has been commercialized in recent years. Considering the energy balance of biogas reforming processes, the incorporation of H_2O and O_2 into biogas increases energy efficiency. Compared with dry reforming of biogas and steam reforming of methane, the tri-reforming uses 45.8% and 19.7% less energy, respectively (Zhao et al., 2019a). The tri-reforming of biogas typically takes place at temperatures of 700–950°C and pressure of 1 bar in a fixed-bed reactor. The CH_4 to CO_2 ratio, CH_4 to H_2O ratio, and CH_4 to O_2 ratio are typically in the range of 1–5, 0.3–5, and 2–15, respectively. Similar to biogas bi-reforming, the catalysts used in biogas tri-reforming are mainly Ni-based catalysts with different supports such as Al_2O_3, SiO_2, ZrO_2, and CeO_2. The CH_4 conversion is mainly higher than 72%, and the CO_2 conversion is in the range of 22%–100%, respectively. The produced H_2 to CO ratio is typically 1.0–2.3. Catalysts exhibit different coke rates, which could reach 0.028 $g_{coke}/(g_{cat}*h)$.

It is important that catalysts exhibit high stability during the biogas reforming process, which is required for the commercial biogas application. An appropriate catalyst support is helpful for the superior metal dispersion and metal–support interaction. Singha et al. (Singha et al., 2016b) studied the tri-reforming of biogas over Ni/ZrO_2 catalysts, which exhibited no deactivation for more than 100 h with almost complete

conversions of CH_4, CO_2, and H_2O. The high nickel dispersion and metal–support interaction of the catalyst increased its surface oxygen species and improved its reactivity. The oxygen atoms at the interface between ZrO_2 and Ni decreased the bond energy of the oxygen species, resulting in the oxygen becoming more easily reducible. These characteristics enhanced the catalytic activity of the Ni/ZrO_2 catalyst (Singha et al., 2016b). Similarly, Vita et al. (Vita et al., 2014) found that Ni/CeO_2 catalysts exhibited constant activity over 150 h of reaction (Vita et al., 2014). The catalysts typically need to be stable for at least 1 year of industry use. The high stability of catalysts can significantly reduce costs related to expensive catalyst precursors and synthesis process. Although some methods have been developed for the recycling of deactivated catalysts, the recycling process is high cost and the recycling times are limited. Therefore, it is important to develop catalysts that exhibit high activity and stability for biogas reforming.

Similar to above dry reforming and bi-reforming of biogas, the tri-reforming performance is affected by the reaction conditions. Damanabi et al. (Damanabi et al., 2019) found that the CH_4 and CO_2 conversions both decreased with the increase of the pressure (1–10 bar). Vita et al. (Vita et al., 2014) found that the conversions of CH_4 and CO_2 increased by 3% and 4%, respectively, but the H_2 to CO molar ratio decreased by 2% as the reaction temperature increased from 800 to 900°C. A high temperature would favor the dry reforming of methane and steam reforming of methane due to their strong endothermic nature, resulting in higher conversions of CH_4 and CO_2. The conversion of CH_4 increased whereas the conversion of CO_2 decreased with the increased O_2 to CH_4 molar ratio (from 0.05 to 0.10). A high O_2 concentration can promote the conversion of CH_4. The conversion of CH_4 increased gradually whereas the conversion of CO_2 decreased largely with the increased H_2O to CH_4 molar ratio (from 0.3 to 0.7). The H_2 to CO molar ratio increased with the increased H_2O to CH_4 molar ratio (from 0.3 to 0.7). A high H_2O concentration can favor the steam reforming of methane with a lower contribution of the dry reforming of methane. In addition, the high H_2O concentration can facilitate the WGS reaction (Vita et al., 2014). Sadeghi et al. (Sadeghi et al., 2018) found the optimized conditions for maximizing the overall energy efficiency were 1,127°C, CH_4 to CO_2 to air to H_2O molar ratio = 1/0.1/2.38/0.6, and 10.8 bar. Under optimized process conditions, the overall energy efficiency reached 92%. The CH_4 conversion, CO_2 conversion, and produced H_2 to CO ratio were 99.99%, 8.2%, and 2.0, respectively. A higher steam concentration in the reactants can increase the reactor exergy efficiency due to the higher H_2 concentration in the product. A lower CO_2 concentration in the reactants is helpful to improve the reactor energy efficiency and reduce the product cost (Sadeghi et al., 2018). The modification of the reforming reactor system (Fekri Lari et al., 2019) was also found to be able to improve the CO_2 conversion.

The CH_4 conversion and the H_2 to CO ratio can be enhanced by increasing the amount of air or H_2O in the reactants. However, the dry reforming reaction can be suppressed, causing a low or negative CO_2 conversion. The negative CO_2 conversion can result from the WGS reaction (Chein and Hsu, 2018). Maciel et al. (Maciel et al., 2010) proposed a reaction mechanism of the biogas tri-reforming process. Dry and steam reforming reactions took place to produce H_2 and CO. The CH_4 and O_2 could react to yield H_2 and CO. However, the combustion-reforming could happen, where CH_4 and O_2 reacted to yield H_2O and CO_2. The methane cracking took place to yield C and H_2. The Boudouard reaction took place to yield C and CO_2 (Maciel et al., 2010).

A high reaction temperature is favored to obtain a high CH_4 conversion and CO_2 conversion due to the endothermic nature but can reduce the H_2 to CO ratio. A high O_2 concentration (in biogas) within a suitable range can promote the conversion of CH_4. The presence of O_2 is useful for industrial application of biogas reforming because it could cause some exothermic side reactions, which can compensate for the energy consumption during the biogas tri-reforming process. However, how to avoid hot spots in the reactor while adding O_2 is crucial. A high H_2O concentration within a suitable range can increase the conversion of CH_4 and the H_2 to CO ratio. However, the CO_2 conversion will be reduced at a high H_2O concentration.

The development on catalysts and reaction condition optimization (e.g., the addition of more O_2 into the reactor) has been successfully made in recent years to prevent the coke formation. Among many nickel-based catalysts used in biogas reforming, the Ni nanoparticles on the CeO_2-ZrO_2 support seem most promising. The nanoparticle size is helpful to enhance the Ni dispersion. The CeO_2-ZrO_2 support exhibits strong interaction with Ni metal and high oxygen storage capability, which can prevent metal sintering and reduce carbon deposition. In addition, the incorporation of Zr in the support can help disperse Ni particles. For the Ni/$Mg_{0.5}Ti_{0.5}O$, Ni/$Mg_{0.75}Ti_{0.25}O$, and NiMg/$Ce_{0.6}Zr_{0.4}O_2$ catalysts, the study of effects of atom

ratio of Mg to Ti and Ce to Zr is lacking. It would be interesting to investigate how the different atom ratios of metals affect the performance of catalysts. A main challenge for biogas tri-reforming is the low CO_2 conversion due to the competition between H_2O and CO_2 to react with methane. Some researchers studied the tri-reforming of biogas at a high pressure such as 10 bar, but the low CO_2 conversion at high pressures can be one issue for following FTS reaction to produce liquid fuel. As bi-reforming of biogas, the reports on the H_2O conversion are lacking due to the component tracking challenge. In addition, how to feed H_2O constantly and accurately during the tri-reforming process can help. The successful incorporation of H_2O and O_2 into biogas for tri-reforming with a high conversion efficiency is a major breakthrough achieved in recent years. The high reaction temperature ($\geq$700°C) used for tri-reforming of biogas indicates that new advanced technologies (e.g., plasma and solar) might be used to lower the reaction temperature to save energy and prevent catalyst deactivation.

Compared with biogas dry reforming, the presence of H_2O in bi-reforming can inhibit the coke formation on catalysts. There is no need to remove the moisture from raw biogas in the biogas bi-reforming. The presence of H_2O can also reduce the energy consumption during the biogas bi-reforming process, as the use of a high reaction temperature in biogas reforming results in a high processing cost. The catalysts utilized in biogas bi-reforming have similar phenomena to biogas dry reforming: Ni as the main active metal and Al_2O_3 as a common support. A higher H_2 to CO ratio (1.1–2.7) is generated in biogas bi-reforming than that in biogas dry reforming (0.7–1.0) due to the methane steam reforming reaction in bi-reforming. Steam reforming of methane has been a commercial technology. However, the methane dry reforming reaction can be suppressed to decrease the CO_2 conversion in biogas bi-reforming. The H_2 to CO ratio generated from biogas dry reforming is suitable for syngas to be used to generate heat. However, the biogas can be directly used to generate heat instead of producing syngas via dry reforming. The H_2 to CO ratio generated from biogas bi-reforming is suitable for syngas to be used to generate heat, methanol, liquid fuel, or hydrogen. When the produced H_2 to CO molar ratio is in the range of <1.5, 1.5–2.0, 1.7–2.2, and >2.2, the syngas is suitable to generate heat, methanol, liquid fuel, and hydrogen, respectively. The control of H_2O content in biogas bi-reforming can adjust the H_2 to CO ratio for a specific target application.

Compared with biogas bi-reforming, the presence of O_2 in tri-reforming can further inhibit coke formation to prevent the catalyst deactivation. The presence of O_2 can further reduce the energy consumption to reduce cost. There is no need to remove the O_2 from raw biogas for tri-reforming use. The O_2 can be nearly fully converted during biogas tri-reforming process due to the low content of O_2 (<6%) in biogas. These advantages of the presence of O_2 may lead to a high CH_4 conversion (typically >72%) in biogas tri-reforming. The catalysts utilized in biogas tri-reforming have similar phenomena to biogas bi-reforming: Ni as a main active metal and common supports include Al_2O_3 and ZrO_2. The H_2 to CO ratio generated from biogas tri-reforming is typically 1.0–2.3, which is suitable for syngas to be used to generate heat, methanol, liquid fuel, or hydrogen. Biogas tri-reforming is a simplified process to produce syngas but an emerging technology. Additional steam and oxygen are typically needed to add into the reactor system to obtain high reactant conversions and suitable H_2 to CO ratio for a specific target application. However, the addition of steam and oxygen can increase the cost. The additional O_2 can increase the risk of oxidation of metal particles (e.g., from metallic state Ni^0 to Ni^{2+}) because the metallic state is considered the active phase for biogas reforming. Adding too much O_2 can cause the methane combustion reaction to generate CO_2. If additional air is added into the tri-reforming reactor instead of O_2, the handling of inert N_2 can be an issue. The H_2O typically is not fully converted so that the handling of unreacted H_2O can be another issue for biogas tri-reforming. The unreacted H_2O can aggregate to form condensed liquid water in the pipe tubing to block the gas flowing. The CH_4 dry reforming reaction can also be suppressed by the competition of H_2O to react with CH_4, which can decrease the CO_2 conversion in biogas tri-reforming. Ensuring the accurate and constant flow of the H_2O feed into the tri-reforming reactor is a challenge. A superior heat and mass management is also needed in biogas tri-reforming.

Low Temperature Biogas Reforming

The typical high temperature (~700–950°C) used in biogas reforming can cause carbon deposition and metal Ni sintering, which can result in the catalysts deactivating. In addition, the high-temperature operation leads to high operation costs (Wang et al., 2018b). Therefore, the development of catalysts and technologies for biogas reforming at low temperatures (<600°C) is needed. Low-temperature biogas reforming typically takes place at a temperature of 25–550°C and pressure of 1 bar, shown in Tables 5 and S2. The fixed-bed reactor and plasma reactor are mainly used for the reaction. The plasma reactor is typically a dielectric barrier discharger reactor. The use of plasma in biogas reforming provides the advantages of

Catalyst	Reaction Conditions	CH_4 Conv. (%)	CO_2 Conv. (%)	H_2/CO	Coke Rate ($g_{coke}/(g_{cat}*h)$)	Ref.
Ni-Pt/$Ce_{0.6}Zr_{0.4}O_2$	430°C, CH_4/CO_2 = 1/1, ~60,000 h^{-1}, 1 bar, u-tube reactor	8	14	0.4	5.5×10^{-4}	(Sokefun et al., 2019)
ZrO_x/Ni-MnO_x/SiO_2	400°C, CH_4/CO_2 = 1/1, 1 bar, fixed-bed reactor	3	5	0.6	1×10^{-3}	(Yao et al., 2017)
ZrO_x/Ni-MnO_x/SiO_2	500°C, CH_4/CO_2 = 1/1, 1 bar, fixed-bed reactor	18	23	0.6	1.4×10^{-3}	(Yao et al., 2017)
$Ni_{0.22}La_{0.025}$/$Mg_{0.53}Al_{0.225}$	550°C, CH_4/CO_2 = 1/1, 20,000 h^{-1}, tubular quartz reactor	~32	~35	~0.9	~0.84	(Liu et al., 2016)
Ni-Mg-Al hydrotalcite	550°C, CH_4/CO_2 = 1/1, 20,000 h^{-1}, tubular quartz reactor	~40	~40	~1.0	–	(Dębek et al., 2016)
Rh-Co/SBA-15	550°C, CH_4/CO_2 = 1/1, 67 L*(g*h)$^{-1}$, 1 bar	~50	~43	~1.1	–	(El Hassan et al., 2016)
Ni/Al_2O_3-MgO	Room temperature, CH_4/CO_2 = 1/1, 364 h^{-1}, 300 J/mL, 1 bar, dielectric barrier discharge plasma reactor	75	73	1.0	~3.7×10^{-3}	(Khoja et al., 2018)
La_2O_3/Al_2O_3	25°C, CH_4/CO_2 = 1/2, 24 kv, 8 W, 800 Hz, plasma discharge coaxial packed-bed reactor	33	12	0.67	–	(Yap et al., 2018)
La_2O_3/Al_2O_3	300°C, CH_4/CO_2 = 1/2, 22 kv, 8 W, 800 Hz, plasma discharge coaxial packed-bed reactor	48	10	0.63	–	(Yap et al., 2018)
Ni-K/Al_2O_3	160°C, CH_4/CO_2 = 1/0.67, 16 W, coaxial dielectric barrier discharge plasma reactor	32	23	1.9	0.035	(Zeng et al., 2018)
$NiFe_2O_4$#SiO_2	~193°C, CH_4/CO_2 = 1/1, 160 W, coaxial dielectric barrier discharge plasma reactor	80	70	1.0	1.2×10^{-4}	(Zheng et al., 2015)
Ni-La/ZrO_2	311°C, CH_4/CO_2 = 1/1, 7 mA, 0.8 kV, 5.6 W, reactor with electric field	34	43	0.8	–	(Yabe et al., 2017)
No catalyst	~387°C, CH_4/CO_2 = 1/1, 92 h^{-1}, 370 J/mL, dielectric barrier discharge plasma alumina reactor	74	68	~0.9	–	(Khoja et al., 2017)
Ag-La loaded protonated carbon nitrides nanotubes (pCNNT)	100°C, CH_4/CO_2 = 1/1, fixed-bed reactor, visible light from solar simulator, 1 bar	–	–	0.2	–	(Tahir et al., 2019)
Ni-CeO_2-Al_2O_3	550°C, CH_4/CO_2 = 1/1, fixed-bed reactor	~36	~41	~0.9	–	(Liang et al., 2020)
$Cu_{19.8}Ru_{0.2}$	Room temperature, CH_4/CO_2 = 1/1, Harrick reactor, white light, 1 bar, 19.2 W/cm^2	~58	–	~1.0		(Zhou et al., 2020)
Rh/La_2O_3-ZrO_2	400°C, $CH_4/CO_2/H_2O$ = 1/1/3, 30,000 h^{-1}, 1 bar, fixed-bed tubular reactor	~9	–	–	–	(Angeli et al., 2016)
Pt-NiMg/$Ce_{0.6}Zr_{0.4}O_2$	500°C, $CH_4/CO_2/H_2O$ = 1/1/1, 136,000 h^{-1}, 1 bar	78	32	1.2	–	(Elsayed et al., 2018)

Table 5. Recent Studies on Low-temperature Biogas Reforming to Syngas

(Continued on next page)

Catalyst	Reaction Conditions	CH_4 Conv. (%)	CO_2 Conv. (%)	H_2/CO	Coke Rate ($g_{coke}/(g_{cat}*h)$)	Ref.
Pt-NiMg/$Ce_{0.6}Zr_{0.4}O_2$	500°C, $CH_4/CO_2/H_2O$ = 1/0.33/0.67, 136,000 h^{-1}, 1 bar	33	36	1.9	Negligible	(Elsayed et al., 2018)
Ni@SiO_2	550°C, 1 bar, $CH_4/CO_2/O_2/H_2O$ = 1/0.5/0.1/0.5, fixed-bed reactor	~23	~3	~3.6	0.025	(Majewski and Wood, 2014)
Ni-Mg/$La_{0.1}Zr_{0.9}O_{2-x}$	200°C, 3 mA, 60,000 mL*$(g*h)^{-1}$, $CH_4/CO_2/O_2/H_2O$ = 1/0.33/0.17/0.33, fixed-bed reactor with electric field	~12	–	3.2	–	(Yabe et al., 2018)
Ni-Mg/$La_{0.1}Zr_{0.9}O_2$	200°C, $CH_4/CO_2/O_2/H_2O$ = 1/0.33/0.17/0.33, 3.0 mA, 2.3 W, fixed-bed reactor with electric field	30	–	1.9	–	(Oguri et al., 2017)

Table 5. Continued
See also Table S2.

low energy input, easy operation, and low installation cost. The energy efficiency of the plasma reactor can be improved by using different heterogeneous catalysts (Khoja et al., 2018). Generally, the CH_4 to CO_2 ratio for biogas reforming is in the range of 0.5–1.5, the CH_4 to H_2O ratio for bi-reforming and tri-reforming is in the range of 0.3–3.0, and the CH_4 to O_2 ratio for tri-reforming is in the range of 5–10. The catalysts used in low-temperature biogas reforming are mainly Ni based and precious metal based (e.g., Rh, Ru, and Pd). Different catalyst supports such as $Ce_{0.6}Zr_{0.4}O_2$, ZrO_2, SiO_2, Al_2O_3, and SBA-15 have been used. The CH_4 and CO_2 conversions obtained from biogas dry reforming are both generally lower than 81%, and the produced H_2 to CO ratio is in the range of 0.2–2.0. The CH_4 conversion obtained from biogas bi-reforming and tri-reforming is generally lower than 79%, and the produced H_2 to CO ratio is in the range of 1.2–3.6. The CO_2 conversion obtained from biogas bi-reforming and tri-reforming is generally lower than 37%. The coke rate of catalysts varies from being negligible to ~0.84 $g_{coke}/(g_{cat}*h)$.

The low reactant conversions are the major challenge for low-temperature biogas reforming due to the endothermic nature of biogas reforming. The low reaction temperature regime can induce significant selectivity losses due to some side reactions (e.g., WGS) during biogas reforming. To improve the reactant conversions, researchers have developed various advanced catalysts. Majewski and Wood (Majewski and Wood, 2014) studied the tri-reforming of biogas over Ni@SiO_2 core-shell catalysts at 550°C. The core-shell structure of the Ni@SiO_2 catalysts limits access to the silica surface to prevent the structure damage of the support and the reduction of the catalysts' surface area. The core-shell structure provides advantages of high utilization of metal species and enhancement of catalytic activity. At a low reaction temperature (e.g., 550°C), the thermodynamic equilibrium favored the forward direction of the WGS reaction causing conversions of CO and H_2O to H_2 and CO_2. In addition, the CO_2 could be produced by the complete oxidation of CH_4. The increased CO_2 and H_2 concentration in generated syngas contributed to the low CO_2 conversion (<5%) and high H_2 to CO ratio (>3) (Majewski and Wood, 2014).

Elsayed et al. (Elsayed et al., 2018) studied the bi-reforming of biogas over Pt-NiMg/$Ce_{0.6}Zr_{0.4}O_2$ catalysts at 500°C. For low-temperature biogas bi-reforming, a challenge can arise because the rWGS reaction is more prevalent, generating less H_2, whereas reaction kinetics dominates over thermodynamics for dry reforming. An optimum reactant ratio in the feed can be investigated to still allow the dry reforming reaction to occur while improving the H_2 to CO ratio. Different reactant feed compositions, CH_4 to CO_2 to H_2O ratio of 1/1/1 and 1/0.33/0.67, were investigated. When the CO_2 to CH_4 ratio decreased, the H_2 to CO ratio increased from 1.2 to 1.9. The CH_4 conversion decreased from 78% to 33% as the feed became stoichiometric. The CO_2 conversion increased from 32% to 36% because the CO_2 was diluted. The results indicate that reasonable conversions of CH_4 and CO_2 and H_2 to CO ratio near 2 can be achieved at a low reaction temperature, which may enable intensified processes for the conversion of biogas to value-added products (Elsayed et al., 2018). To further improve the reactant conversions and reduce the cost, more research is needed for the low-temperature biogas reforming. The development of novel catalysts, optimization of catalyst synthesis, and introduction of new technologies can be a focus in the future. Developing advanced catalysts without using new technologies to obtain desired reactant conversions and H_2 to CO ratio is a challenge.

The reduction of catalysts plays a significant role in biogas reforming. For example, the NiO in the nickel-based catalysts needs to be reduced to metal Ni prior to the reforming reaction. Yao et al. (Yao et al., 2017) studied the dry reforming of biogas over ZrO_x/Ni-MnO_x/SiO_2 catalysts at 500°C. It was reported that Zr improved catalytic activity but the reaction would suffer from coke deposition. The promoter Mn improves the dispersion of Ni species, which enables the catalyst to minimize coke deposition. Catalytic tests showed that the reduction temperature (500°C, 550°C, 600°C, 800°C) had a significant influence on the catalyst activity. The reduced ZrO_x/Ni-MnO_x/SiO_2 catalysts were characterized using techniques including temperature-programmed reduction (TPR), X-ray diffraction (XRD), and transmission electron microscopy (TEM). The TPR results showed that the reduction temperature had an influence on the state of the metal Ni species and Mn species of the catalysts. The XRD results exhibited that the diffraction peak of metal Ni increased, whereas the diffraction peak of NiO decreased with increased reduction temperature. The TEM results exhibited that the reduction temperature affected the particle size of the Ni species on the catalyst. The ZrO_x/Ni-MnO_x/SiO_2 catalysts reduced at 550°C exhibited relatively high content of surface Ni species and small Ni species particles with narrow particle size distribution (mainly 5–6 nm), which resulted in a high catalytic activity (Yao et al., 2017). The catalyst activation process has an influence on the catalyst's structural features such as metal particle size, metal particle size distribution, and metal species content. Small metal particle size, narrow metal particle size distribution, high metal dispersion due to appropriate promoters (e.g., Mn), and high content of surface metal species will contribute to a high catalytic activity. Beyond the reduction temperature, other catalyst activation parameters such as reduction gas, gas flow rate, and reduction time can be investigated and optimized.

To lower the reaction temperature and obtain reasonable reactant conversions for biogas reforming, new technologies including the plasma and electric field have been developed. Khoja et al. (Khoja et al., 2018) studied the dry reforming of biogas over Ni/Al_2O_3-MgO catalysts at room temperature in a cold plasma dielectric barrier discharge reactor, shown in Figure 5B. The reactor system mainly consists of gas cylinders, mass flow controllers, alternating current power supply, alumina dielectric tube, condenser, and gas detector. The obtained CH_4 and CO_2 conversions were 75% and 73%, respectively (Khoja et al., 2018). Yabe et al. (Yabe et al., 2018) studied the tri-reforming of biogas over Ni-Mg/$La_{0.1}Zr_{0.9}O_{2-x}$ catalysts at 200°C in an electrode reactor, shown in Figure 5C. The Ni-Mg/$La_{0.1}Zr_{0.9}O_{2-x}$ catalysts exhibited methane oxidation suppression because NiO-MgO on the catalyst is not reduced at such a low temperature. The steam reforming of methane reaction performed well due to the surface protonics in the electric field. The conversion of O_2 was ~52%. The electric field utilized for the tri-reforming of biogas at low temperatures (e.g., 200°C) shows some interest in reducing the energy needed for the process (Yabe et al., 2018).

The feed composition, reaction temperature, voltage, current, catalyst species, and catalyst reduction temperature have an effect on the low-temperature biogas reforming performance. The addition of catalysts in the plasma reactor could promote the conversions of CH_4 and CO_2. The increase of the reaction temperature could promote the CH_4 conversion. However, it is important to reach a balance between the high reactant conversions and low reaction temperature. The low reaction temperature (<600°C) used for the biogas dry reforming seems to help reduce the coke rate of catalysts, compared with that at higher reaction temperatures (700–900°C). The utilization of new technologies and advanced catalysts into low-temperature biogas reforming with a low energy input is a major breakthrough achieved in recent years. However, the carbon deposition on the catalyst is still an issue for the low-temperature biogas reforming application. Achieving high product selectivity at a low temperature regime is also a challenge. The current CH_4 and CO_2 conversions are still low ($\leq$80% and $\leq$73%, respectively). The appropriate combination of plasma technology and advanced catalysts could lower the reaction temperature without decreasing the reactant conversions largely.

REFORMING CATALYST SYNTHESIS, CHARACTERIZATION, AND REGENERATION

Catalyst Synthesis

The catalysts used for biogas reforming exhibit different shapes including powder, pellet, core-shell, monolith, and foam (Figure 6A). Generally, the catalysts during the early stage of development are in the powder form. The number of potential candidate powder catalysts is reduced during the screening process, which includes synthesis and characterization. The powder catalysts need to be shaped into macroscopic forms (e.g., pellet) for industrial use to minimize the pressure drop in the reactor. Catalysts used in the industry should not only have the required mechanical properties (e.g., strength and attrition resistance) and functionality but also be able to reproduce the performance of laboratory-scale preparation (Mitchell et al., 2013). Different synthesis methods have been developed to obtain different catalysts with various shapes for biogas reforming use (Table 6).

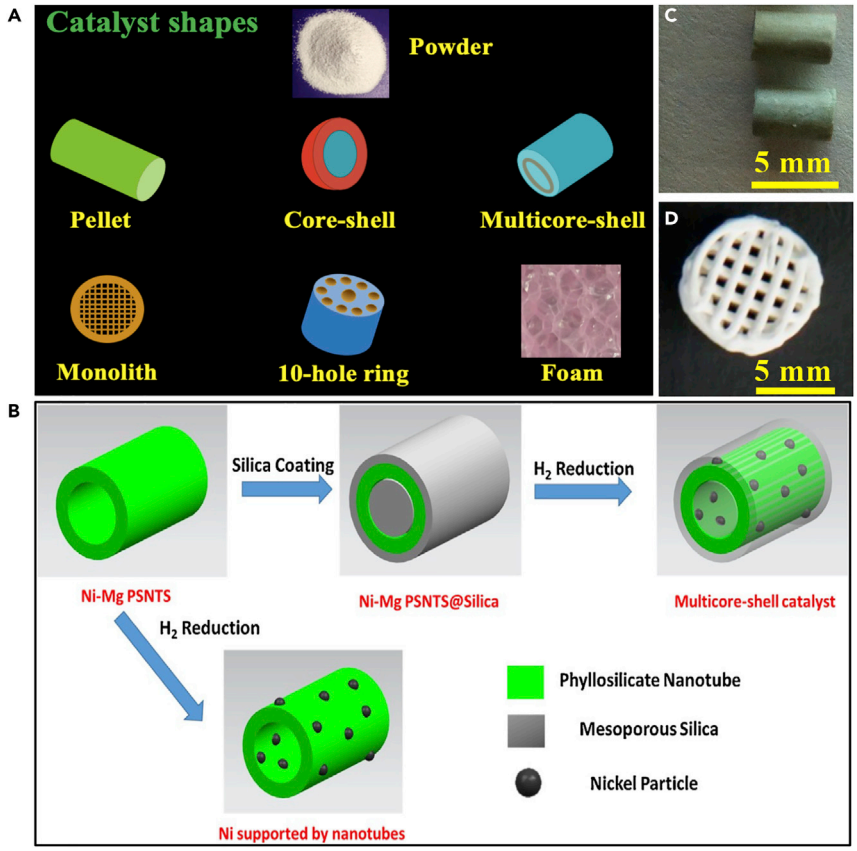

Figure 6. The Images

(A) Images of catalysts of various shapes used in biogas reforming.

(B) The diagram of the preparation of multicore-shell catalysts derived from Ni-Mg PSNTS@silica. Reproduced with permission from (Bian et al., 2016). Copyright © 2016 Elsevier B.V.

(C) NiMg/$Ce_{0.6}Zr_{0.4}O_2$/Al_2O_3 pellet catalysts used for surrogate biogas tri-reforming.

(D) 3D-printed zeolite monolith catalysts with square channels. Reproduced with permission from (Thakkar et al., 2016). Copyright © 2016 American Chemical Society.

In laboratory scale, catalysts in powder form are usually used for the screening process in biogas reforming. For example, Zanganeh et al. (Zanganeh et al., 2013) studied the dry reforming of biogas over $Ni_xMg_{1-x}O$ powder catalysts, which were synthesized using a coprecipitation method from solutions of Ni(NO_3)$_2$●6H_2O and Mg(NO_3)$_2$●6H_2O using K_2CO_3 as a precipitant. The excellent anti-coking performance of the $Ni_xMg_{1-x}O$ catalyst was attributed to the high dispersion of reduced Ni species, nickel-support interaction, and basicity of the support surface (Zanganeh et al., 2013). After the screening, the powders are shaped into macroscopic forms for future large-scale utilization. Maintaining the same catalytic performance without being brittle is a main challenge for catalysts being transferred from powder to macroscopic form. Wang et al. (Wang et al., 2010) synthesized NiO-MgO solid solution cordierite monolith catalysts using a wet impregnation method that impregnated NiO and MgO on the cordierite monolith support. The catalyst had three main phases: Ni phase, NiO phase, and NiO-MgO solid solution phase. The high stability and activity of the NiO-MgO solid solution cordierite monolith catalyst were attributed to the high nickel dispersion on the catalyst (Wang et al., 2010). During the biogas reforming process, the high metal dispersion on the catalyst provides the high resistance of coke formation.

Catalysts with other macroscopic forms such as core-shell and multicore-shell have been developed for biogas reforming too. Das et al. (Das et al., 2018) studied low-temperature dry reforming of biogas over Ni-SiO_2@CeO_2 core-shell catalysts. Uniform silica nanospheres were synthesized using a Stöber method using tetra-ethyl orthosilicate. A nickel phyllosilicate layer was formed on the SiO_2 spheres using an ammonia evaporation method and the obtained SiO_2@Ni-phyllosilicate was coated with a layer of CeO_2

Catalyst	Shape	Synthesis Method	Dimension	Ref.
NiO-MgO cordierite	Monolithic	Wet impregnation	50 × 40 × 1 mm (column height × outer diameter × wall thickness)	(Wang et al., 2010)
$Ni_xMg_{1-x}O$	Powder	Co-precipitation	13–21 nm (particle size)	(Zanganeh et al., 2013)
Ni/La-Si	Powder	One pot sol-gel	177–250 μm (particle size)	(Chen et al., 2019)
NiO-Mg/Ce-ZrO_2/Al_2O_3	10-hole ring	–	19 × 16 mm (particle size)	(Arab Aboosadi et al., 2011)
NiW/Al_2O_3	Pellet	One pot sol-gel	1–2 mm (particle size)	(Arbag et al., 2015)
$NiMg/Ce_{0.6}Zr_{0.4}O_2$	Pellet	Wet impregnation and extrusion	1.5 mm (diameter)	(Zhao et al., 2018b)
$NiMg/Ce_{0.6}Zr_{0.4}O_2/Al_2O_3$	Pellet	Wet impregnation	4.1 × 3.2 mm (length × diameter)	(Zhao et al., 2018a)
Ni/Al_2O_3	Pellet	Wet impregnation	–	(Park et al., 2015)
Ni/Al_2O_3/Ni	Foam	Sol-gel and impregnation	–	(Park et al., 2015)
Ni@SiO_2	Core-shell	Water-in-oil microemulsion	~5 × 10 × 30 nm (Ni particle size × SiO_2 shell thickness × SiO_2 sphere diameter)	(Wang et al., 2018a)
Ni-SiO_2@CeO_2	Core-shell	Stöber treatment, ammonia evaporation, and precipitation	–	(Das et al., 2018)
Ni-Mg phyllosilicate nanotubes@SiO_2	Multicore-shell	Hydrothermal treatment and silica coating	–	(Bian et al., 2016)

Table 6. Shape, Dimension, and Synthesis Method of Catalysts Used for Biogas Reforming

using a precipitation method. CeO_2 was chosen as the shell due to its high oxygen storage capacity and redox potential, which can reduce the coke formation under severe dry reforming conditions. The Ni-SiO_2@CeO_2 core-shell catalyst exhibited an excellent coke inhibition property without coke detected after 72 h of reforming. The high activity of the catalyst was attributed to its high Ni dispersion and reducibility (Das et al., 2018). Bian et al. (Bian et al., 2016) studied the dry reforming of biogas over Ni-Mg PSNTS@silica multicore-shell catalysts (Figure 6B), which were synthesized using a hydrothermal method. With the silica coating, the thermal stability of the Ni-Mg PSNTS@silica multicore-shell catalyst was greatly improved (Bian et al., 2016). The design of the core-shell and multicore-shell can prevent the coke formation on the catalyst, probably due to the high metal dispersion. However, the catalyst synthesis and activation process need to be strictly controlled to obtain highly dispersed and uniform metal particles.

Catalysts in pellet form are usually used in an industrial scale for biogas reforming. Pellets can be shaped from powder by simple extrusion, which is cost- effective. Arbag et al. (Arbag et al., 2015) studied the dry reforming of biogas over W- and Ni-incorporated mesoporous Al_2O_3 pellet catalysts, which were synthesized using a one-pot sol-gel route method. The W- and Ni-incorporated mesoporous Al_2O_3 pellet catalysts exhibited a high catalytic activity throughout a 150 h of time-on-stream operation at 750°C. The incorporation of W can significantly enhance and stabilize catalyst performance. Coke formation on the catalyst was minimized due to the redox ability of WO_x (Arbag et al., 2015). The synthesized $NiMg/Ce_{0.6}Zr_{0.4}O_2/Al_2O_3$ pellet catalysts (Figure 6C) have been used for biogas tri-reforming to produce syngas with high reactant conversions and desirable selectivity and stability (Zhao et al., 2018a). However, the space velocity was low due to the large volume of Al_2O_3. To increase the space velocity suitable for large-scale application, the $NiMg/Ce_{0.6}Zr_{0.4}O_2$ pellets (without the Al_2O_3 support) have been developed via extrusion, where similar catalyst performance was achieved (Zhao et al., 2018b). However, pellet catalysts exhibit issues due to potential mass transfer limitation and heat transfer limitation in the continuous flow reactors.

Heat and mass transfer of catalysts are important factors in the biogas reforming process due to the combination of endothermic and exothermic reactions. In our previous research (Zhao et al., 2018b), the tri-reforming of biogas was run over cylindrical $NiMg/Ce_{0.6}Zr_{0.4}O_2$ pellet catalysts at 882°C and 3 bar in a fixed-bed reactor. The $NiMg/Ce_{0.6}Zr_{0.4}O_2$ pellet catalysts exhibited internal diffusion limitations because the

Weisz-Prater criteria (C_{wp}) was higher than 1. The pressure drop in this tri-reforming process was negligible. The pellet catalyst with small particle size (diameter of 1.5 mm) had a higher effectiveness factor than that with large particle size (diameter of 3.18 mm). The pellet catalyst with small particle size was estimated to exhibit internal mass transfer and external heat transfer but no external mass transfer and internal heat transfer. However, the NiMg/$Ce_{0.6}Zr_{0.4}O_2$ powder catalysts tested in similar reaction conditions did not exhibit internal mass transfer limitations (Zhao et al., 2018b). Similarly, the Pd-Ni-Mg/ceria-zirconia and Pt-Ni-Mg/ceria-zirconia powder catalysts did not exhibit internal diffusion limitations, and the external mass transfer limitations were negligible during the biogas dry reforming process (Elsayed et al., 2016).

Other technologies have been investigated to further improve the catalytic performance and minimize the potential transport and pressure drop issues for catalysts. For example, 3D printing can handle complex shapes with high design flexibility (Mokashi et al., 2019; Tang et al., 2018; Zhao et al., 2019c). It offers the advantages of low waste generation and energy consumption. In our current research on 3D printing of catalysts for biogas reforming, a zeolite monolith catalyst was successfully 3D printed and demonstrated. Similarly, Thakkar et al. (Thakkar et al., 2016) have successfully 3D printed the zeolite monolith catalyst (Figure 6D). The synthesis of conventional monolith catalyst needs a specially designed extruder for the extrusion process, which causes high extrusion costs. The geometry of the conventional monolith channels is typically circular or square. However, the 3D printing of monolith catalysts makes it easy to modify the shape and size of catalysts, especially for catalysts with complex structure. With the assistance of 3D-printing technology, other shapes that can minimize transfer limitation and pressure drop issues will be investigated and developed.

Based on research described above, catalysts have been developed with various shapes including powder, cylinder pellet, monolith, core shell, hole O-ring, and disk. The catalysts are mainly Ni-based catalysts, with supports of MgO, SiO_2, Al_2O_3, and $Ce_{0.6}Ze_{0.4}O_2$. Industrial catalysts are usually in the form of monoliths, pellets, or other structures, which can minimize the pressure drop in the reactor (Zhao et al., 2019b). Powders are typically structured via a unit operation (e.g., forming or shaping) into macroscopic bodies. During the structuring process, powders should be refined (e.g., ball milling) to form a well-defined feed, and the shaped bodies should be treated with satisfied mechanical properties and chemical stability to ensure long lifetime and smooth operation. The successful shaping of advanced powder catalysts with high catalytic activity is a recent major breakthrough. However, scale-up of catalysts is a major hurdle in the implementation of a new catalytic technology (Mitchell et al., 2013). The preparation methods for catalyst synthesis mainly include wet impregnation, precipitation, 3D printing, deposition, one pot sol-gel, and extrusion. Current suitable catalyst scale-up methods include pelletization, spray drying (form micrometre-sized), granulation (form millimetre-sized), and extrusion (form centimetre-sized) (Mitchell et al., 2013). Extrusion is a cost-effective and simple technique for producing standard industrial catalysts, but 3D printing shows a potential for customized catalysts with complex shapes.

Catalyst Characterization

The catalytic activity of catalysts is a combined effect of reaction parameters (such as transfer limitation, biogas feed composition, and reaction temperature) and catalyst characteristics. Tables 7 and S3 show some typical properties of catalysts used in biogas reforming. The properties of catalysts (e.g., Brunauer-Emmett-Teller [BET] surface area, pore size, pore volume, basic site, metal dispersion) have a relationship to the catalytic performance during the biogas reforming process. The screening of properties can be one strategy for evaluating catalysts. The synthesis-property-function relationships of catalysts are crucial to selecting appropriate formulation and structuring form. One challenge is that the property–function relationships of catalysts are not clear. During the biogas reforming process, carbon formation may fill some pores of the catalysts, which can change their surface characteristics.

The synthesis method and procedure have a significant influence on the catalyst's properties (e.g., surface area and pore volume) as does the selection of metal precursors. For example, the Co/Al_2O_3 catalysts exhibited BET surface area of 118–144 m^2/g due to the different cobalt precursors ($CoSO_4$ and $Co(NO_3)_2$) (Ding and Yan, 2002). Wang et al. (Wang et al., 2010) synthesized the NiO-MgO solid solution cordierite monolith catalysts and found the BET surface area of the cordierite was 11 m^2/g. With the wet impregnation of Al_2O_3 superfine powders, the NiO-MgO solid solution cordierite monolith catalyst had a higher BET surface area, which was 40.2 m^2/g (Wang et al., 2010). Zanganeh et al. (Zanganeh et al., 2013) studied the dry reforming of biogas over $Ni_xMg_{1-x}O$ solid solution catalysts. The surface area of metal oxide powders at high temperatures depends on their intrinsic properties, particularly phase transformation and melting point. The nickel loading in the range of 3–7 wt% had a

Catalyst	BET Surface Area (m^2/g)	Pore Volume (cm^3/g)	Pore Size (Å)	Basic Sites (mmol/g)	Metal Dispersion (%)	Ref.
NiO-MgO cordierite	40.2	–	–	–	–	(Wang et al., 2010)
$Ni_xMg_{1-x}O$	65–115	0.50–1.08	260–494	–	–	(Zanganeh et al., 2013)
Al_2O_3	192	0.30	63–75	–	–	(Ding and Yan, 2002; Zou et al., 2016)
Co/Al_2O_3	118–144	0.23–0.24	66–78	–	–	(Ding and Yan, 2002)
Ni/Al_2O_3	130	0.24	75	0.03	1.0	(Ding and Yan, 2002; García-Vargas et al., 2014)
Ni/ZrO_2	128	0.16	51	0.002	0.3–2.0	(Kumar et al., 2019; Singha et al., 2016a; Song et al., 2010)
ZrO_2	130	0.11	35	–	–	(Singha et al., 2016a; Song et al., 2010)
$Ce_{0.6}Zr_{0.4}O_2$	93–232	0.06–0.40	32–57	–	–	(Sukonket et al., 2011)
$Ni/Ce_{0.6}Zr_{0.4}O_2$	59–215	0.06–0.30	41–53	–	4.2–7.4	(Sukonket et al., 2011)
Ni/CeO_2	1.8–9.2	0.02–0.08	89	0.02	~1	(Pal et al., 2015; Pino et al., 2011; Singha et al., 2016a; Vita et al., 2014)
Ni-Mg/β-SiC	21	0.09	–	0.01	–	(García-Vargas et al., 2015)
Ni-alumina aerogel	370	1.18	127	–	19	(Yoo et al., 2015)
Ni-alumina xerogel	322	0.58	72	–	12	(Yoo et al., 2015)
Ni/SiC	26	0.18	–	0.003	1.6	(García-Vargas et al., 2014)
Ni/YSZ (yttria-stabilized zirconia)	11	0.06	–	0.02	1.5	(García-Vargas et al., 2014)
Ni/zeolite L	95	0.45	96	–	4.7	(Izquierdo et al., 2014)
Rh-Ni/zeolite L	64	0.63	198	–	10.5	(Izquierdo et al., 2014)
Mg/CeO_2-ZrO_2	138	0.16	45	–	–	(Kumar et al., 2019; Singha et al., 2016a)
Ni/MgO	241	0.74	124	–	0.6	(Kumar et al., 2019; Singha et al., 2016a)
$Ni/Ce_{0.15}Zr_{0.85}O_2$	122	0.18	61	–	–	(Kumar et al., 2019; Singha et al., 2016a)
$Ni-Mg/CeO_2$-ZrO_2	126–133	0.18–0.20	46–47	–	–	(Kumar et al., 2019; Singha et al., 2016a)
Ce/Al_2O_3	195	0.76	150	–	–	(Izquierdo et al., 2013)
Zr/Al_2O_3	180	0.67	144	–	–	(Izquierdo et al., 2013)
$Ni-Ce/Al_2O_3$	163	0.59	144	–	0.06	(Izquierdo et al., 2013)
$Ni-Ce-Zr/Al_2O_3$	151	0.60	153	–	0.08	(Izquierdo et al., 2013)
$Rh-Ni-Ce/Al_2O_3$	157	0.60	150	–	0.12	(Izquierdo et al., 2013)
NiMo-C	138	0.27	73	–	–	(Zou et al., 2016)
NiMoC-La	143	0.27	73	–	–	(Zou et al., 2016)
NiMoC-Co	130	0.25	74	–	–	(Zou et al., 2016)
NiMoC-K	104	0.18	62	–	–	(Zou et al., 2016)
Ni/CeO_2-ZrO_2	4	–	–	0.0008	1.5	(Kumar et al., 2019)
Ni/SBA-15	36	–	–	0.004	2.2	(Kumar et al., 2019)

Table 7. Properties of Catalysts Used in Biogas Reforming

(Continued on next page)

Catalyst	BET Surface Area (m^2/g)	Pore Volume (cm^3/g)	Pore Size (Å)	Basic Sites (mmol/g)	Metal Dispersion (%)	Ref.
Ni-Y/KIT-6	199	0.2	40	–	–	(Świrk et al., 2019)
Ru/SiO_2	930	1.01	48	–	–	(Das et al., 2019)
$Sr_{0.92}Y_{0.08}Ti_{1-x}Ru_xO_{3-d}$	37	0.27	296	–	–	(Kim et al., 2019a)

Table 7. Continued
See also Table S3.

minor effect on the BET surface area of the $Ni_xMg_{1-x}O$ solid solution catalysts. However, when the nickel loading increased to 10 wt%, the surface area increased significantly. With the further increase of nickel loading (15–25 wt %), the surface area of the $Ni_xMg_{1-x}O$ solid solution catalysts decreased (Zanganeh et al., 2013). García-Vargas et al. (García-Vargas et al., 2014) loaded nickel in four different supports including Al_2O_3, CeO_2, SiC, and YSZ. The support had a significant effect on the surface characteristics of the Ni-based catalysts. The surface area and pore volume were in the range of 7–69 m^2/g and 0.06–0.24 cm^3/g, respectively (García-Vargas et al., 2014). The synthesis parameters including phase transformation, metal loading, and support species have a large influence on the surface characteristics of catalysts. The synthesis procedure needs a strict control to obtain the desired properties of catalysts.

The surface area of catalysts can be reduced with metal loading. Ding and Yan studied the dry reforming of biogas over Al_2O_3 catalysts, which had a BET surface area of 192 m^2/g, pore volume of 0.30 cm^3/g, and pore size of 63–75 Å (Ding and Yan, 2002; Zou et al., 2016). After Co or Ni was loaded on the Al_2O_3support, the Co/Al_2O_3 or Ni/Al_2O_3 catalysts had a lower BET surface area and pore volume than Al_2O_3 (Ding and Yan, 2002; García-Vargas et al., 2014). Some of the pores of the Al_2O_3 support might have been filled with metal oxides after the metal loading, which caused the decrease of the surface area and pore volume. Similarly, with the addition of Ni and Mg on the β-SiC support, the surface area of the Ni-Mg/β-SiC catalysts decreased, reported by García-Vargas et al. (García-Vargas et al., 2015). With the impregnation of 5 wt% of Ni on the $Ce_{0.6}Zr_{0.4}O_2$ support, the surface area of the $Ni/Ce_{0.6}Zr_{0.4}O_2$ catalysts decreased, as reported by Sukonket et al. (Sukonket et al., 2011). In addition, the surface area and pore volume of the $Ni/Ce_{0.6}Zr_{0.4}O_2$ catalysts decreased with the increase of the calcination temperature from 650 to 800°C.

Based on research described above, the BET surface areas of reforming catalysts are mainly in the range of 2–370 m^2/g. The BET surface area of catalysts is affected by many parameters including the metal precursor, pore structure of supports, synthesis method, and dispersion of active metal on the support. A suitable metal loading (e.g., 10 wt%) on the support can reach the highest surface area of the catalyst. The pore volumes of reforming catalysts are mainly in the range of 0.004–1.18 cm^3/g. Generally, the addition of metals on the support will result in decreased pore volume of catalysts because the metals can lead to partial blockage of the support channels. The pore sizes of reforming catalysts are mainly in the range of 32–494 Å. The pore size of catalysts can affect the product selectivity: small molecules of products can diffuse out of catalyst pores, but large molecules of products can block the catalyst pores. The pore volume and pore size of catalysts can be affected by the particle size, synthesis method, and synthesis procedure. The dispersion of nickel metal on various supports (e.g., Al_2O_3, ZrO_2, CeO_2, MgO, zeolite) varies largely from 0.06% to 19%. A high metal dispersion of catalysts is effective to reduce the carbon deposition during biogas reforming process. The metal dispersion of catalysts can be affected by the precursor species, support species, synthesis method, and metal loading level. For example, incorporating a small amount of noble metal (e.g., Rh) can increase the dispersion of nickel metal on the catalyst (Izquierdo et al., 2013, 2014). The basic sites of reforming catalysts are mainly in the range of 0.0008–0.04 mmol/g. The optimal catalyst can exhibit these properties: surface area of >100 m^2/g, pore volume of >0.2 cm^3/g, pore size of ~50 Å, basic site of >0.02 mmol/g, and metal dispersion of >2%. No clear relationship is found yet between the catalyst's property and biogas reforming reaction type. The catalyst's surface area, pore volume, and pore size do not vary largely as a function of the active metal (e.g., Ni and Co), probably due to the same support with only small amounts of active metals. However, the catalyst's surface area, pore volume, and basic site vary largely as a function of the support (e.g., Al_2O_3, SiO_2, MgO, CeO_2, and ZrO_2). In the future, more studies on the relationship between catalyst physicochemical properties and catalytic activity can be conducted.

Catalyst	Lifetime	Regeneration	Ref.
Boron nitride defect-confined Ni	≥125 h	–	(Bu et al., 2020)
Ni/CeO_2	≥150 h	–	(Vita et al., 2014)
Ni-Mo-MgO	≥850 h	–	(Song et al., 2020)
$Ni/MgAl_2O_4$	Insignificant carbon formation after 2 years	–	(Mortensen and Dybkjær, 2015)
$0.15\%Ni/1.7\%Ln/Al_2O_3$	CH_4 conversion decreased from 92% to 62% after 600 h	–	(Slagtern et al., 1997)
Ni/ZrO_2	CH_4 conversion decreased from 86% to 84% after 600 h	–	(Wei et al., 2000)
Ni-0.5Mo/SBA-15	CH_4 conversion remained at ~94% for 600 h	–	(Huang et al., 2011)
$8\%Ni/SBA\text{-}15/Al_2O_3/FeCrAl$	CH_4 conversion decreased from 92% to 89% after 1,400 h	–	(Wang et al., 2008)
$9\%\ La_2NiO_4/Al_2O_3$	–	In air at 600°C	(Liu and Au, 2003)
Ni/SiO_2MgO	–	$O_2 + CO_2$ was better than CO_2 (O_2 accelerates coke removal)	(Assabumrungrat et al., 2009)
$NiCo/MgO\text{-}ZrO_2$	–	1 h regeneration: air was better than N_2 or H_2	(Fan et al., 2011)
Ni/Al_2O_3	–	Flow O_2, then reduced with H_2 at 650°C for 1 h	(Quincoces, 2004)

Table 8. Lifetime and Regeneration of Biogas Reforming Catalysts

Catalyst Regeneration

Lifetime (Table 8) is an important factor for catalyst use in industry. Catalysts could be deactivated by coke deposition, sintering of metallic phase, and sintering of support (Vita et al., 2014). However, the spent catalysts can be regenerated to recover their catalytic activity. The typical regeneration methods for spent reforming catalysts include heating in air, activation in steam, and reduction using H_2. A main challenge for the catalyst regeneration is the addition of regeneration cost and decreased catalytic performance.

Carbon deposition on the catalyst can be observed using an apparatus such as a transmission electron microscope. Wang et al. (Wang et al., 2019) studied the dry reforming of biogas over $La(Co_{0.1}Ni_{0.9})_{0.5}Fe_{0.5}O_3$ catalysts. The nanosheet-like carbon species can be observed on the used $La(Co_{0.1}Ni_{0.9})_{0.5}Fe_{0.5}O_3$ catalyst, indicating the deposition of carbon on the catalyst during the biogas reforming process. Methane decomposition (Equation 11) and Boudouard reaction (Equation 7) can result in serious carbon deposition issues for the catalyst. The deposited carbon species on the catalyst can be removed by oxygen species adsorbed either on the perovskite matrix or on the metallic particle. The oxygen vacancy can provide active sites for the dissociation of CO_2, whereas the active oxygen species can promote the removal of the deposited carbon species. The spin-state features and multiple valences of Co cations may affect the active oxygen species in the perovskite, which affected the removal of deposited carbon species. The overall low carbon formation rate of the $La(Co_{0.1}Ni_{0.9})_{0.5}Fe_{0.5}O_3$ catalyst might be attributed to the stable perovskite phase that enhanced the metal–support interaction (Wang et al., 2019).

$$CH_4 \rightarrow C + 2H_2 \quad \Delta H^\circ = 74.9 kJ/mol \qquad \text{(Equation 11)}$$

Researchers have developed various catalysts to improve the lifetime during the biogas reforming process. Vita et al. (Vita et al., 2014) studied the tri-reforming of simulated biogas over Ni/CeO_2 catalysts, which showed stability during 150 h of reaction. The coexistence of different nickel phases (such as Ni^0 and NiO) and the characteristics of the CeO_2 support can play a role in the stability of the Ni/CeO_2 catalyst (Vita et al., 2014). Mortensen and Dybkjær (Mortensen and Dybkjær, 2015) studied the industrial-scale steam reforming of CO_2-rich gas. The nickel-based catalysts revealed insignificant carbon formation (500–1,000 ppm) after 2 years of operation under severe conditions. In general, large nickel particles

(e.g., >10 nm) are more prone to carbon formation. Noble metals are typically more resistant than Ni toward carbon formation. The reforming of CO_2-rich gas in an industrial setting would require co-feeding of steam to reduce carbon formation (Mortensen and Dybkjær, 2015). Slagtern et al. (Slagtern et al., 1997) studied the dry reforming of biogas over 0.15%Ni/1.7%Ln/Al_2O_3 catalysts. The initial coke formation was 0.13 wt% after 20 h of operation and then became 0.16 wt% after ~100 h. The Ni sintering was initially a major reason for deactivating the 0.15%Ni/1.7%Ln/Al_2O_3 catalyst, whereas coking became increasingly important with longer reaction time. The coking was initially high and then stabilized with a longer reaction time (Slagtern et al., 1997).

Wei et al. (Wei et al., 2000) studied the dry reforming of biogas over Ni/ZrO_2 catalysts, which exhibited a coke rate of 1.8×10^{-4} $g_{coke}/(g_{cat}*h)$ after 600 h. There might be a periodic cycle of carbon deposition and elimination on the nickel surface of the Ni/ZrO_2 catalyst (Wei et al., 2000). Huang et al. (Huang et al., 2011) studied the dry reforming of biogas over Ni-0.5Mo/SBA-15 catalysts. The CH_4 conversion remained at ~94%, and the coke rate was 7.3×10^{-4} $g_{coke}/(g_{cat}*h)$ after 600 h, indicating the superior stability of the Ni-0.5Mo/SBA-15 catalysts. The carbon deposition was a main reason for deactivating the catalyst during biogas dry reforming of biogas; the sintering of nickel particles was another reason. The main factors that prevented the carbon deposition of the Ni-0.5Mo/SBA-15 catalyst were strong basicity, strong metal–support interaction, small metal particles, and the formation of Mo_2C species. The changes in catalyst composition and reactivity of active phases can affect the structure and morphology of the deposited carbon (Huang et al., 2011). The lifetime of catalysts can be affected by the coexistence of different metal phases. The addition of appropriate noble metal can promote the catalyst stability. Understanding the coke formation mechanism during the biogas reforming is a challenge. Whether there is a periodic cycle of carbon deposition and elimination on the catalyst can be further studied and confirmed. Some new advanced technologies (e.g., *in situ* TEM) can be utilized to observe the catalysts in real time under real experimental conditions.

Coke can be removed through the flowing of O_2, air, steam, and other gases. Liu and Au (Liu and Au, 2003) found that the catalyst activity and carbon deposition depended on parameters such as surface composition, metal–support interaction, metal crystalline structure, support acidity, and support basicity. The used La_2NiO_4/Al_2O_3 catalysts in biogas dry reforming process almost restored the catalytic performance after regeneration at 600°C in air by burning off the carbon. The La_2NiO_4/Al_2O_3 catalyst exhibited decreasing coke formation with the catalyst calcination temperature increase from 500 to 800°C due to the formation of a stable $NiAl_2O_4$ spinel structure (Liu and Au, 2003). Quincoces et al. (Quincoces, 2004) studied the dry reforming of biogas over Ni/Al_2O_3 catalysts. The used Ni/Al_2O_3 catalysts were regenerated with O_2, followed by reduction with H_2. The CH_4 conversion over regenerated Ni/Al_2O_3 catalysts decreased by 28% than fresh Ni/Al_2O_3 catalysts (Quincoces, 2004).

In summary, the lifetime of reforming catalysts can vary between 150 h and 2 years. A periodic cycle of carbon deposition and elimination may take place on the catalysts. The lifetime of catalysts is affected by the catalyst synthesis method such as calcination and activation procedure, pore structure of catalysts, support characteristics of catalysts, and reaction conditions during biogas reforming process. A high metal-support interaction, more oxygen species, strong basicity, small metal particles, and the utilization of noble metals on catalysts can inhibit the carbon formation, thus increasing the lifetime of catalysts. In addition, complete removal of impurities in feedstock gases can prevent catalyst poisoning. One challenge for the catalyst regeneration is to keep the same catalytic activity as exhibited by the fresh catalyst. Flowing air or O_2 seems a promising method to effectively regenerate catalysts, but the temperature and oxygen concentration need to be optimized. The catalysts can be regenerated either outside the reactor or directly inside. However, the regeneration may cause catalyst destruction and agglomeration of metals, which will reduce catalyst lifetime. The regeneration of used catalysts can also increase the cost of the biogas reforming process. Catalysts with a long enough lifetime will be desired for industrial applications.

INDUSTRIAL APPLICATION

Syngas Application

Syngas derived from biogas reforming is a gas mixture that mainly consists of H_2 and CO. It may contain CO_2, CH_4, N_2, and other gases, depending on the biogas composition, reforming reaction performance, and posttreatment. Syngas can be utilized as raw material for the production of fuels (e.g., hydrogen, synthetic gasoline, dimethyl ether, ethanol, methanol) and other valuable chemicals (Hernandez and Martin,

2018; Lee et al., 2003b; Majewski and Wood, 2014). In addition, syngas can be applied in fuel cells and be directly used to produce energy and heat (Vita et al., 2014). Syngas used directly for heat and power can typically be processed in boilers or turbines. Syngas can be effectively used as an end product based on its specific H_2 to CO ratio. When the produced syngas contains an H_2 to CO molar ratio in the range of 1.5–2, it can be used to synthesize methanol, dimethyl ether, or diesel fuel (Majewski and Wood, 2014). One challenge for syngas application involves the question of how to efficiently convert the syngas to final products because the H_2 to CO molar ratio in various syngas sources varies. To utilize syngas for liquid fuel through FTS over Co-based catalysts, the suitable H_2 to CO molar ratio should be near 2.0. The H_2 to CO ratio in syngas can be tuned by the addition of H_2 or removal of some CO. Another challenge for syngas application is the presence of impurities in syngas. These impurities can lead to side reactions in the syngas application process. The impurities have to be removed to maintain the catalyst activity and protect the reaction units.

Researchers have recently developed methods to remove impurities from syngas. Spies et al. (Spies et al., 2017) used a warm (e.g., 250–450°C) cleanup technique to purify the coal-derived syngas for downstream conversions such as methanol synthesis. The coal-derived syngas mainly contained H_2, CO, CO_2, N_2, CH_4, and C_2H_4. A multicontaminant removal method using different materials including ZnO, Na_2CO_3, CuNi, Ir-Ni/$MgAl_2O_4$, and CuZnAl was employed. More than 99% of sulfur in the syngas can be removed using this method. The ZnO sorbents were proven desulfurization materials with fast kinetics and substantial capacity (Spies et al., 2017). Hernandez and Martin (Hernandez and Martin, 2018) purified the syngas (mainly containing H_2, CO, CO_2, N_2, H_2O, and hydrocarbons) derived from biogas tri-reforming by using a flash separator to remove water first. The traces of hydrocarbons and N_2 were removed using a pressure swing adsorption (PSA) system. Second, the H_2 to CO ratio was adjusted through a H_2 tuned-up section consisting of a PSA membrane unit for H_2 recovery, a bypass, and a WGS reactor. Last, CO_2 was removed using zeolite 5A or 13X (Hernandez and Martin, 2018). The effective removal of impurities from syngas can prevent damage to reactors and decreased catalyst activity. The better ways to effectively remove impurities from syngas with low-processing costs needs more study. The efficient separation of H_2 from CO in syngas would be an interesting topic to study in the future.

Techno-economics of Biogas Conversion

In some parts of the United States, biogas is flared due to infrastructure challenges, wasting valuable resources that could be converted to energy and/or chemicals. Techno-economics analyses (Tables 9 and S4) summarize the economic feasibility of biogas utilization and application via using different software such as Aspen Plus and Aspen HYSYS v9.0. The analysis can be performed in both small-scale and large-scale systems. A major challenge for biogas application is the low conversion efficiency. The biogas conversion efficiency here is determined based on energy recovery unless specified.

Biogas can be simply used to generate electricity. However, the low conversion efficiency of biogas to electricity is an issue for biogas utilization. For example, White et al. (White et al., 2011) analyzed small-scale biogas conversion systems located on multiple farms in ON, Canada. The study found that beef farms with $\geq$78 animals and dairy farms with $\geq$33 animals can operate economically attractive biogas systems (White et al., 2011). Pipatmanomai et al. (Pipatmanomai et al., 2009) conducted an economic assessment of biogas conversion to electricity in small pig farms (170 breeder swines and 255 piglets) in Thailand at 45% of government subsidy. The payback period of this system without H_2S removal was approximately 4 years. With H_2S removal, the payback period was approximately 8 years. The electricity price and government subsidy have a major effect on the payback period. The H_2S removal can add high operational costs to the proposed system, but it is strongly recommended to reduce the emission of pollution gas and prevent reactor engine corrosion (Pipatmanomai et al., 2009). To improve conversion efficiency, biogas can be utilized to generate other products instead of electricity.

Hydrogen has a high calorific value and can be used as a fuel. The use of hydrogen for energy offers the advantages of zero carbon and greenhouse gas emissions. However, hydrogen is highly combustible and explosive. Lachén et al. (Lachén et al., 2018) carried out a techno-economic assessment of biogas conversion to hydrogen. Raw materials were water, electricity, biogas, catalyst, iron oxide, cobalt ferrite, and membrane. The pure hydrogen yield reached 68% at 575°C. The production cost was assumed to be in the range of $4.49–16.85/kg (i.e. €4–15/kg), based on the operating temperature (475–575°C) and the grade of integration (IG, IG = 0, 0.25, 0.5, and 1) (Lachén et al., 2018). Madeira et al. (Madeira et al., 2017) conducted

Product	Product Price	Conversion Process	Conversion Efficiency (%)	Payback Period (year)	Other	Ref.
Electricity	–	Use an engine	~35	<10	Small scale cattle farms	(White et al., 2011)
Electricity	0.067 $/kWh	Engine with electric generator	20.8	~4–8	Small pig farm	(Pipatmanomai et al., 2009)
H_2	~9.99 $/kg	Biogas dry reforming and steam-iron process	>45	–	Plant model (1,350 kg/h biogas)	(Lachén et al., 2018)
H_2	–	Steam reforming, shift reaction, and PSA	79	7	Large-scale wastewater plant (generating ~4019 m^3/day biogas)	(Madeira et al., 2017)
H_2	–	Biogas autothermal reforming	65	–	BioRobur plant (generating 100 Nm^3/h H_2)	(Montenegro Camacho et al., 2017)
Methanol	0.9 $/gallon	Biogas cleaning/ reforming and methanol synthesis	–	–	Plant model (12,080,000 m^3/year biogas)	(Hernández and Martín, 2016)
Methanol	~400 $/ metric ton	Biogas cleaning/ reforming and methanol synthesis	–	Not economically feasible	Large-scale plant (generating 5,900 Nm^3/h biogas)	(Sheets and Shah, 2018)
Liquid fuel	~0.79 $/ kg (diesel)	Tri-reforming and FTS	54 (carbon conversion efficiency)	Not economically feasible	Plant model (27.22 kg/s CO_2 rich natural gas)	(Graciano et al., 2018)
Liquid fuel	–	Tri-reforming and FTS	45	–	Commercial scale plant (2,500 scfm LFG)	(Zhao et al., 2019a)
Liquid fuel	–	Biogas cleaning/ reforming, FTS, hydrocracking, and distillation	54 (mass basis)	–	Plant model (2,000 Nm^3/h biogas)	(Okeke and Mani, 2017)
Compressed natural gas	–	Gas pressurizing and impurity removal	–	–	Medium-sized landfill model	(Winslow et al., 2019)
Wax	~2.77 $/kg	Biogas steam reforming, FTS, and product separation	56	~7	Small-scale plant model (~200 kg/h biogas)	(Herz et al., 2017)

Table 9. Techno-economics Analysis of Biogas Conversion
See also Table S4.

an exergetic and economic evaluation of cassava wastewater biogas conversion to hydrogen. The biogas and hydrogen production cost was estimated as $0.0518/kWh and $0.13/kWh, respectively (Madeira et al., 2017). Braga et al. (Braga et al., 2013) conducted a techno-economic analysis of biogas conversion to hydrogen for fuel cell application. The analysis was based on the biogas generated by a bovine manure biodigester located in São Paulo, Brazil. The biogas conversion process mainly consisted of steam reforming, dry reforming, and shift reaction. Biogas reforming efficiency was 80%. The hydrogen production cost was estimated as $0.27/kWh with a payback period of 8 years (Braga et al., 2013). Montenegro Camacho et al. (Montenegro Camacho et al., 2017) conducted a techno-economic analysis of hydrogen production from the autothermal reforming of biogas. The cost of generating 100 Nm^3/h of hydrogen was $2.78/kg (i.e., €2.5/kg) after 10 years of amortization. The longer the BioRobur plant life is, the more feasible the initial investment is. In addition, the raw material (e.g., municipal solid waste, agroindustry scraps) for the biogas production has a major effect on the hydrogen cost (Montenegro Camacho et al., 2017).

The conversion efficiency of biogas to hydrogen is relatively high, which can reach 80%. This conversion technology can be economically advantageous within ~8 years.

Methanol is the simplest alcohol and is widely used for industrial purposes. Biogas can be converted into methanol for chemical applications. Hernández and Martín (Hernández and Martín, 2016) optimized the operational process of biogas conversion to methanol using a mathematical approach. Part of the biogas was utilized to provide the energy needed for this process. The production cost of converting biogas into methanol was estimated as $1.75/gallon (Hernández and Martín, 2016). Sheets and Shah (Sheets and Shah, 2018) conducted a techno-economic analysis of the biogas conversion to methanol from a large-scale landfill or anaerobic digestion facility. The plant mainly consisted of biogas cleaning via pressurized water scrubbing, biogas reforming, syngas to methanol conversion, methanol purification, and energy recovery from unconverted gas. The methanol production cost was $2.11/kg, and it became $1.99/kg with credits for low-pressure steam (Sheets and Shah, 2018).

Liquid fuel is a value-added product that can be used to replace petroleum fuel to reduce the environmental pollution. Researchers have developed some pathways to convert biogas to liquid fuel. Graciano et al. (Graciano et al., 2018) conducted a model-based analysis of converting biogas (CO_2-rich natural gas: mainly containing ~48 mol % CH_4 and 30 mol % CO_2) to liquid transportation fuels via tri-reforming and FTS at a tax rate of 32%/year. The plant-wide electricity consumption can be nearly fully covered by a Rankine cycle unit. However, the economic viability of the process is highly dependent on the biogas price (Graciano et al., 2018). Okeke and Mani (Okeke and Mani, 2017) carried out a techno-economic assessment of biogas-to-liquid-fuels conversion technology. The unconverted methane, syngas, and syncrude were utilized to generate electricity to meet internal plant demand while the excess power was sold to the grid. The liquid fuel price was $5.67/gal ($5.29/gasoline gallon equivalent) when the plant feed capacity was 2,000 Nm^3/h. However, when the plant feed capacity increased to 20,000 Nm^3/h, the liquid fuel price reduced to $2.06/gal ($1.92/gasoline gallon equivalent) (Okeke and Mani, 2017). In our previous research (Zhao et al., 2019a), a novel technology of combining tri-reforming and FTS (TriFTS) was created to convert landfill gas to liquid fuel. A preliminary economic analysis of a commercial-scale TriFTS process was conducted based on the bench-scale experimental results with a tax rate of 20%. The simulation results indicated that 45% of the energy contained in the feed LFG can be recovered in the liquid fuel produced, with the rest meeting the energy demand of the TriFTS conversion process. The break-even cost of the diesel fuel produced was estimated as $2.71/gallon if the LFG is assumed to be free of cost (Zhao et al., 2019a). Compared with generating electricity, the conversion efficiency of biogas into liquid fuel is much higher. The economic viability of the biogas conversion to liquid fuel is highly dependent on the feedstock price and current market fuel price.

Biogas can also be converted to other products (e.g., compressed natural gas [CNG] and wax). CNG is simply natural gas, mainly comprising methane, that is stored under high pressure for use as vehicle fuel. Wax is typically used for coating and candles. Winslow et al. (Winslow et al., 2019) conducted an economic assessment on LFG to vehicle fuel conversion for a waste hauling operation with 10 tractor-trailers (each tractor-trailer hauled ~19 Mg of MSW per trip to generate 1,900 m^3 CH_4). The CNG was produced from LFG at the landfill for vehicle use. The LFG refining process consisted of pressurizing the gas and removing impurities (e.g., siloxane, CO_2, and hydrogen sulfide). The net present value per diesel gallon equivalent (DGE) of operating this scenario over a 30-year period was determined to be $2.31 at a renewable identification number (RIN) value of $0/DGE (Winslow et al., 2019). Herz et al. (Herz et al., 2017) evaluated the biogas conversion to waxes (i.e., long-chained hydrocarbons that are solid at ambient conditions) through steam reforming and FTS. The process is profitable without governmental support, compared with the established combined heat and power technology (Herz et al., 2017).

Generally, biogas can be converted to heat, hydrogen, methanol, liquid fuel, CNG, and wax. The overall efficiency of biogas conversion is approximately 35%–80%, based on the product type. Biogas conversion can be economically feasible with a typical payback period of ~4–8 years. However, the plant feed capacity, raw material price, government subsidy, and market price of final product have an effect on the economic viability. Recently, T2C-Energy LLC (Tampa, Florida) successfully tested the pilot scale of converting LFG to liquid fuels using a technology of combining tri-reforming and FTS. However, commercial operations are still progressing. Fulcrum BioEnergy Inc. (Pleasanton, California) and Velocys (Plain City, Ohio) have also developed technologies that can cost-effectively produce low-carbon liquid fuels from municipal solid waste. In general, most biogas is used for electricity production or CNG, but no commercial operations exist yet for the production of liquid fuels or chemicals. A major challenge for the biogas reforming industry is to further reduce costs.

CONCLUSIONS

Summary

Biogas reforming technologies have gained greater attention in recent years. However, no systematic study has been performed to optimize the syngas synthesis from biogas. This paper systematically reviewed the state of the art of biogas reforming, reaction mechanism, catalyst synthesis/characterization/regeneration, and syngas application. Biogas, especially from wastes, has great potential for conversion to syngas for diesel fuel use as improved climate factors. Compared with traditional fossil fuel, the fuel produced from biogas can reduce the cost of waste management and provide environmentally friendly transportation fuel.

Biogas reforming is affected by several factors including temperature, pressure, feed gas composition, space velocity, and catalyst activity. High reaction temperature (e.g., >800°C) is favored to obtain high CH_4 and CO_2 conversions due to the endothermic nature, but high pressure can suppress reactions to decrease CH_4 and CO_2 conversions. A relatively lower GHSV (e.g., <60,000 h^{-1}) can lead to higher reactant conversions due to higher residence time of reactants on the catalyst surface. Nickel-based catalysts are usually used for the reforming of biogas, and Ni nanoparticles on the CeO_2-ZrO_2 support seem a promising catalyst. Concerned about reducing energy input and coke formation, novel technologies such as plasma and solar have been developed for low-temperature biogas reforming use. However, the reactant conversions are not high yet and need to be improved further.

Compared with other reforming methods (e.g., dry and bi-reforming), tri-reforming of biogas seems to be an advanced technology toward high conversions of reactants. However, the CO_2 conversion needs to be improved during the tri-reforming process. In the future, advanced and economic catalysts with higher activity need to be developed to improve reactant conversions. In addition, the kinetics of catalyst activity could be investigated. The reforming conditions for reactants with different compositions could be further optimized. Unreacted reactants such as water could be recycled to improve the production economics. Finally, more economic evaluation and scale-up of biogas reforming (especially tri-reforming) should be investigated.

Challenges and Future Directions

The major technical challenge is that converting biogas to syngas needs to be cost-competitive. Energy consumption at high temperatures is one of the most costly aspects, and the cost of catalysts plays a significant role. The catalysts can be deactivated after a certain period. Understanding how to regenerate the used catalysts or develop catalysts with long lifetimes becomes important.

Future directions include:

(1) Systematic experimental process development is needed to optimize the syngas synthesis from biogas. The molar ratio of the produced H_2 to CO and reactant conversions during biogas reforming can be affected by biogas composition, reaction temperature, reaction pressure, space velocity, time-on-stream, and catalyst property. There is a need to better control the molar ratio of the produced H_2 to CO, which is critical for the following fuel or methanol or other chemical synthesis. The process conditions need to be optimized for maximizing the reactant conversions and the overall energy efficiency.

(2) Research interest in direct conversion of methane to chemicals and fuels is growing as a method to improve productivity and energy efficiency (Holmen, 2009; Karakaya and Kee, 2016; Schwach et al., 2017; Wang et al., 2017). Large reserves of methane indicate that a market exists for the large-scale conversion of methane on-site. Direct conversion of methane to liquid fuels without going through an intermediate syngas generation step can be potentially more environmentally friendly and cost-effective. In addition, one-step reforming of CH_4 and CO_2 into chemicals and fuels is a promising route. Catalysts with a high selectivity toward desired products should be designed and developed.

(3) Process integration/intensification can help optimize the fuel produced from biogas, such as combining reforming and Fischer-Tropsch synthesis. Combining different systems together may help to improve the reactant conversions, recover the byproduct, and enhance the energy efficiency. An effective hybrid system may reduce the whole processing cost.

SUPPLEMENTAL INFORMATION

Supplemental Information can be found online at https://doi.org/10.1016/j.isci.2020.101082.

ACKNOWLEDGMENTS

This article is based upon work supported by the U.S. Department of Energy (DOE) under award DE-SC0015221. The authors BJ and JK would also acknowledge funding from DOE through award DE-EE0008488. This paper has been authored in part by UT-Battelle, LLC, under contract DE-AC05-00OR22725 with the US DOE. The US government retains and the publisher, by accepting the article for publication, acknowledges that the US government retains a nonexclusive, paid-up, irrevocable, worldwide license to publish or reproduce the published form of this manuscript, or allow others to do so, for US government purposes. DOE will provide public access to these results of federally sponsored research in accordance with the DOE Public Access Plan (http://energy.gov/downloads/doe-public-access-plan).

AUTHOR CONTRIBUTIONS

Conceptualization: X.Z., B.J., and J.K. Writing of Original Draft: X.Z. Revision: X.Z., B.J., J.K., and S.O. Supervision: B.J., J.K., and S.O. Funding Acquisition: B.J. and J.K.

DECLARATION OF INTERESTS

Dr. Babu Joseph and Dr. John Kuhn disclose an interest in T2C-Energy, LLC. Dr. Xianhui Zhao, Dr. Babu Joseph, and Dr. John Kuhn disclose an interest in patents on related subjects issued to University of South Florida.

REFERENCES

Abdullah, A.H., Mat, R., Somderam, S., Abd Aziz, A.S., and Mohamed, A. (2018). Hydrogen sulfide adsorption by zinc oxide-impregnated zeolite (synthesized from Malaysian kaolin) for biogas desulfurization. J. Ind. Eng. Chem. *65*, 334–342.

Alipour-Dehkordi, A., and Khademi, M.H. (2019). Use of a micro-porous membrane multi-tubular fixed-bed reactor for tri-reforming of methane to syngas: CO_2, H_2O or O_2 side-feeding. Int. J. Hydrogen Energy *44*, 32066–32079.

Alsaffar, M.A., Ayodele, B.V., and Mustapa, S.I. (2020). Scavenging carbon deposition on alumina supported cobalt catalyst during renewable hydrogen-rich syngas production by methane dry reforming using artificial intelligence modeling technique. J. Clean. Prod. *247*, 119168.

Anchieta, C.G., Assaf, E.M., and Assaf, J.M. (2019). Effect of ionic liquid in Ni/ZrO_2 catalysts applied to syngas production by methane tri-reforming. Int. J. Hydrogen Energy *44*, 9316–9327.

Angeli, S.D., Turchetti, L., Monteleone, G., and Lemonidou, A.A. (2016). Catalyst development for steam reforming of methane and model biogas at low temperature. Appl. Catal. B Environ. *181*, 34–46.

Arab Aboosadi, Z., Jahanmiri, A.H., and Rahimpour, M.R. (2011). Optimization of tri-reformer reactor to produce synthesis gas for methanol production using differential evolution (DE) method. Appl. Energy *88*, 2691–2701.

Arbag, H., Yasyerli, S., Yasyerli, N., Dogu, G., Dogu, T., Osojnik Črnivec, I.G., and Pintar, A. (2015). Coke minimization during conversion of biogas to syngas by bimetallic tungsten–nickel incorporated mesoporous alumina synthesized by the one-pot route. Ind. Eng. Chem. Res. *54*, 2290–2301.

Assabumrungrat, S., Charoenseri, S., Laosiripojana, N., Kiatkittipong, W., and Praserthdam, P. (2009). Effect of oxygen addition on catalytic performance of $Ni/SiO_2{\cdot}MgO$ toward carbon dioxide reforming of methane under periodic operation. Int. J. Hydrogen Energy *34*, 6211–6220.

Ayodele, B.V., and Cheng, C.K. (2015). Process modelling, thermodynamic analysis and optimization of dry reforming, partial oxidation and auto-thermal methane reforming for hydrogen and syngas production. Chem. Prod.Process Model. *10*, 211–220.

Bi, S., Qiao, W., Xiong, L., Ricci, M., Adani, F., and Dong, R. (2019). Effects of organic loading rate on anaerobic digestion of chicken manure under mesophilic and thermophilic conditions. Renew. Energy *139*, 242–250.

Bian, Z., Suryawinata, I.Y., and Kawi, S. (2016). Highly carbon resistant multicore-shell catalyst derived from Ni-Mg phyllosilicate nanotubes@silica for dry reforming of methane. Appl. Catal. B Environ. *195*, 1–8.

Bierer, B., Kress, P., Nägele, H.J., Lemmer, A., and Palzer, S. (2019). Investigating flexible feeding effects on the biogas quality in full-scale anaerobic digestion by high resolution, photoacoustic-based NDIR sensing. Eng. Life Sci. *19*, 700–710.

Bobadilla, L.F., Garcilaso, V., Centeno, M.A., and Odriozola, J.A. (2017). Monitoring the reaction mechanism in model biogas reforming by in situ transient and steady-state DRIFTS measurements. ChemSusChem *10*, 1193–1201.

Braga, L.B., Silveira, J.L., da Silva, M.E., Tuna, C.E., Machin, E.B., and Pedroso, D.T. (2013). Hydrogen production by biogas steam reforming: a technical, economic and ecological analysis. Renew. Sustain. Energy Rev. *28*, 166–173.

Broun, R., and Sattler, M. (2016). A comparison of greenhouse gas emissions and potential

electricity recovery from conventional and bioreactor landfills. J. Clean. Prod. *112*, 2664–2673.

Bu, K., Deng, J., Zhang, X., Kuboon, S., Yan, T., Li, H., Shi, L., and Zhang, D. (2020). Promotional effects of B-terminated defective edges of Ni/boron nitride catalysts for coking- and sintering-resistant dry reforming of methane. Appl. Catal. B Environ. *267*, 118692.

Cao, P., Adegbite, S., Zhao, H., Lester, E., and Wu, T. (2018). Tuning dry reforming of methane for F-T syntheses: a thermodynamic approach. Appl. Energy *227*, 190–197.

Charisiou, N.D., Douvartzides, S.L., Siakavelas, G.I., Tzounis, L., Sebastian, V., Stolojan, V., Hinder, S.J., Baker, M.A., Polychronopoulou, K., and Goula, M.A. (2019). The relationship between reaction temperature and carbon deposition on nickel catalysts based on Al_2O_3, ZrO_2 or SiO_2 supports during the biogas dry reforming reaction. Catalysts *9*, 676.

Chein, R.-Y., and Hsu, W.-H. (2018). Analysis of syngas production from biogas via the tri-reforming process. Energies *11*, 1075.

Chen, X., Jiang, J., Li, K., Tian, S., and Yan, F. (2017). Energy-efficient biogas reforming process to produce syngas: the enhanced methane conversion by O_2. Appl. Energy *185*, 687–697.

Chen, C., Wang, X., Chen, X., Liang, X., Zou, X., and Lu, X. (2019). Combined steam and CO_2 reforming of methane over one-pot prepared Ni/La-Si catalysts. Int. J. Hydrogen Energy *44*, 4780–4793.

Chen, S., Zaffran, J., and Yang, B. (2020). Descriptor design in the computational screening of Ni-based catalysts with balanced activity and stability for dry reforming of methane reaction. ACS Catal. *10*, 3074–3083.

Cui, Y., Zhang, H., Xu, H., and Li, W. (2007). Kinetic study of the catalytic reforming of CH_4 with CO_2 to syngas over Ni/α-Al_2O_3 catalyst: the effect of temperature on the reforming mechanism. Appl. Catal. A Gen. *318*, 79–88.

Damanabi, A.T., Servatan, M., Mazinani, S., Olabi, A.G., and Zhang, Z. (2019). Potential of tri-reforming process and membrane technology for improving ammonia production and CO_2 reduction. Sci. Total Environ. *664*, 567–575.

Das, S., Ashok, J., Bian, Z., Dewangan, N., Wai, M.H., Du, Y., Borgna, A., Hidajat, K., and Kawi, S. (2018). Silica–Ceria sandwiched Ni core–shell catalyst for low temperature dry reforming of biogas: coke resistance and mechanistic insights. Appl. Catal. B Environ. *230*, 220–236.

Das, S., Shah, M., Gupta, R.K., and Bordoloi, A. (2019). Enhanced dry methane reforming over Ru decorated mesoporous silica and its kinetic study. J. CO2 Util. *29*, 240–253.

de la Cruz-Flores, V.G., Martinez-Hernandez, A., and Gracia-Pinilla, M.A. (2020). Deactivation of Ni-SiO_2 catalysts that are synthetized via a modified direct synthesis method during the dry reforming of methane. Appl. Catal. A Gen. *594*, 117455.

Dębek, R., Galvez, M.E., Launay, F., Motak, M., Grzybek, T., and Da Costa, P. (2016). Low temperature dry methane reforming over Ce, Zr and CeZr promoted Ni–Mg–Al hydrotalcite-derived catalysts. Int. J. Hydrogen Energy *41*, 11616–11623.

del Valle-Zermeño, R., Romero-Güiza, M.S., Chimenos, J.M., Formosa, J., Mata-Alvarez, J., and Astals, S. (2015). Biogas upgrading using MSWI bottom ash: an integrated municipal solid waste management. Renew. Energy *80*, 184–189.

Díez-Ramírez, J., Dorado, F., Martínez-Valiente, A., García-Vargas, J.M., and Sánchez, P. (2016). Kinetic, energetic and exergetic approach to the methane tri-reforming process. Int. J. Hydrogen Energy *41*, 19339–19348.

Ding, R., and Yan, Z. (2002). Adsorption properties studies of the nickel catalysts for carbon dioxide reforming of methane. Fuel Chem. Div. Preprints *47*, 103–105.

El Hassan, N., Kaydouh, M.N., Geagea, H., El Zein, H., Jabbour, K., Casale, S., El Zakhem, H., and Massiani, P. (2016). Low temperature dry reforming of methane on rhodium and cobalt based catalysts: active phase stabilization by confinement in mesoporous SBA-15. Appl. Catal. A Gen. *520*, 114–121.

Elsayed, N.H., Roberts, N.R.M., Joseph, B., and Kuhn, J.N. (2016). Comparison of Pd–Ni–Mg/ceria–zirconia and Pt–Ni–Mg/ceria–zirconia catalysts for syngas production via low temperature reforming of model biogas. Top. Catal. *59*, 138–146.

Elsayed, N.H., Elwell, A., Joseph, B., and Kuhn, J.N. (2017). Effect of silicon poisoning on catalytic dry reforming of simulated biogas. Appl. Catal. A Gen. *538*, 157–164.

Elsayed, N.H., Maiti, D., Joseph, B., and Kuhn, J.N. (2018). Precious metal doped Ni–Mg/ceria–zirconia catalysts for methane conversion to syngas by low temperature bi-reforming. Catal. Lett. *148*, 1003–1013.

EPA (2014). EPA issues final rule for renewable fuel standard (RFS) pathways II and modifications to the RFS program, ultra low sulfur diesel requirements, and E15 misfueling mitigation requirements, U.S.E.P. Agency, ed.. https://nepis.epa.gov/Exe/ZyPDF.cgi?Dockey=P100JPPP.pdf.

Evans, S.E., Staniforth, J.Z., Darton, R.J., and Ormerod, R.M. (2014). A nickel doped perovskite catalyst for reforming methane rich biogas with minimal carbon deposition. Green Chem. *16*, 4587–4594.

Fan, M.-S., Abdullah, A.Z., and Bhatia, S. (2011). Hydrogen production from carbon dioxide reforming of methane over Ni–Co/MgO–ZrO_2 catalyst: process optimization. Int. J. Hydrogen Energy *36*, 4875–4886.

Fei, X., Zekkos, D., and Raskin, L. (2016). Quantification of parameters influencing methane generation due to biodegradation of municipal solid waste in landfills and laboratory experiments. Waste Manag. *55*, 276–287.

Fekri Lari, M., Farsi, M., and Rahimpour, M.R. (2019). Modification of a tri-reforming reactor based on the feeding policy to couple with methanol and GTL units. Chem. Eng. Res. Des. *144*, 107–114.

Gangadharan, P., Kanchi, K.C., and Lou, H.H. (2012). Evaluation of the economic and environmental impact of combining dry reforming with steam reforming of methane. Chem. Eng. Res. Des. *90*, 1956–1968.

Gao, Y., Jiang, J., Meng, Y., Aihemaiti, A., Ju, T., Chen, X., and Yan, F. (2020). A novel nickel catalyst supported on activated coal fly ash for syngas production via biogas dry reforming. Renew. Energy *149*, 786–793.

García-Vargas, J.M., Valverde, J.L., Dorado, F., and Sánchez, P. (2014). Influence of the support on the catalytic behaviour of Ni catalysts for the dry reforming reaction and the tri-reforming process. J. Mol. Catal. A Chem. *395*, 108–116.

García-Vargas, J.M., Valverde, J.L., Díez, J., Dorado, F., and Sánchez, P. (2015). Catalytic and kinetic analysis of the methane tri-reforming over a Ni–Mg/β-SiC catalyst. Int. J. Hydrogen Energy *40*, 8677–8687.

Graciano, J.E.A., Chachuat, B., and Alves, R.M.B. (2018). Conversion of CO_2-rich natural gas to liquid transportation fuels via trireforming and Fischer–Tropsch synthesis: model-based assessment. Ind. Eng. Chem. Res. *57*, 9964–9976.

Han, D., Kim, Y., Cho, W., and Baek, Y. (2020). Effect of oxidants on syngas synthesis from biogas over 3 wt % Ni-Ce-MgO-ZrO_2/Al_2O_3 catalyst. Energies *13*, 297.

He, G., Liang, W., Tsai, C.L., Xia, X., Baumann, S., Jiang, H., and Meulenberg, W.A. (2019). Chemical environment-induced mixed conductivity of titanate as a highly stable oxygen transport membrane. iScience *19*, 955–964.

Hernandez, B., and Martin, M. (2018). Optimization for biogas to chemicals via tri-reforming. Analysis of Fischer-Tropsch fuels from biogas. Energy Convers. Manag. *174*, 998–1013.

Hernández, B., and Martín, M. (2016). Optimal process operation for biogas reforming to methanol: effects of dry reforming and biogas composition. Ind. Eng. Chem. Res. *55*, 6677–6685.

Herz, G., Reichelt, E., and Jahn, M. (2017). Design and evaluation of a Fischer-Tropsch process for the production of waxes from biogas. Energy *132*, 370–381.

Holmen, A. (2009). Direct conversion of methane to fuels and chemicals. Catal. Today *142*, 2–8.

Hossain, M.A., Ayodele, B.V., Cheng, C.K., and Khan, M.R. (2019). Optimization of renewable hydrogen-rich syngas production from catalytic reforming of greenhouse gases (CH_4 and CO_2) over calcium iron oxide supported nickel catalyst. J. Energy Inst. *92*, 177–194.

Huang, T., Huang, W., Huang, J., and Ji, P. (2011). Methane reforming reaction with carbon dioxide over SBA-15 supported Ni–Mo bimetallic catalysts. Fuel Process. Technol. *92*, 1868–1875.

Izquierdo, U., Barrio, V.L., Requies, J., Cambra, J.F., Güemez, M.B., and Arias, P.L. (2013). Tri-reforming: a new biogas process for synthesis gas and hydrogen production. Int. J. Hydrogen Energy *38*, 7623–7631.

Izquierdo, U., Barrio, V.L., Bizkarra, K., Gutierrez, A.M., Arraibi, J.R., Gartzia, L., Bañuelos, J., Lopez-Arbeloa, I., and Cambra, J.F. (2014). Ni and RhNi catalysts supported on Zeolites L for hydrogen and syngas production by biogas reforming processes. Chem. Eng. J. *238*, 178–188.

Izquierdo, U., García-García, I., Gutierrez, Á., Arraibi, J., Barrio, V., Cambra, J., and Arias, P. (2018). Catalyst deactivation and regeneration processes in biogas tri-reforming process. The effect of hydrogen sulfide addition. Catalysts *8*, 12.

Jabbour, K., Saad, A., Inaty, L., Davidson, A., Massiani, P., and El Hassan, N. (2019). Ordered mesoporous Fe-Al_2O_3 based-catalysts synthesized via a direct "one-pot" method for the dry reforming of a model biogas mixture. Int. J. Hydrogen Energy *44*, 14889–14907.

Jang, W.-J., Jeong, D.-W., Shim, J.-O., Kim, H.-M., Roh, H.-S., Son, I.H., and Lee, S.J. (2016). Combined steam and carbon dioxide reforming of methane and side reactions: thermodynamic equilibrium analysis and experimental application. Appl. Energy *173*, 80–91.

Jiang, H., Li, H., Xu, H., and Zhang, Y. (2007). Preparation of Ni/$Mg_xTi_{1-x}O$ catalysts and investigation on their stability in tri-reforming of methane. Fuel Process. Technol. *88*, 988–995.

Karakaya, C., and Kee, R.J. (2016). Progress in the direct catalytic conversion of methane to fuels and chemicals. Prog. Energy Combust. Sci. *55*, 60–97.

Khoja, A.H., Tahir, M., and Amin, N.A.S. (2017). Dry reforming of methane using different dielectric materials and DBD plasma reactor configurations. Energy Convers. Manag. *144*, 262–274.

Khoja, A.H., Tahir, M., and Amin, N.A.S. (2018). Cold plasma dielectric barrier discharge reactor for dry reforming of methane over Ni/ɣ-Al_2O_3-MgO nanocomposite. Fuel Process. Technol. *178*, 166–179.

Kim, A.R., Lee, H.Y., Lee, D.H., Kim, B.-W., Chung, C.-H., Moon, D.J., Jang, E.J., Pang, C., and Bae, J.W. (2015). Combined steam and CO_2 reforming of CH_4 on $LaSrNiO_x$ mixed oxides supported on Al_2O_3-modified SiC support. Energy Fuel *29*, 1055–1065.

Kim, G.S., Lee, B.Y., Ham, H.C., Han, J., Nam, S.W., Moon, J., and Yoon, S.P. (2019a). Highly active and stable $Sr_{0.92}Y_{0.08}Ti_{1-x}Ru_xO_{3-d}$ in dry reforming for hydrogen production. Int. J. Hydrogen Energy *44*, 202–212.

Kim, S., Crandall, B.S., Lance, M.J., Cordonnier, N., Lauterbach, J., and Sasmaz, E. (2019b). Activity and stability of NiCe@SiO_2 multi–yolk–shell nanotube catalyst for tri-reforming of methane. Appl. Catal. B Environ. *259*, 118037.

Kozonoe, C.E., de Paiva Floro Bonfim, R., Brito Alves, R.M., and Schmal, M. (2019). The Fe-Co-Cu supported on MWCNT as catalyst for the tri-reforming of methane – investigating the structure changes of the catalysts. Fuel *256*, 115917.

Kumar, N., Shojaee, M., and Spivey, J. (2015). Catalytic bi-reforming of methane: from greenhouse gases to syngas. Curr. Opin. Chem. Eng. *9*, 8–15.

Kumar, R., Kumar, K., Choudary, N.V., and Pant, K.K. (2019). Effect of support materials on the performance of Ni-based catalysts in tri-reforming of methane. Fuel Process. Technol. *186*, 40–52.

Kumar, R., Kumar, K., Pant, K.K., and Choudary, N.V. (2020). Tuning the metal-support interaction of methane tri-reforming catalysts for industrial flue gas utilization. Int. J. Hydrogen Energy *45*, 1911–1929.

Lachén, J., Durán, P., Menéndez, M., Peña, J.A., and Herguido, J. (2018). Biogas to high purity hydrogen by methane dry reforming in TZFBR+MB and exhaustion by Steam-Iron Process. Techno–economic assessment. Int. J. Hydrogen Energy *43*, 11663–11675.

Lee, J.-H., Joo, O.-S., Baek, Y.-S., Yu, Y.H., and Jung, K.-D. (2003a). Accumulation of the carbonaceous species on the Ni/Al_2O_3 catalyst during CO_2 reforming of methane. Bull. Korean Chem. Soc. *24*, 1623–1626.

Lee, S.-H., Cho, W., Ju, W.-S., Cho, B.-H., Lee, Y.-C., and Baek, Y.-S. (2003b). Tri-reforming of CH_4 using CO_2 for production of synthesis gas to dimethyl ether. Catal. Today *87*, 133–137.

Li, M., and van Veen, A.C. (2018). Coupled reforming of methane to syngas ($2H_2$-CO) over Mg-Al oxide supported Ni catalyst. Appl. Catal. A Gen. *550*, 176–183.

Li, W., Zhao, Z., Ding, F., Guo, X., and Wang, G. (2015a). Syngas production via steam–CO_2 dual reforming of methane over LA-Ni/ZrO_2 catalyst prepared by l-arginine ligand-assisted strategy: enhanced activity and stability. ACS Sustain. Chem. Eng. *3*, 3461–3476.

Li, W., Zhao, Z., Ren, P., and Wang, G. (2015b). Effect of molybdenum carbide concentration on the Ni/ZrO_2 catalysts for steam-CO_2 bi-reforming of methane. RSC Adv. *5*, 100865–100872.

Li, K., Pei, C., Li, X., Chen, S., Zhang, X., Liu, R., and Gong, J. (2020). Dry reforming of methane over $La_2O_2CO_3$-modified Ni/Al_2O_3 catalysts with moderate metal support interaction. Appl. Catal. B Environ. *264*, 118448.

Liang, T.-Y., Chen, H.-H., and Tsai, D.-H. (2020). Nickel hybrid nanoparticle decorating on alumina nanoparticle cluster for synergistic catalysis of methane dry reforming. Fuel Process. Technol. *201*, 106335.

Lin, R., Deng, C., Cheng, J., Xia, A., Lens, P.N.L., Jackson, S.A., Dobson, A.D.W., and Murphy, J.D. (2018). Graphene facilitates biomethane production from protein-derived glycine in anaerobic digestion. iScience *10*, 158–170.

Lino, A.V.P., Colmenares Calderon, Y.N., Mastelaro, V.R., Assaf, E.M., and Assaf, J.M. (2019). Syngas for Fischer-Tropsch synthesis by methane tri-reforming using nickel supported on $MgAl_2O_4$ promoted with Zr, Ce and Ce-Zr. Appl. Surf. Sci. *481*, 747–760.

Liu, B.S., and Au, C.T. (2003). Carbon deposition and catalyst stability over La_2NiO_4/γ-Al_2O_3 during CO_2 reforming of methane to syngas. Appl. Catal. A Gen. *244*, 181–195.

Liu, H., Wierzbicki, D., Debek, R., Motak, M., Grzybek, T., Da Costa, P., and Gálvez, M.E. (2016). La-promoted Ni-hydrotalcite-derived catalysts for dry reforming of methane at low temperatures. Fuel *182*, 8–16.

Maciel, L.J.L., de Souza, A.E.Á.M., Cavalcanti-Filho, V.O., Knoechelmann, A., and de Abreu, C.A.M. (2010). Kinetic evaluation of the tri-reforming process of methane for syngas production. React. Kinet. Mech. Cat. *101*, 407–416.

Madeira, J.G.F., Delgado, A.R.S., Boloy, R.A.M., Coutinho, E.R., and Loures, C.C.A. (2017). Exergetic and economic evaluation of incorporation of hydrogen production in a cassava wastewater plant. Appl. Therm. Eng. *123*, 1072–1078.

Majewski, A.J., and Wood, J. (2014). Tri-reforming of methane over Ni@SiO_2 catalyst. Int. J. Hydrogen Energy *39*, 12578–12585.

Mitchell, S., Michels, N.L., and Perez-Ramirez, J. (2013). From powder to technical body: the undervalued science of catalyst scale up. Chem. Soc. Rev. *42*, 6094–6112.

Mokashi, C.S., Schipper, D.L., Qasaimeh, M.A., and Lee, R.E.C. (2019). A system for analog control of cell culture dynamics to reveal capabilities of signaling networks. iScience *19*, 586–596.

Montenegro Camacho, Y.S., Bensaid, S., Piras, G., Antonini, M., and Fino, D. (2017). Techno-economic analysis of green hydrogen production from biogas autothermal reforming. Clean. Technol. Environ. *19*, 1437–1447.

Mortensen, P.M., and Dybkjær, I. (2015). Industrial scale experience on steam reforming of CO_2-rich gas. Appl. Catal. A Gen. *495*, 141–151.

Nandini, A., Pant, K.K., and Dhingra, S.C. (2005). K-, CeO_2-, and Mn-promoted Ni/Al_2O_3 catalysts for stable CO_2 reforming of methane. Appl. Catal. A Gen *290*, 166–174.

News. (2016). News,C.E. Dry reforming puts CO2 to work, *94*, p. 30. https://cen.acs.org/articles/94/i17/Dry-reforming-puts-CO2-work.html.

NREL (2013). Biogas potential in the United States, U.S.D.o. Energy, ed.. https://www.nrel.gov/docs/fy14osti/60178.pdf.

Oguri, T., Sugiura, K., Yabe, T., Ogo, S., and Sekine, Y. (2017). Combustion suppression in tri-reforming of methane over Ni supported catalysts at low temperatures in electric field. J. Jpn. Petrol Inst. *60*, 232–240.

Okeke, I.J., and Mani, S. (2017). Techno-economic assessment of biogas to liquid fuels conversion technology via Fischer-Tropsch synthesis. Biofuel Bioprod. Bior. *11*, 472–487.

Olah, G.A., Goeppert, A., Czaun, M., and Prakash, G.K. (2013). Bi-reforming of methane from any source with steam and carbon dioxide exclusively to metgas (CO-$2H_2$) for methanol and hydrocarbon synthesis. J. Am. Chem. Soc. *135*, 648–650.

Olah, G.A., Goeppert, A., Czaun, M., Mathew, T., May, R.B., and Prakash, G.K. (2015). Single step bi-reforming and oxidative bi-reforming of

methane (natural gas) with steam and carbon dioxide to metgas (CO-2H_2) for methanol synthesis: self-sufficient effective and exclusive oxygenation of methane to methanol with oxygen. J. Am. Chem. Soc. *137*, 8720–8729.

Pal, P., Singha, R.K., Saha, A., Bal, R., and Panda, A.B. (2015). Defect-induced efficient partial oxidation of methane over nonstoichiometric Ni/CeO_2 nanocrystals. J. Phys. Chem. C *119*, 13610–13618.

Paladino Lino, A.V., Assaf, E.M., and Assaf, J.M. (2019). X-ZrO_2 addition (X= Ce, La, Y and Sm) on Ni/$MgAl_2O_4$ applied to methane tri-reforming for syngas production. J. CO2 Util. *33*, 273–283.

Park, D., Lee, C., Moon, D.J., and Kim, T. (2015). Design, analysis, and performance evaluation of steam-CO_2 reforming reactor for syngas production in GTL process. Int. J. Hydrogen Energy *40*, 11785–11790.

Pino, L., Vita, A., Cipitì, F., Laganà, M., and Recupero, V. (2011). Hydrogen production by methane tri-reforming process over Ni–ceria catalysts: effect of La-doping. Appl. Catal. B Environ. *104*, 64–73.

Pipatmanomai, S., Kaewluan, S., and Vitidsant, T. (2009). Economic assessment of biogas-to-electricity generation system with H_2S removal by activated carbon in small pig farm. Appl. Energy *86*, 669–674.

Quincoces, C. (2004). Ni/γ-Al_2O_3 catalyst from kaolinite for the dry reforming of methane. Mater. Lett. *58*, 272–275.

Rahmat, N., Yaakob, Z., Rahman, N.A., and Jahaya, S.S. (2019). Renewable hydrogen-rich syngas from CO_2 reforming of CH_4 with steam over Ni/$MgAl_2O_4$ and its process optimization. Int. J. Environ. Sci. Technol. *17*, 843–856.

Ren, P., and Zhao, Z. (2019). Unexpected coke-resistant stability in steam-CO_2 dual reforming of methane over the robust Mo_2C-Ni/ZrO_2 catalyst. Catal.Commun. *119*, 71–75.

Roy, P.S., Song, J., Kim, K., Park, C.S., and Raju, A.S.K. (2018). CO_2 conversion to syngas through the steam-biogas reforming process. J. CO2 Util. *25*, 275–282.

Sadeghi, M., Jafari, M., Yari, M., and Mahmoudi, S.M.S. (2018). Exergoeconomic assessment and optimization of a syngas production system with a desired H_2/CO ratio based on methane tri-reforming process. J. CO2 Util. *25*, 283–301.

Saebea, D., Authayanun, S., and Arpornwichanop, A. (2019). Process simulation of bio-dimethyl ether synthesis from tri-reforming of biogas: CO_2 utilization. Energy *175*, 36–45.

Sarker, B.R., Wu, B., and Paudel, K.P. (2018). Optimal number and location of storage hubs and biogas production reactors in farmlands with allocation of multiple feedstocks. Appl. Math. Model. *55*, 447–465.

Sarker, B.R., Wu, B., and Paudel, K.P. (2019). Modeling and optimization of a supply chain of renewable biomass and biogas: processing plant location. Appl. Energy *239*, 343–355.

Scarlat, N., Dallemand, J.-F., and Fahl, F. (2018). Biogas: developments and perspectives in Europe. Renew. Energy *129*, 457–472.

Schwach, P., Pan, X., and Bao, X. (2017). Direct conversion of methane to value-added chemicals over heterogeneous catalysts: challenges and prospects. Chem. Rev. *117*, 8497–8520.

Sheets, J.P., and Shah, A. (2018). Techno-economic comparison of biogas cleaning for grid injection, compressed natural gas, and biogas-to-methanol conversion technologies. Biofuel Bioprod. Bior. *12*, 412–425.

Siang, T.J., Bach, L.G., Singh, S., Truong, Q.D., Ho, V.T.T., Huy Phuc, N.H., Alenazey, F., and Vo, D.-V.N. (2019). Methane bi-reforming over boron-doped Ni/SBA-15 catalyst: longevity evaluation. Int. J. Hydrogen Energy *44*, 20839–20850.

Singh, S., Bahari, M.B., Abdullah, B., Phuong, P.T.T., Truong, Q.D., Vo, D.-V.N., and Adesina, A.A. (2018). Bi-reforming of methane on Ni/SBA-15 catalyst for syngas production: influence of feed composition. Int. J. Hydrogen Energy *43*, 17230–17243.

Singha, R.K., Das, S., Pandey, M., Kumar, S., Bal, R., and Bordoloi, A. (2016a). Ni nanocluster on modified CeO_2–ZrO_2 nanoporous composite for tri-reforming of methane. Catal.Sci. Technol. *6*, 7122–7136.

Singha, R.K., Shukla, A., Yadav, A., Adak, S., Iqbal, Z., Siddiqui, N., and Bal, R. (2016b). Energy efficient methane tri-reforming for synthesis gas production over highly coke resistant nanocrystalline Ni–ZrO_2 catalyst. Appl. Energy *178*, 110–125.

Slagtern, Å., Olsbye, U., Blom, R., Dahl, I.M., and Fjellvåg, H. (1997). Characterization of Ni on La modified Al_2O_3 catalysts during CO_2 reforming of methane. Appl. Catal. A Gen. *165*, 379–390.

Sokefun, Y.O., Joseph, B., and Kuhn, J.N. (2019). Impact of Ni and Mg loadings on dry reforming performance of Pt/ceria-zirconia catalysts. Ind. Eng. Chem. Res. *58*, 9322–9330.

Song, C., and Pan, W. (2004). Tri-reforming of methane: a novel concept for catalytic production of industrially useful synthesis gas with desired H_2/CO ratios. Catal. Today *98*, 463–484.

Song, Y.-Q., Liu, H.-M., and He, D.-H. (2010). Effects of hydrothermal conditions of ZrO_2 on catalyst properties and catalytic performances of Ni/ZrO_2 in the partial oxidation of methane. Energy Fuel *24*, 2817–2824.

Song, Y., Ozdemir, E., Ramesh, S., Adishev, A., Subramanian, S., Harale, A., Albuali, M., Fadhel, B.A., Jamal, A., Moon, D., et al. (2020). Dry reforming of methane by stable Ni–Mo nanocatalysts on single-crystalline MgO. Science *367*, 777–781.

Spies, K.A., Rainbolt, J.E., Li, X.S., Braunberger, B., Li, L., King, D.L., and Dagle, R.A. (2017). Warm cleanup of coal-derived syngas: multicontaminant removal process demonstration. Energy Fuel *31*, 2448–2456.

Sukonket, T., Khan, A., Saha, B., Ibrahim, H., Tantayanon, S., Kumar, P., and Idem, R. (2011). Influence of the catalyst preparation method, surfactant amount, and steam on CO_2 reforming of CH_4 over 5Ni/$Ce_{0.6}Zr_{0.4}O_2$ catalysts. Energy Fuel *25*, 864–877.

Sun, Q., Li, H., Yan, J., Liu, L., Yu, Z., and Yu, X. (2015). Selection of appropriate biogas upgrading technology-a review of biogas cleaning, upgrading and utilisation. Renew. Sustain. Energy Rev. *51*, 521–532.

Świrk, K., Gálvez, M.E., Motak, M., Grzybek, T., Rønning, M., and Da Costa, P. (2019). Syngas production from dry methane reforming over yttrium-promoted nickel-KIT-6 catalysts. Int. J. Hydrogen Energy *44*, 274–286.

Tahir, B., Tahir, M., and Amin, N.A.S. (2019). Ag-La loaded protonated carbon nitrides nanotubes (pCNNT) with improved charge separation in a monolithic honeycomb photoreactor for enhanced bireforming of methane (BRM) to fuels. Appl. Catal. B Environ. *248*, 167–183.

Tang, L., Cheng, S., Zhang, L., Mi, H., Mou, L., Yang, S., Huang, Z., Shi, X., and Jiang, X. (2018). Printable metal-polymer conductors for highly stretchable bio-devices. iScience *4*, 302–311.

Thakkar, H., Eastman, S., Hajari, A., Rownaghi, A.A., Knox, J.C., and Rezaei, F. (2016). 3D-Printed zeolite monoliths for CO_2 removal from enclosed environments. ACS Appl. Mater. Interfaces *8*, 27753–27761.

Vita, A., Pino, L., Cipiti, F., Lagana, M., and Recupero, V. (2014). Biogas as renewable raw material for syngas production by tri-reforming process over $NiCeO_2$ catalysts: optimal operative condition and effect of nickel content. Fuel Process. Technol. *127*, 47–58.

Vita, A., Italiano, C., Fabiano, C., Laganà, M., and Pino, L. (2015). Influence of Ce-precursor and fuel on structure and catalytic activity of combustion synthesized Ni/CeO_2 catalysts for biogas oxidative steam reforming. Mater. Chem. Phys. *163*, 337–347.

Walker, D.M., Pettit, S.L., Wolan, J.T., and Kuhn, J.N. (2012). Synthesis gas production to desired hydrogen to carbon monoxide ratios by tri-reforming of methane using Ni–MgO–(Ce,Zr)O_2 catalysts. Appl. Catal. A Gen. *445-446*, 61–68.

Wang, K., Li, X., Ji, S., Huang, B., and Li, C. (2008). Preparation of Ni-based metal monolithic catalysts and a study of their performance in methane reforming with CO_2. ChemSusChem *1*, 527–533.

Wang, C., Wang, T., Ma, L., Gao, Y., and Wu, C. (2010). Steam reforming of biomass raw fuel gas over NiO–MgO solid solution cordierite monolith catalyst. Energy Convers. Manag. *51*, 446–451.

Wang, L., Yi, Y., Wu, C., Guo, H., and Tu, X. (2017). One-step reforming of CO_2 and CH_4 into high-value liquid chemicals and fuels at room temperature by plasma-driven catalysis. Angew. Chem. Int. Ed. *56*, 13679–13683.

Wang, F., Han, B., Zhang, L., Xu, L., Yu, H., and Shi, W. (2018a). CO_2 reforming with methane over small-sized Ni@SiO_2 catalysts with unique features of sintering-free and low carbon. Appl. Catal. B Environ. *235*, 26–35.

Wang, Y., Yao, L., Wang, S., Mao, D., and Hu, C. (2018b). Low-temperature catalytic CO_2 dry

reforming of methane on Ni-based catalysts: a review. Fuel Process. Technol. *169*, 199–206.

Wang, H., Dong, X., Zhao, T., Yu, H., and Li, M. (2019). Dry reforming of methane over bimetallic Ni-Co catalyst prepared from $La(Co_xNi_{1-x})_{0.5}Fe_{0.5}O_3$ perovskite precursor: catalytic activity and coking resistance. Appl. Catal. B Environ. *245*, 302–313.

Wei, J., Xu, B., Li, J., Cheng, Z., and Zhu, Q. (2000). Highly active and stable Ni/ZrO_2 catalyst for syngas production by CO_2 reforming of methane. Appl. Catal. A Gen. *196*, L167–L172.

White, A.J., Kirk, D.W., and Graydon, J.W. (2011). Analysis of small-scale biogas utilization systems on Ontario cattle farms. Renew. Energy *36*, 1019–1025.

Winslow, K.M., Laux, S.J., and Townsend, T.G. (2019). An economic and environmental assessment on landfill gas to vehicle fuel conversion for waste hauling operations. Resour. Conserv Recy. *142*, 155–166.

Yabe, T., Mitarai, K., Oshima, K., Ogo, S., and Sekine, Y. (2017). Low-temperature dry reforming of methane to produce syngas in an electric field over La-doped Ni/ZrO_2 catalysts. Fuel Process. Technol. *158*, 96–103.

Yabe, T., Yamada, K., Oguri, T., Higo, T., Ogo, S., and Sekine, Y. (2018). Ni–Mg supported catalysts on low-temperature electrocatalytic tri-reforming of methane with suppressed oxidation. ACS Catal. *8*, 11470–11477.

Yang, E.-h., Kim, N.Y., Noh, Y.-s., Lim, S.S., Jung, J.-S., Lee, J.S., Hong, G.H., and Moon, D.J. (2015). Steam CO_2 reforming of methane over $La_{1-x}Ce_xNiO_3$ perovskite catalysts. Int. J. Hydrogen Energy *40*, 11831–11839.

Yao, L., Wang, Y., Shi, J., Xu, H., Shen, W., and Hu, C. (2017). The influence of reduction temperature on the performance of $ZrO_x/Ni\text{-}MnO_x/SiO_2$ catalyst for low-temperature CO_2 reforming of methane. Catal. Today *281*, 259–267.

Yap, D., Tatibouët, J.-M., and Batiot-Dupeyrat, C. (2018). Catalyst assisted by non-thermal plasma in dry reforming of methane at low temperature. Catal. Today *299*, 263–271.

Yentekakis, I.V., Goula, G., Hatzisymeon, M., Betsi-Argyropoulou, I., Botzolaki, G., Kousi, K., Kondarides, D.I., Taylor, M.J., Parlett, C.M.A., Osatiashtiani, A., et al. (2019). Effect of support oxygen storage capacity on the catalytic performance of Rh nanoparticles for CO_2 reforming of methane. Appl. Catal. B Environ. *243*, 490–501.

Yentekakis, I.V., Goula, G., Panagiotopoulou, P., Katsoni, A., Diamadopoulos, E., Mantzavinos, D., and Delimitis, A. (2015). Dry reforming of methane: catalytic performance and stability of Ir catalysts supported on $\gamma\text{-}Al_2O_3$, $Zr_{0.92}Y_{0.08}O_{2-\delta}$ (YSZ) or $Ce_{0.9}Gd_{0.1}O_{2-\delta}$ (GDC) supports. Top. Catal. *58*, 1228–1241.

Yoo, J., Bang, Y., Han, S.J., Park, S., Song, J.H., and Song, I.K. (2015). Hydrogen production by tri-reforming of methane over nickel–alumina aerogel catalyst. J. Mol. Catal. A Chem. *410*, 74–80.

Zanganeh, R., Rezaei, M., and Zamaniyan, A. (2013). Dry reforming of methane to synthesis gas on NiO–MgO nanocrystalline solid solution catalysts. Int. J. Hydrogen Energy *38*, 3012–3018.

Zareei, S. (2018). Evaluation of biogas potential from livestock manures and rural wastes using GIS in Iran. Renew. Energy *118*, 351–356.

Zeng, Y.X., Wang, L., Wu, C.F., Wang, J.Q., Shen, B.X., and Tu, X. (2018). Low temperature reforming of biogas over K-, Mg- and Ce-promoted Ni/Al_2O_3 catalysts for the production of hydrogen rich syngas: understanding the plasma-catalytic synergy. Appl. Catal. B Environ. *224*, 469–478.

Zhang, J., and Li, F. (2015). Coke-resistant $Ni@SiO_2$ catalyst for dry reforming of methane. Appl. Catal. B Environ. *176-177*, 513–521.

Zhang, Y., Zhang, S., Gossage, J.L., Lou, H.H., and Benson, T.J. (2014). Thermodynamic analyses of tri-reforming reactions to produce syngas. Energy Fuel *28*, 2717–2726.

Zhang, X., Yang, C., Zhang, Y., Xu, Y., Shang, S., and Yin, Y. (2015). Ni–Co catalyst derived from layered double hydroxides for dry reforming of methane. Int. J. Hydrogen Energy *40*, 16115–16126.

Zhang, F., Liu, Z., Chen, X., Rui, N., Betancourt, L.E., Lin, L., Xu, W., Sun, C.-j., Abeykoon, A.M.M., Rodriguez, J.A., et al. (2020a). Effects of Zr doping into ceria for the dry reforming of methane over $Ni/CeZrO_2$ catalysts: in situ studies with XRD, XAFS, and AP-XPS. ACS Catal. *10*, 3274–3284.

Zhang, T., Liu, Z., Zhu, Y.-A., Liu, Z., Sui, Z., Zhu, K., and Zhou, X. (2020b). Dry reforming of methane on Ni-Fe-MgO catalysts: influence of Fe on carbon-resistant property and kinetics. Appl. Catal. B Environ. *264*, 118497.

Zhao, X., Ngo, H.T., Walker, D.M., Weber, D., Maiti, D., Cimenler, U., Petrov, A.D., Joseph, B., and Kuhn, J.N. (2018a). Tri-reforming of surrogate biogas over Ni/Mg/ceria–zirconia/alumina pellet catalysts. Chem. Eng. Commun. *205*, 1129–1142.

Zhao, X., Walker, D.M., Maiti, D., Petrov, A.D., Kastelic, M., Joseph, B., and Kuhn, J.N. (2018b). NiMg/ceria-zirconia cylindrical pellet catalysts for tri-reforming of surrogate biogas. Ind. Eng. Chem. Res. *57*, 845–855.

Zhao, X., Naqi, A., Walker, D.M., Roberge, T., Kastelic, M., Joseph, B., and Kuhn, J.N. (2019a). Conversion of landfill gas to liquid fuels through a TriFTS (tri-reforming and Fischer–Tropsch synthesis) process: a feasibility study. Sustain. Energy Fuels *3*, 539–549.

Zhao, X., Stachurski, P., Shah, S., Maiti, D., Ramani, S., Wright, A., Walker, D.M., Joseph, B., and Kuhn, J.N. (2019b). Design and optimization of NiMg/ceria-zirconia catalyst pellets. Powder Technol. *357*, 214–222.

Zhao, X., Tekinalp, H., Meng, X., Ker, D., Benson, B., Pu, Y., Ragauskas, A.J., Wang, Y., Li, K., Webb, E., et al. (2019c). Poplar as biofiber reinforcement in composites for large-scale 3D printing. ACS Appl. Bio Mater. *2*, 4557–4570.

Zheng, X., Tan, S., Dong, L., Li, S., and Chen, H. (2015). Plasma-assisted catalytic dry reforming of methane: highly catalytic performance of nickel ferrite nanoparticles embedded in silica. J. Power Sources *274*, 286–294.

Zhou, L., Martirez, J.M.P., Finzel, J., Zhang, C., Swearer, D.F., Tian, S., Robatjazi, H., Lou, M., Dong, L., Henderson, L., et al. (2020). Light-driven methane dry reforming with single atomic site antenna-reactor plasmonic photocatalysts. Nat. Energy *5*, 61–70.

Zou, H., Chen, S., Huang, J., and Zhao, Z. (2016). Effect of additives on the properties of nickel molybdenum carbides for the tri-reforming of methane. Int. J. Hydrogen Energy *41*, 16842–16850.

iScience, Volume *23*

Supplemental Information

Biogas Reforming to Syngas: A Review

Xianhui Zhao, Babu Joseph, John Kuhn, and Soydan Ozcan

Table S1. Other Recent Studies on Tri-reforming of Biogas to Syngas. (Related to Table 4)

Catalyst	Reaction conditions	CH_4 conv. (%)	CO_2 conv. (%)	H_2/CO	Coke rate ($g_{coke}/(g_{cat}*h)$)	Ref.
Nickel-alumina xerogel	700°C, 269,000 mL/(g*h), 1 bar, fixed-bed reactor	76.6	–	1.9–2.0	4.7E-3	(Yoo et al., 2015)
Ni/zeolite L	800°C, 162 h^{-1}, 1 bar, fixed-bed reactor	~86	~24	~1.9	–	(Izquierdo et al., 2014)
Rh-Ni/zeolite L	800°C, 162 h^{-1}, 1 bar, fixed-bed reactor	96.4	~33	~1.8	–	(Izquierdo et al., 2014)
Ni/YSZ-CeO_2	800°C, 10,000 h^{-1}, $CH_4/CO_2/O_2/H_2O$ = 1/1/0.1/1	100	100	1.0–1.1	–	(Kang et al., 2007)
Ni/$Mg_{0.5}Ti_{0.5}O$	850°C, 1.78 g*h/mol, 10 bar, $CH_4/CO_2/O_2/H_2O$ = 1/0.48/0.1/0.54, fixed-bed reactor	~85	~62	–	–	(Jiang et al., 2007a)
Ni/$Mg_{0.75}Ti_{0.25}O$	850°C, 1.78 g*h/mol, 1 bar, $CH_4/CO_2/O_2/H_2O$ = 1/0.48/0.1/0.54, fixed-bed reactor	~95	~80	~1.6	–	(Jiang et al., 2007a)
NiMg/$Ce_{0.6}Zr_{0.4}O_2$	800°C, 61,000 h^{-1}, 1 bar, $CH_4/CO_2/O_2/H_2O$ = 1/0.7/0.2/0.23, fixed-bed reactor	97	78	2.1	5.1E-4	(Walker et al., 2012)
Ni/Ce-Al_2O_3	800°C, 161 $g_{gas}/(g_{cat}*h)$, 1 bar, CH_4/O_2 = 4, fixed-bed reactor	97	22	2.0	–	(Izquierdo et al., 2013)
Ni/Ce-Zr-Al_2O_3	800°C, 161 $g_{gas}/(g_{cat}*h)$, 1 bar, CH_4/O_2 = 4, fixed-bed reactor	99	34	1.5	–	(Izquierdo et al., 2013)
Rh-Ni/Ce-Al_2O_3	800°C, 161 $g_{gas}/(g_{cat}*h)$, 1 bar, CH_4/O_2 = 4, fixed-bed reactor	99	39	1.7	–	(Izquierdo et al., 2013)
Ni/Ce-ZrO_2	800°C, fixed-bed reactor	96	82	1.4	–	(Lee et al., 2003)
Ni@SiO_2	750°C, 1 bar, $CH_4/CO_2/O_2/H_2O$ = 1/0.5/0.1/3.0, fixed-bed reactor	73	43	1.7	0.028	(Majewski and Wood, 2014)
Ni/Al_2O_3	950°C, 10,000 h^{-1}, 1 bar, $CH_4/CO_2/O_2/H_2O$ = 50/12.5/25/12.5, fixed-bed reactor	~95	~25	–	–	(Jiang et al., 2007b)

Ni-MgO	850°C, 32,000 mL/(h*g_{cat}), 1 bar, $CH_4/CO_2/O_2/H_2O$ = 1/0.48/0.1/0.54, fixed-bed reactor	~98	~79	~1.5	–	(Song and Pan, 2004)
Ni-Mg-CeZrO	850°C, 32,000 mL/(h*g_{cat}), 1 bar, $CH_4/CO_2/O_2/H_2O$ = 1/0.48/0.1/0.54, fixed-bed reactor	~98	~73	~1.5	–	(Song and Pan, 2004)
Ni-ZrO_2	850°C, 32,000 mL/(h*g_{cat}), 1 bar, $CH_4/CO_2/O_2/H_2O$ = 1/0.48/0.1/0.54, fixed-bed reactor	~98	~73	~1.6	–	(Song and Pan, 2004)
Ni/Al_2O_3	850°C, 32,000 mL/(h*g_{cat}), 1 bar, $CH_4/CO_2/O_2/H_2O$ = 1/0.48/0.1/0.54, fixed-bed reactor	~98	~73	~1.6	–	(Song and Pan, 2004)
Ni-CeO_2	850°C, 32,000 mL/(h*g_{cat}), 1 bar, $CH_4/CO_2/O_2/H_2O$ = 1/0.48/0.1/0.54, fixed-bed reactor	~95	~73	~1.6	–	(Song and Pan, 2004)
Ni-CeZrO	850°C, 32,000 mL/(h*g_{cat}), 1 bar, $CH_4/CO_2/O_2/H_2O$ = 1/0.48/0.1/0.54, fixed-bed reactor	~93	~71	~1.6	–	(Song and Pan, 2004)
NiMo-C	850°C, $CH_4/CO_2/O_2/H_2O$ = 1/0.39/0.16/0.30, fixed-bed reactor	~96	~100	–	–	(Zou et al., 2016)
NiMoC-La	850°C, $CH_4/CO_2/O_2/H_2O$ = 1/0.39/0.16/0.30, fixed-bed reactor	~93	~88	–	–	(Zou et al., 2016)
NiMoC-Co	850°C, $CH_4/CO_2/O_2/H_2O$ = 1/0.39/0.16/0.30, fixed-bed reactor	~93	~100	–	–	(Zou et al., 2016)
NiMoC-Mg	850°C, $CH_4/CO_2/O_2/H_2O$ = 1/0.39/0.16/0.30, fixed-bed reactor	~90	~84	–	–	(Zou et al., 2016)
NiMoC-K	850°C, $CH_4/CO_2/O_2/H_2O$ = 1/0.39/0.16/0.30, fixed-bed reactor	~17	~0	–	–	(Zou et al., 2016)
Ni/Ce-Al_2O_3	800°C, 1 bar, 161 g_{gas}*(g_{cat}*h)$^{-1}$, $CH_4/CO_2/O_2$/liquid H_2O =	~99	~36	~1.9	–	(Izquierdo et al., 2018)

	1/0.67/0.25/0.0008, fixed-bed reactor					
Ni/Zr-Al_2O_3	800°C, 1 bar, 161 $g_{gas}*(g_{cat}*h)^{-1}$, $CH_4/CO_2/O_2$/liquid H_2O = 1/0.67/0.25/0.0008, fixed-bed reactor	99	34	~2	–	(Izquierdo et al., 2018)
Rh-Ni/Ce-Al_2O_3	800°C, 1 bar, 161 $g_{gas}*(g_{cat}*h)^{-1}$, $CH_4/CO_2/O_2$/liquid H_2O = 1/0.67/0.25/0.0008, fixed-bed reactor	~99	~32	~2	–	(Izquierdo et al., 2018)
Ni/Al_2O_3	800°C, 1 bar, 17,220 $mL*(g*h)^{-1}$, $CH_4/CO_2/O_2/H_2O$ = 1/0.23/0.07/0.46, fixed-bed reactor	–	–	2.3	0.014	(Kumar et al., 2019)
Ni/ZrO_2	800°C, 1 bar, 17,220 $mL*(g*h)^{-1}$, $CH_4/CO_2/O_2/H_2O$ = 1/0.23/0.07/0.46, fixed-bed reactor	–	–	2.2	3.6E-3	(Kumar et al., 2019)
Ni/TiO_2	800°C, 1 bar, 17,220 $mL*(g*h)^{-1}$, $CH_4/CO_2/O_2/H_2O$ = 1/0.23/0.07/0.46, fixed-bed reactor	–	–	1.9	2E-5	(Kumar et al., 2019)
Ni/SBA-15	800°C, 1 bar, 17,220 $mL*(g*h)^{-1}$, $CH_4/CO_2/O_2/H_2O$ = 1/0.23/0.07/0.46, fixed-bed reactor	–	–	2.2	1E-4	(Kumar et al., 2019)
Ni/MgO	800°C, 1 bar, 17,220 $mL*(g*h)^{-1}$, $CH_4/CO_2/O_2/H_2O$ = 1/0.23/0.07/0.46, fixed-bed reactor	–	–	1.8	1.4E-3	(Kumar et al., 2019)

Table S2. Other Recent Studies on Low-temperature Biogas Reforming to Syngas. (Related to Table 5)

Catalyst	Reaction conditions	CH_4 conv. (%)	CO_2 conv. (%)	H_2/CO	Coke rate ($g_{coke}/(g_{cat}*h)$)	Ref.
Pd-Ni-Mg/$Ce_{0.6}Zr_{0.4}O_2$	366°C, CH_4/CO_2 = 1/1, 68,000 h^{-1}, 1-bar, u-tube reactor	–	10	–	–	(Elsayed et al., 2016)
Pd-Ni-Mg/$Ce_{0.6}Zr_{0.4}O_2$	383°C, CH_4/CO_2 = 1/1, 68,000 h^{-1}, 1-bar, u-tube reactor	10	–	–	–	(Elsayed et al., 2016)
Ni/La_2O_3-ZrO_2	400°C, CH_4/CO_2 = 1/1, fixed-bed reactor	~7	~11	~0.5	–	(Sokolov et al., 2013)
Ni-CaO/ZrO_2-La_2O_3	500°C, CH_4/CO_2 = 1/1, 1 bar, fixed-bed reactor	~ 63	~ 80	~ 0.5	–	(Bachiller-Baeza et al., 2013)
Ni/γ-Al_2O_3	500°C, CH_4/CO_2 = 1/1, 18,000 $cm^3/(g*h)$, 1 bar, fixed-bed reactor	23	17	–	–	(Wang and Lu, 1998)
No catalyst	25°C, CH_4/CO_2 = 1/2, 4 W, 1 bar, cold corona plasma reactor	28	20	0.7	–	(Aziznia et al., 2012)
Ni/γ-Al_2O_3	25°C, CH_4/CO_2 = 1/2, 4 W, 1 bar, cold corona plasma reactor	36	23	0.6	–	(Aziznia et al., 2012)
No catalyst	70°C, CH_4/CO_2 = 1/1, 19.5 kv, 4 KHz, 5.7 mJ, 23 W, 1 bar, pulsed plasma reactor	61	50	1.3	–	(Ghorbanzadeh et al., 2009)
Ni/Al_2O_3	160°C, CH_4/CO_2 = 1/0.67, 16 W, coaxial dielectric barrier discharge plasma reactor	27	20	2.0	0.029	(Zeng et al., 2018)
Ni/γ-Al_2O_3	~230 °C, CH_4/CO_2 = 1/1, 50 W, coaxial dielectric barrier discharge plasma reactor	56	30	–	~[1.7E-3, 6.4E-3]	(Tu and Whitehead, 2012)
Pd/Al_2O_3	240°C, CH_4/CO_2 = 1/2, 5.7–6 kHz, 1.2 bar,	51	28	–	–	(Sentek et al., 2010)

	dielectric barrier discharge plasma reactor					
Ru/ZrO_2-La_2O_3	450°C, $CH_4/CO_2/H_2O$ = 1/1/0.5, 1 bar, fixed-bed reactor	~15	~3	~2.5	–	(Soria et al., 2011)

Table S3. Properties of Some Other Catalysts Used in Biogas Reforming. (Related to Table 7)

Catalyst	BET surface area (m^2/g)	Pore volume (cm^3/g)	Pore size (Å)	Basic sites (mmol/g)	Metal dispersion (%)	Ref.
CeO_2	–	–	–	0.01	–	(García-Vargas et al., 2012; Pal et al., 2015)
Ni-La-CeO_2	–	–	–	0.03–0.04	–	(Pino et al., 2011)
Ni/YSZ-CeO_2	10	0.004	–	–	–	(Kang et al., 2007)
Imperial chemical industries (ICI)	13	0.08	–	–	–	(Kang et al., 2007)
Holder Topsoe (HT)	18	0.05	–	–	–	(Kang et al., 2007)
Ce-Zr/Al_2O_3	192	0.74	151	–	–	(Izquierdo et al., 2013)
Ni-Zr/Al_2O_3	167	0.62	146	–	–	(Izquierdo et al., 2013)
NiMoC-Ce	132	0.26	73	–	–	(Zou et al., 2016)
NiMoC-Mg	120	0.22	69	–	–	(Zou et al., 2016)
Ni@SiO_2	68	–	–	–	–	(Majewski and Wood, 2014; Majewski et al., 2013)
Ni/YSZ-O_2	14	0.12	–	0.01	1.6	(García-Vargas et al., 2014)
CeO_2-ZrO_2	178	0.26	58	–	–	(Singha et al., 2016)

Table S4. Other Information of the Techno-economics Analysis of Biogas Conversion.

(Related to Table 9)

Product	Plant life (year)	Cost	Ref.
Electricity	–	Initial investment cost: $5,462–5,795; Operating and maintenance cost: $755–1,629/year; Annual saving and benefit: $2,024–2,576/year	(Pipatmanomai et al., 2009)
H_2	–	Investment cost in reforming system: $3,142,897	(Madeira et al., 2017)
H_2	10	Capital cost: $968,923; Operational cost: ~$103,438/year	(Montenegro Camacho et al., 2017)
Methanol	–	Capital cost: $46,000,000	(Hernández and Martín, 2016)
Methanol	20	Capital cost: ~$170,000,000; Operational cost: $48,000,000/year	(Sheets and Shah, 2018)
Liquid fuel	30	Total permanent investment cost: ~$42,000 bbl/day	(Graciano et al., 2018)
Liquid fuel	15	Total direct manufacturing cost: $5,720,000; Capital cost: $8,500,000	(Zhao et al., 2019)
Liquid fuel	20	Capital cost: $96,520,000; Operational cost: $11,450,000/year	(Okeke and Mani, 2017)
Compressed natural gas	30	Capital cost: $2,429,000; Operational cost: $192,100/year	(Winslow et al., 2019)
Wax	–	Capital cost: $3,080,000; Operational cost: $83.21/bbl	(Herz et al., 2017)

Supplemental References:

Aziznia, A., Bozorgzadeh, H.R., Seyed-Matin, N., Baghalha, M., and Mohamadalizadeh, A. (2012). Comparison of dry reforming of methane in low temperature hybrid plasma-catalytic corona with thermal catalytic reactor over Ni/γ-Al_2O_3. J Nat Gas Chem *21*, 466-475.

Bachiller-Baeza, B., Mateos-Pedrero, C., Soria, M.A., Guerrero-Ruiz, A., Rodemerck, U., and Rodríguez-Ramos, I. (2013). Transient studies of low-temperature dry reforming of methane over Ni-CaO/ZrO_2-La_2O_3. Appl Catal B-Environ *129*, 450-459.

Elsayed, N.H., Roberts, N.R.M., Joseph, B., and Kuhn, J.N. (2016). Comparison of Pd–Ni–Mg/ceria–zirconia and Pt–Ni–Mg/ceria–zirconia catalysts for syngas production via low temperature reforming of model biogas. Top Catal *59*, 138-146.

García-Vargas, J.M., Valverde, J.L., de Lucas-Consuegra, A., Gómez-Monedero, B., Sánchez, P., and Dorado, F. (2012). Precursor influence and catalytic behaviour of Ni/CeO_2 and Ni/SiC catalysts for the tri-reforming process. Appl Catal a-Gen *431-432*, 49-56.

García-Vargas, J.M., Valverde, J.L., Dorado, F., and Sánchez, P. (2014). Influence of the support on the catalytic behaviour of Ni catalysts for the dry reforming reaction and the tri-reforming process. J Mol Catal A-Chem *395*, 108-116.

Ghorbanzadeh, A., Lotfalipour, R., and Rezaei, S. (2009). Carbon dioxide reforming of methane at near room temperature in low energy pulsed plasma. Int J Hydrogen Energ *34*, 293-298.

Graciano, J.E.A., Chachuat, B., and Alves, R.M.B. (2018). Conversion of CO_2-rich natural gas to liquid transportation fuels via trireforming and Fischer–Tropsch synthesis: Model-based assessment. Ind Eng Chem Res *57*, 9964-9976.

Hernández, B., and Martín, M. (2016). Optimal process operation for biogas reforming to methanol: effects of dry reforming and biogas composition. Ind Eng Chem Res *55*, 6677-6685.

Herz, G., Reichelt, E., and Jahn, M. (2017). Design and evaluation of a Fischer-Tropsch process for the production of waxes from biogas. Energy *132*, 370-381.

Izquierdo, U., Barrio, V.L., Bizkarra, K., Gutierrez, A.M., Arraibi, J.R., Gartzia, L., Bañuelos, J., Lopez-Arbeloa, I., and Cambra, J.F. (2014). Ni and RhNi catalysts supported on Zeolites L for hydrogen and syngas production by biogas reforming processes. Chem Eng J *238*, 178-188.

Izquierdo, U., Barrio, V.L., Requies, J., Cambra, J.F., Güemez, M.B., and Arias, P.L. (2013). Tri-reforming: A new biogas process for synthesis gas and hydrogen production. Int J Hydrogen Energ *38*, 7623-7631.

Izquierdo, U., García-García, I., Gutierrez, Á., Arraibi, J., Barrio, V., Cambra, J., and Arias, P. (2018). Catalyst deactivation and regeneration processes in biogas tri-reforming process. The effect of hydrogen sulfide addition. Catalysts *8*, 12.

Jiang, H., Li, H., Xu, H., and Zhang, Y. (2007a). Preparation of $Ni/Mg_xTi_{1-x}O$ catalysts and investigation on their stability in tri-reforming of methane. Fuel Process Technol *88*, 988-995.
Jiang, H., Li, H., and Zhang, Y. (2007b). Tri-reforming of methane to syngas over Ni/Al_2O_3—thermal distribution in the catalyst bed. J Fuel Chem Technol *35*, 72-78.
Kang, J.S., Kim, D.H., Lee, S.D., Hong, S.I., and Moon, D.J. (2007). Nickel-based tri-reforming catalyst for the production of synthesis gas. Appl Catal A-gen *332*, 153-158.
Kumar, R., Kumar, K., Choudary, N.V., and Pant, K.K. (2019). Effect of support materials on the performance of Ni-based catalysts in tri-reforming of methane. Fuel Process Technol *186*, 40-52.
Lee, S.-H., Cho, W., Ju, W.-S., Cho, B.-H., Lee, Y.-C., and Baek, Y.-S. (2003). Tri-reforming of CH_4 using CO_2 for production of synthesis gas to dimethyl ether. Catal Today *87*, 133-137.
Madeira, J.G.F., Delgado, A.R.S., Boloy, R.A.M., Coutinho, E.R., and Loures, C.C.A. (2017). Exergetic and economic evaluation of incorporation of hydrogen production in a cassava wastewater plant. Appl Therm Eng *123*, 1072-1078.
Majewski, A.J., and Wood, J. (2014). Tri-reforming of methane over $Ni@SiO_2$ catalyst. Int J Hydrogen Energ *39*, 12578-12585.
Majewski, A.J., Wood, J., and Bujalski, W. (2013). Nickel–silica core@shell catalyst for methane reforming. Int J Hydrogen Energ *38*, 14531-14541.
Montenegro Camacho, Y.S., Bensaid, S., Piras, G., Antonini, M., and Fino, D. (2017). Techno-economic analysis of green hydrogen production from biogas autothermal reforming. Clean Technol Envir *19*, 1437-1447.
Okeke, I.J., and Mani, S. (2017). Techno-economic assessment of biogas to liquid fuels conversion technology via Fischer-Tropsch synthesis. Biofuel Bioprod Bior *11*, 472-487.
Pal, P., Singha, R.K., Saha, A., Bal, R., and Panda, A.B. (2015). Defect-induced efficient partial oxidation of methane over nonstoichiometric Ni/CeO_2 nanocrystals. J Phys Chem C *119*, 13610-13618.
Pino, L., Vita, A., Cipitì, F., Laganà, M., and Recupero, V. (2011). Hydrogen production by methane tri-reforming process over Ni–ceria catalysts: Effect of La-doping. Appl Catal B-Environ *104*, 64-73.
Pipatmanomai, S., Kaewluan, S., and Vitidsant, T. (2009). Economic assessment of biogas-to-electricity generation system with H_2S removal by activated carbon in small pig farm. Appl Energ *86*, 669-674.
Sentek, J., Krawczyk, K., Młotek, M., Kalczewska, M., Kroker, T., Kolb, T., Schenk, A., Gericke, K.-H., and Schmidt-Szałowski, K. (2010). Plasma-catalytic methane conversion with carbon dioxide in dielectric barrier discharges. Appl Catal B-Environ *94*, 19-26.
Sheets, J.P., and Shah, A. (2018). Techno-economic comparison of biogas cleaning for grid injection, compressed natural gas, and biogas-to-methanol conversion technologies. Biofuel Bioprod Bior *12*, 412-425.
Singha, R.K., Das, S., Pandey, M., Kumar, S., Bal, R., and Bordoloi, A. (2016). Ni nanocluster on modified CeO_2–ZrO_2 nanoporous composite for tri-reforming of methane. Catal Sci Technol *6*, 7122-7136.

Sokolov, S., Kondratenko, E.V., Pohl, M.-M., and Rodemerck, U. (2013). Effect of calcination conditions on time on-stream performance of Ni/La_2O_3–ZrO_2 in low-temperature dry reforming of methane. Int J Hydrogen Energ *38*, 16121-16132.
Song, C., and Pan, W. (2004). Tri-reforming of methane: a novel concept for synthesis of industrially useful synthesis gas with desired H_2/CO ratios using CO_2 in flue gas of power plants without CO_2 separation. Am Chem Soc Div Fuel Chem Prepr *49*, 128-131.
Soria, M.A., Mateos-Pedrero, C., Guerrero-Ruiz, A., and Rodríguez-Ramos, I. (2011). Thermodynamic and experimental study of combined dry and steam reforming of methane on Ru/ZrO_2-La_2O_3 catalyst at low temperature. Int J Hydrogen Energ *36*, 15212-15220.
Tu, X., and Whitehead, J.C. (2012). Plasma-catalytic dry reforming of methane in an atmospheric dielectric barrier discharge: Understanding the synergistic effect at low temperature. Appl Catal B-Environ *125*, 439-448.
Walker, D.M., Pettit, S.L., Wolan, J.T., and Kuhn, J.N. (2012). Synthesis gas production to desired hydrogen to carbon monoxide ratios by tri-reforming of methane using Ni–MgO–(Ce,Zr)O_2 catalysts. Appl Catal A-gen *445-446*, 61-68.
Wang, S., and Lu, G.Q.M. (1998). CO_2 reforming of methane on Ni catalysts: Effects of the support phase and preparation technique. Appl Catal B-Environ *16*, 269-277.
Winslow, K.M., Laux, S.J., and Townsend, T.G. (2019). An economic and environmental assessment on landfill gas to vehicle fuel conversion for waste hauling operations. Resour Conserv Recy *142*, 155-166.
Yoo, J., Bang, Y., Han, S.J., Park, S., Song, J.H., and Song, I.K. (2015). Hydrogen production by tri-reforming of methane over nickel–alumina aerogel catalyst. J Mol Catal A-Chem *410*, 74-80.
Zeng, Y.X., Wang, L., Wu, C.F., Wang, J.Q., Shen, B.X., and Tu, X. (2018). Low temperature reforming of biogas over K-, Mg- and Ce-promoted Ni/Al_2O_3 catalysts for the production of hydrogen rich syngas: Understanding the plasma-catalytic synergy. Appl Catal B-Environ *224*, 469-478.
Zhao, X., Naqi, A., Walker, D.M., Roberge, T., Kastelic, M., Joseph, B., and Kuhn, J.N. (2019). Conversion of landfill gas to liquid fuels through a TriFTS (tri-reforming and Fischer–Tropsch synthesis) process: a feasibility study. Sustain Energ Fuels *3*, 539-549.
Zou, H., Chen, S., Huang, J., and Zhao, Z. (2016). Effect of additives on the properties of nickel molybdenum carbides for the tri-reforming of methane. Int J Hydrogen Energ *41*, 16842-16850.